BIOMECHANICAL ANALYSES OF ANTERIOR VAGINAL WALL PROLAPSE: MR IMAGING AND COMPUTER MODELING STUDIES

by
Luyun Chen

A dissertation submitted in partial fulfillment
Of the requirements for the degree of
Doctor of Philosophy
(Biomedical Engineering)
In The University of Michigan
2008

Doctoral Committee:

Research Professor James A. Ashton-Miller, Co-Chair
Professor John O.L. DeLancey, Co-Chair
Professor Douglas C. Noll
Professor Gregory M. Hulbert

To my parents

Acknowledgements

Thank you Professor James A. Ashton-Miller and Professor John O.L. DeLancey for the guidance, assistance, patience and encouragement; to Professor Douglas C. Noll and Professor Gregory M. Hulbert for serving on my committee and for the helpful advice and comments; to Yvonne Hsu for all the wonderful corporations and contribution on clinical insights; to Biomechanics Research Lab and Pelvic Floor Research Group for stimulating and friendly interdisciplinary research environment; to NIH grants NICHD R01 HD038665, P50 HD044406, for financial support.

Preface

Chapter 2 to chapter 6 of this dissertation were written as separate papers, published or to be submitted to technical journals. For that reason some repetition of material does occur, particularly in the introduction of each chapter.

Table of Contents

List of Figures

List of Tables

List of Appendices

Chapter 1

Introduction

1.1 What is pelvic organ prolapse and how big is the problem?

Pelvic organ prolapse is a distressing and debilitating condition for women. It is a problem that most women don't like to discuss, even when the symptoms interfere with their work, intimate relationships or ability to travel. Pelvic floor prolapse occurs when the network of muscle and connective tissue supporting the female pelvic organs weakens and sags. As a result, the vagina, bladder, uterus or rectum can slip out of position, sometimes protruding into or even inverting the vagina.

Figure 1-1. Photograph of the anterior vaginal wall protruding from the vaginal introitus showing two types of cystocele. Left; distention type AVP with stretched anterior vaginal wall (AVW). Right, displaced AVP with intact AVW that has become detached form supports (cervix, Cx also seen). (© DeLancey)

Figure 1-1 shows pictures of examples of anterior vaginal wall prolapse taken during a clinical exam. The functional consequences of pelvic organ prolapse include, but are not limited to, urinary incontinence, voiding dysfunction, fecal incontinence, sexual dysfunction, and difficulty with defecation. Although some women treat their symptoms conservatively with pessaries, medications, physiotherapy, or behavioral therapy, others resort to protective undergarments and vaginal deodorizers to avoid odors. Women who are the most impaired seek surgical solutions. A majority of the approximately 300,000 female pelvic floor operations performed each year are performed for pelvic organ prolapse (i.e., approximately 200,000 operations each year) (Boyles et al, 2003). This makes pelvic organ prolapse the pelvic floor disorder most often requiring surgical repair and it costs society of over one billion dollars per year (Subak et al, 2002). Approximately one out of 10 American women (Olsen et al, 1997) will require surgery for pelvic floor dysfunction during their lifetime and 29% will undergo re-operation (Olsen et al, 1997). This latter statistic is a relatively high re-operation rate and indicates that the methods of surgical repair may be open to improvement.

Thus, pelvic floor prolapse is not only socially embarrassing and disabling, but the treatments are also costly and can place women at risk of additional surgery. This spectrum of problems creates an enormous socioeconomic burden on our society.

1.2 Why is improving understanding mechanisms of anterior vaginal wall prolapse important?

Anterior vaginal prolapse (AVP), clinically referred to as “cystocele,” is the most common form of pelvic organ prolapse (Hendrix et al, 2002) and an important problem whose successful treatment remains a challenge, even for experienced surgeons. The anterior vagina is the prolapse site with the highest rates of persistent and recurrent support defects (Shull et al, 2000). Blinded follow-up in a recent randomized prospective study of surgical techniques for AVP at an institution known internationally for excellence in urogynecologic surgery found that only 30-45% of patients had satisfactory or optimal results at 24 months (Weber et al, 2001). A review of the published articles for

surgical outcomes showed that recurrence of the AVP accounted for 42% of operative failures for pelvic organ prolapse (Sze et al, 1997). The inability to predict the patients who will experience surgical failure remains a significant barrier to developing more successful treatment. An improved understanding of the mechanisms underlying AVP will aid more successful treatment development and selection.

1.3 What are risk factors for pelvic organ prolapse?

Despite the prevalence of the problem, any understanding of the mechanisms underlying pelvic organ prolapse lag far behind the epidemiology. Risk factors for and correlates of pelvic organ prolapse are primarily based on expert opinion and are supported by limited epidemiologic and clinical evidence. Existing data suggest that age and ethnicity are associated with pelvic organ prolapse (Hendrix et al. 2002). Of greater interest to clinicians, however, are risk factors that maybe amenable to intervention to reduce injury to the pelvic floor. One such potential risk factor is childbirth, and, in particular vaginal birth. In the Oxford Family Planning Asscociation prolapse epidemiology study, parity was the strongest risk factor for pelvic organ prolapse, with an adjusted risk ratio of 10.85 (Mant et al, 1997). Although this trauma to the pelvic floor cannot be easily avoided, there has been increasing interest in understanding the specific aspects of the labor and delivery process that affect the pelvic floor. Lien et al. developed computer models to simulate vaginal birth and study the possible injury mechanisms identifying stretch injury of the ventral pubovisceral muscle as one candidate (Lien et al, 2004, 2005). There is scant evidence about other risk factors that are possibly amenable to efforts to prevent pelvic organ prolapse. In one study or ergonomic significance (Jørgensen et al, 1994), nursing assistants were more likely to undergo surgery for pelvic floor disorders than the general population, but no adjustment was made for vaginal birth. Surgical injury to the pelvic floor and underlying connective tissue disorders have also been implicated in pelvic organ prolapse. Obesity, cigarette smoking with chronic cough, previous hysterectomy, constipation, and estrogen deficiency have all been commonly implicated in the cause of pelvic organ prolapse. However, there is little, if any, evidence that mechanistically relates these factors to the development of AVP.

1.4 What structures are responsible for normal pelvic floor support?

The pelvic floor organs, when removed from the body, exist only as a limp and formless mass. Their shape and position in living women is determined by their attachments to the pubic bones through the muscles and connective tissue of the pelvis. The viscera are often thought of as being supported by the pelvic floor, but are actually a part of it. For example, the support of anterior compartment of pelvic floor consists of levator ani muscle, apical connective mesenteric tissue such as cardinal and uterosacral ligaments, paravaginal connective tissue, and the anterior vaginal wall itself.

Levator ani muscle support

The levator ani muscle, the main muscle comprising the pelvic floor, is believed to play a very important role in pelvic floor support. The levator ani muscle (LA) has a complex shape with muscle fibers running in multiple directions. The muscle structure can be simplified by dividing the levator ani muscle into two regions (Lawson et al, 1974, Kearney et al, 2004). The pubic portion of the muscle arises from the pubic bone and then attaches to the perineal structures and walls of the pelvic organs. The other portion is the iliococcygeal muscle, which forms a relatively flat, horizontal shelf that spans the pelvic opening from one pelvic sidewall to the other (Figure 1-2).

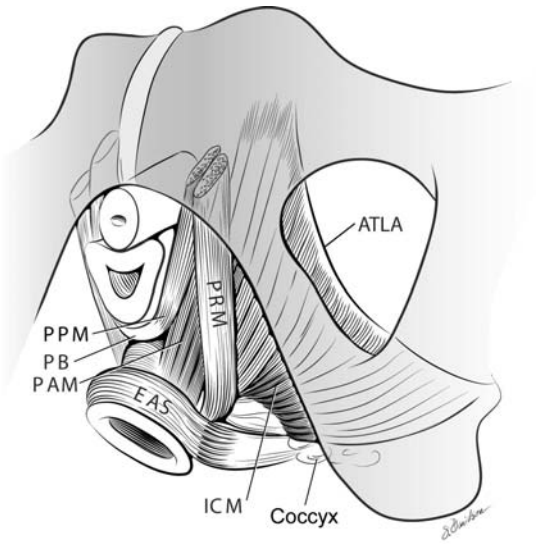

Figure 1-2 Illustration of levator ani muscle. Pubic portion include puboperineal muscle (PPM), puborectalis muscle (PRM) and puboanalis muscle (PAM). ICM: iliococcygeal muscle; ATLA: Arcus tendineus levator ani; EAS: external anal spincter; PB: perineal body. (From DeLancey private collection)

Connective tissue support

The anterior vaginal wall is supported by different connective tissues in different regions (Figure 1-3). The cardinal and uterosacral ligament attach the cervix and uterus to the pelvic side wall and provide the support for the vaginal apex, which is referred as “apical support” or “Level I” support. In the mid-portion of the vagina, the connective tissue attaches the vagina laterally and more directly to the pelvic walls and is used referred as “paravaginal support” or “Level II” support. It is not a separate layer from the vagina, as is sometimes inferred, but is a combination of the anterior vaginal wall and its attachments to the pelvic wall. In the distal vagina, the vaginal wall is directly attached to surrounding structures without any intervening connective tissue. Anteriorly it fuses with the urethra, posteriorly with the perineal body and laterally with the levator ani muscle and is usually referred as “Level III” support.

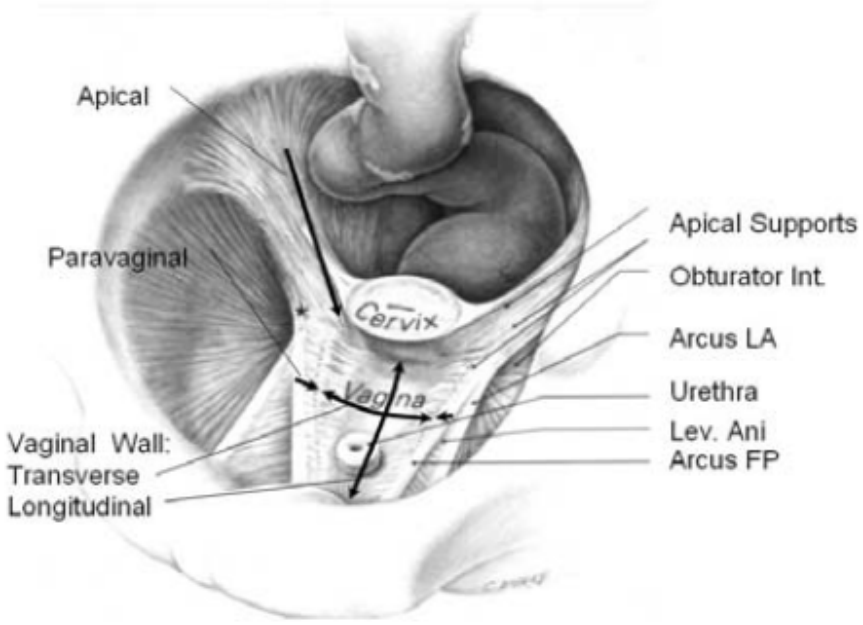

Figure 1-3 Anatomy of anterior vaginal wall support and sites of support failure (Bladder removed) (© DeLancey)

Anterior vaginal wall

The anterior vaginal wall, a very important part of anterior compartment pelvic floor support, makes up the central support "fabric", suspended as it is from the surrounding 'frames' of the pelvis by attachments at two sides (i.e., "paravaginal" support) and the proximal one end (i.e., "apical" support). Its distal end is fused with the levator ani muscle (Level III support).

1.5. A brief historical overview and the present understanding of the mechanisms underlying anterior vaginal wall prolapse.

Pelvic organ prolapse is a remarkably common problem, yet the disease mechanism resulting in its occurrence remains poorly understood. In 1918, Paramore described the support of the vagina as being like a ship in its berth, floating on the water and attached by ropes on either side to a dock (Paramore 1918). The ship is analogous to the vagina, the ropes to the ligaments, and the water to the supportive layer formed by the pelvic muscles. The ropes function to hold the ship (pelvic organs) in the center of its berth as it

rests on the water (pelvic muscles). If, however, the water level were to fall far enough that the ropes would be required to hold the ship without the supporting water, the ropes would all break.

In 1934, Bonney pointed out that the vagina is in the same relationship to the abdominal cavity as the in-turned finger of a surgical glove is to the rest of the glove (Figure 1-4) (Bonney 1934). If the pressure in the glove is increased, it forces the finger to protrude downwards in the same way that increases in abdominal pressure force the vagina to prolapse. Figure 1-5a and Figure 1-5b provide a schematic illustration of this prolapse phenomenon. In Figure 1-5c, the lower end of the vagina is held closed by the pelvic floor muscles, preventing prolapse by constricting the base of the invaginated finger closed. Figure 1-5d shows suspension of the vagina to the pelvic walls. Figure 1-5e demonstrates that spatial relationships are important in the “flap-valve” closure where the suspending fibers hold the vagina in a position against the supporting walls of the pelvis; increases in pressure force the vagina against the wall, thereby pinning it in place. Vaginal support is a combination of constriction, suspension, and structural geometry.

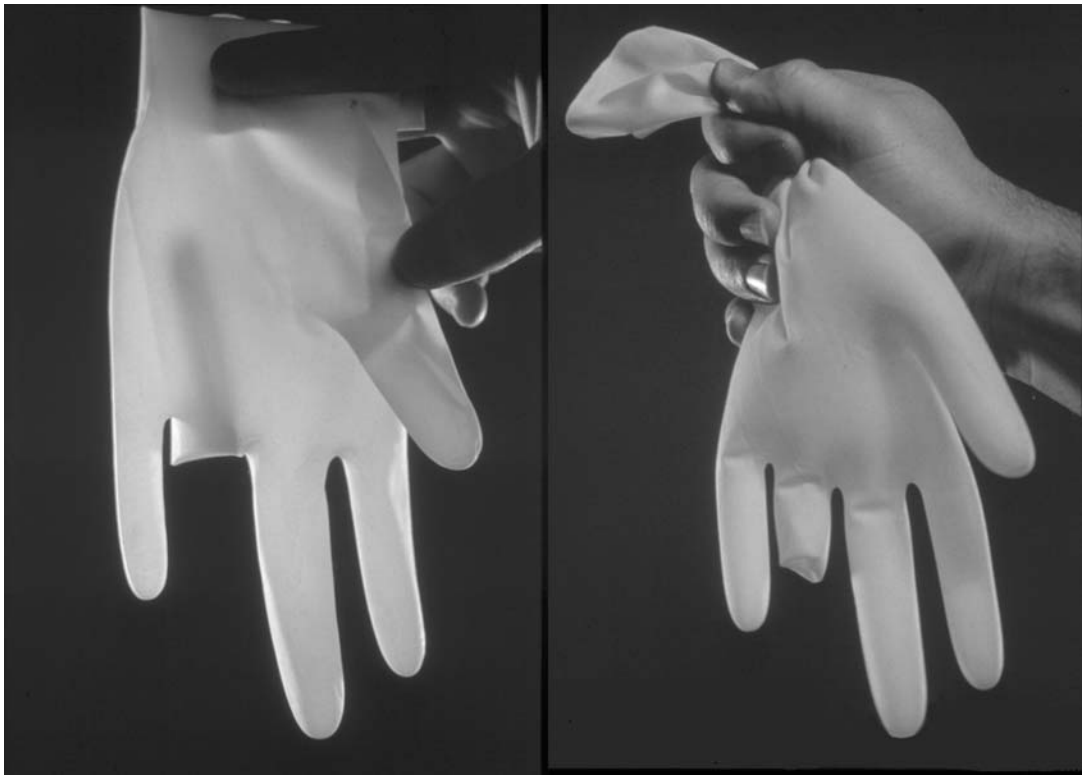

Figure. 1-4. Bonney's analogy of vaginal prolapse. The eversion of an intussuscepted surgical glove finger by increasing pressure within the glove is analogous to prolapse of the vagina © DELANCEY 2002, with permission)

The Ship-in-berth analogy and surgical glove analogy both point out the interaction between levator ani muscle and endopelvic fasica, which is one of the most important biomechanical features of pelvic organ support. However there are no scientific studies of this phenomenon and experiments investigating this interaction and supporting those theories are lacking.

In 2002, at the time this dissertation research was started, there were several competing hypotheses that have been proposed to explain how anterior vaginal wall prolapsed occurs. A first hypothesis involved midline stretching of the vaginal wall, while a second involved peripheral detachment in the paravaginal and apical areas of support to the vaginal wall. The first hypothesis focuses on the stretching of the fibromuscular vaginal tube (fascia) as the disease mechanism of prolapse. This has also been referred to as a distention cystocele (Nichols et al. 1996). The distention cystocele implies that the vagina becomes thin and attenuated in the formation of the cystocele (or

hernia). The other hypothesis focuses more on the connections of the vaginal tube to the pelvic sidewall (Richardson 1976, 1981). When these connections break, a paravaginal defect or a displacement cystocele is thought to occur.(Nichols et al. 1996,Richardson et al. 2000).

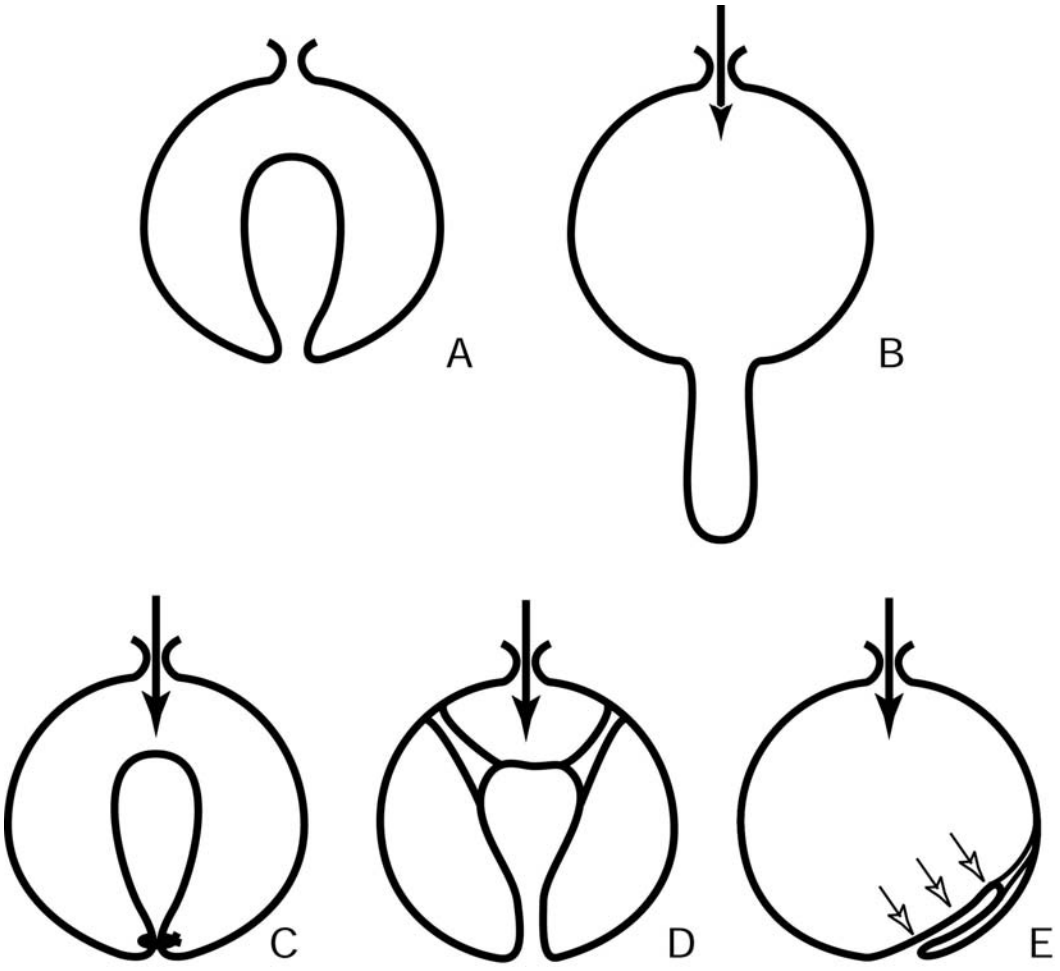

Figure 1-5 . Diagrammatic display of vaginal support. A. Invaginated area in a surrounding compartment; B. The prolapse opens when the pressure (arrow) is increased; C. Closing the bottom of the vagina prevents prolapse by constriction; D. Ligament suspension; E. Flap valve closure where suspending fibers hold the vagina in a position against the wall allowing increases in pressure to pin it in place ©DELANCEY 2002, with permission).

Figure 1-6 shows a systems analsysis model of the extant cystocele formation theories that are supported by scientific studies. Intra-abdominal pressure loaded on anterior compartment causes the tension in the paravaginal supports and vaginal wall

itself. Impairments in paravaginal connective tissue and/or the weakening of anterior vaginal wall result in an abnormal vaginal wall elongation and cause the vagina to bulge based on the geometric constraints provided by the paravaginal attachments.

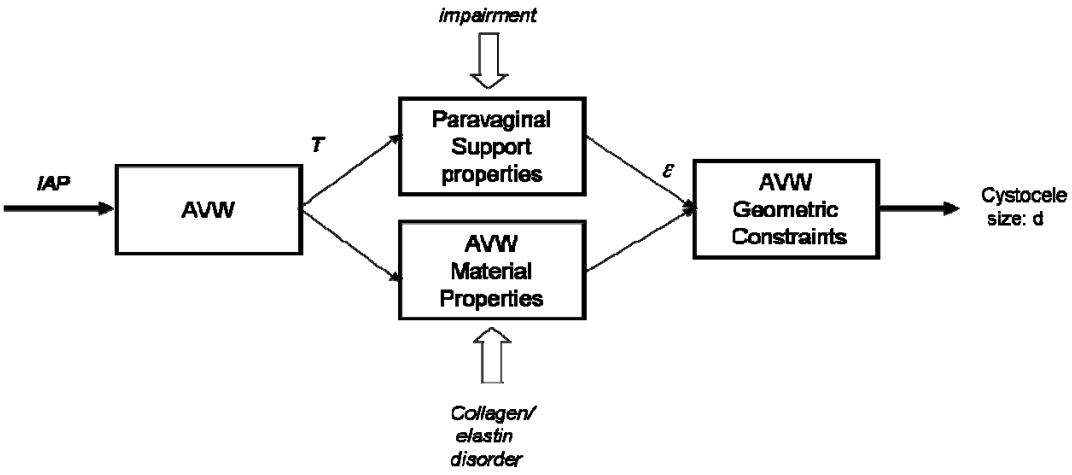

Figure 1-6 The extant understanding of cystocele formation supported by scientific studies.

However, these theories only concentrate on the connective tissue support failure. Levator ani muscle plays an important role in pelvic organ support. A recent study of our group (DeLancey et al. 2007) showed that pubococcygeal muscle (PCM) damage is four times more common in women with prolapse. Neither of these findings can explain this observation. Also, we observed that there are distinguishable vaginal deformation patterns in women with AVP when performing Valsalva (Figure 1-7). Therefore, we hypothesize that the occurrence and magnitude of AVP is not explained by any single mechanism but involves combination of connective tissue support failure at one or more sites, also involving an interaction with pubococcygeal (levator) muscle impairment.

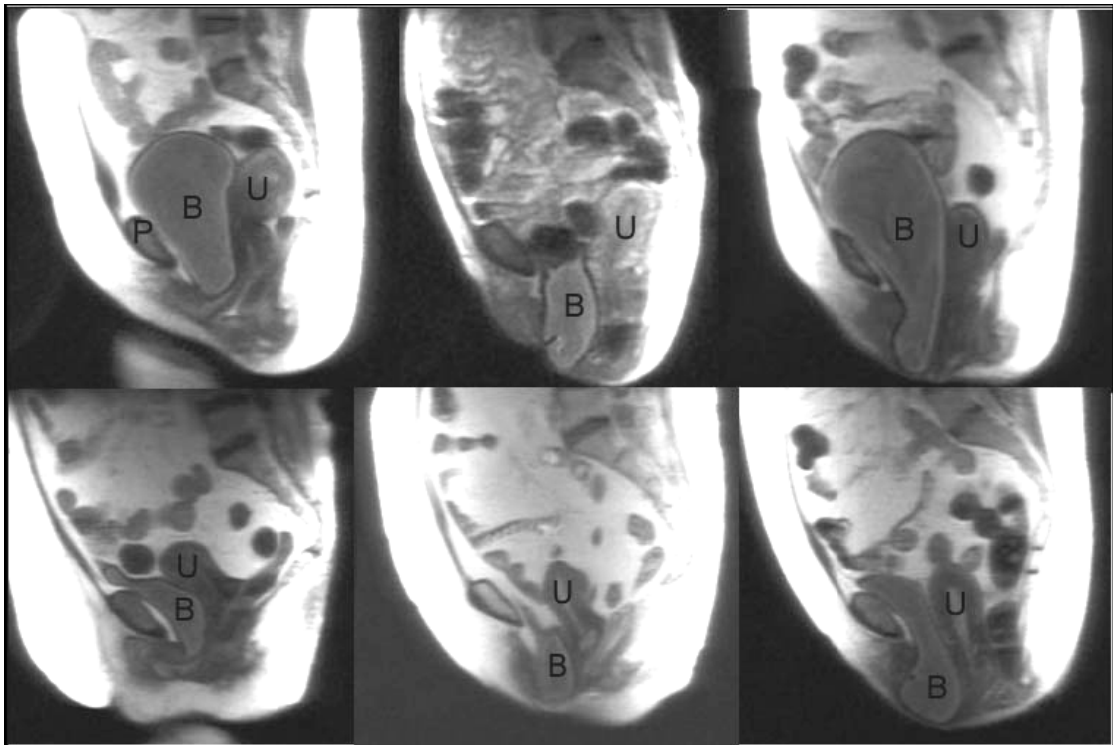

Figure 1-7 Variation between women with AVP (© DeLancey)

1.6 What is the evidence for connective tissue failure in the development of AVP?

The mechanical characteristics of pelvic connective tissue samples taken from women undergoing surgery for prolapse suggest that there may be multiple sites of tissue failure. The shear strength of vaginal wall specimens has been found to be lower in patients with pelvic floor dysfunction than in normal controls (Kondo et al. 1994) and great variability in the tensile and bending strengths of the samples has also been observed (Cosson et al. 2004). The resiliency of the apical support structures, such as the uterosacral ligaments, has also been found to be significantly reduced among women with symptomatic uterovaginal prolapse (Reay et al. 2003). The variation in these studies suggests that there are different sites of failure. Although, in general, each of these studies confirms that women with pelvic floor dysfunction have tissues that, on average, are inferior to control women, there is no single explanation to account for the clinical

variability seen. The proposed AVP mechanism has the potential to build on these finding by considering specific support defects in the vagina or uterosacral ligaments present in an individual woman.

1.7 What is the evidence that suggests levator ani muscle impairment also plays a role in AVP?

That levator ani weakness may be involved in the development of AVP is suggested by a study by DeLancey et al. that showed that the rate of levator ani defect was four-fold higher (DeLancey et al. 2007) and the contraction force developed by the levator ani was 46% lower in women with prolapse compared with controls (Morgan et al.2005). Several other studies have also suggested the clinical importance of levator ani injury. For example, Koelbl et al. (1989) biopsied the region where the levator ani muscle is normally found during surgery on women with cystocele and found a substantial number of women lacking normal muscle at this site. A further study by the same group (Hanzal et al. 1993) showed that 53% of the women who had missing muscle also experienced operative failure, while there were no failures among those with normal muscle on biopsy. These visible manifestations are supported by histological studies revealing muscle fibrosis and evidence of direct myogenic muscle damage among parous and older women. More recently, magnetic resonance (MR) imaging has revealed morphologic and structural changes in the levator ani muscles in women with pelvic floor dysfunction (Tunn et al. 1998, Hoyte et al. 2001, Singh et al. 2003). So, levator ani weakness does appear to be a contributory factor, but the mechanism by which it plays a role remains unclear.

1.8 Hypothesis and Specific Aims

In this dissertation we hypothesize that the occurrence and magnitude of AVP is not explained by any single mechanism but involves combination of connective tissue support failure at one or more anatomic site and also involves an interaction with pubococcygeal muscle impairment. This dissertation involves an approach which

combines measurements in living women, via MR imaging with theoretical biomechanical modeling simulations to test the above hypothesis.

Aim 1: Morphological measurement of anterior vaginal wall support system using MR imaging

There are mainly two purposes for these morphological measurements. The first is to compare the key structural elements' morphology in women with normal support and women with AVP. This includes the anterior vaginal wall support system comprised of the levator ani muscle, the apical and paravaginal support connective tissues, and the anterior vaginal wall. Morphological differences will provide insight into how the AVP patients differ from normal age-matched controls. The other purpose is to establish the average morphology in women with normal support thus providing useful geometric information for biomechanical models (Aim 2).

Aim 2: Biomechanical modeling of AVP

An essential aim of this thesis is to develop biomechanical models of the anterior vaginal wall support system in order to improve the understanding of the mechanism underlying the development of AVP.

The models range from simple, two-dimensional, lumped parameter models to anatomically more accurate finite element models. Biomechanical models can yield powerful insights and are relatively inexpensive, fast and safe to implement. Unlike biological systems in vivo, the model allows one to vary a single factor at a time so that the sensitivity of the system to changes in this factor, or a combination of factors, can be analyzed.

Aim 3. In vivo assessment of the compliance of the anterior compartment and the exploration of more extensive ways to validate model

By incorporating intra-abdominal pressure and structural displacement information, the compliance of the support system can also be estimated. By comparing MR images in the resting and maximum Valsalva states we can explore the feasibility of estimating the deformation field under load using a non-rigid 3-D image registration method and the possibility of using this information to validate the biomechanical model developed in Aim 2.

Hence the overall goal of this dissertation is to try to understand the biomechanical mechanisms underlying the development of anterior vaginal wall prolapse in women.

References

Bonney, V. The principles that should underlie all operations for prolapse. Obstet Gynaecol Br Emp 1934;41: 669.

Boyles SH, Weber AM, Meyn L. Procedures for pelvic organ prolapse in the United States, 1979-1997. Am J Obstet Gynecol. 2003 Jan;188(1):108-15

Boyles SH, Weber AM, Meyn L. Procedures for urinary incontinence in the United States, 1979-1997. Am J Obstet Gynecol 2003;189:·70-5.

Cosson M, Lambaudie E, Boukerrou M, Lobry P, Crépin G, Ego A. A biomechanical study of the strength of vaginal tissues. Results on 16 post-menopausal patients presenting with genital prolapse. Eur J Obstet Gynecol Reprod Biol. 2004 Feb 10;112(2):201-5.

DeLancey JO, Morgan DM, Fenner DE, Kearney R, Guire K, Miller JM, Hussain H, Umek W, Hsu Y, Ashton-Miller JA. Comparison of levator ani muscle defects and function in women with and without pelvic organ prolapse. Obstet Gynecol. 2007 Feb;109(2 Pt 1):295-302.

Hanzal E, Berger E, Koelbl H. Levator ani muscle morphology and recurrent genuine stress incontinence. Obstet Gynecol 1993;81:426-9.

Hendrix SL, Clark A, Nygaard I, Aragaki A, Barnabei V, McTiernan A. Pelvic organ prolapse in the Women's Health Initiative: gravity and gravidity. Am J Obstet Gynecol. 2002 Jun;186(6):1160-6

Hoyte L, Ratiu P. Linear measurements in 2-dimensional pelvic floor imaging: the impact of slice tilt angles on measurement reproducibility. Am J Obstet Gynecol

2001;185:537-44.

Jørgensen S, Hein HO, Gyntelberg F. Heavy lifting at work and risk of genital prolapse and herniated lumbar disc in assistant nurses. Occup Med (Lond). 1994 Feb;44(1):47-9.

Kearney R, Miller JM, Ashton-Miller JA, DeLancey JOL. Obstetric factors associated with levator ani muscle injury after vaginal birth. Obstet Gynecol. 2006; 107(1): 144-9.

Koelbl H, Strassegger H, Riss PA, Gruber H. Morphologic and functional aspects of pelvic floor muscles in patients with pelvic relaxation and genuine stress incontinence. Obstet Gynecol 1989;74:789-95.

Kondo A, Narushima M, Yoshikawa Y, Hayashi H. Pelvic fascia strength in women with stress urinary incontinence in comparison with those who are continent. Neurourol Urodynam 1994;13:507-13.

Lien KC, Mooney B, DeLancey JO, Ashton-Miller JA. Levator ani muscle stretch induced by simulated vaginal birth. Obstet Gynecol 2004;103:31-40.

Lien KC, Morgan DM, DeLancey JO, Ashton-Miller JA. Pudendal nerve stretch during vaginal birth: a 3D computer simulation. Am J Obstet Gynecol. 2005 May;192(5):1669-76.

Lawson JO. Pelvic anatomy. I. Pelvic floor muscles Ann R Coll Surg Engl 1974;54:244-52.

Mant J, Painter R, Vessey M. Epidemiology of genital prolapse: Observations from the Oxford Family Planning Association Study. Br J Obstet Gynaecol 1997;104:579–85.

Morgan DM, Kaur G, Hsu Y, Fenner DE, Guire K, Miller J, Ashton-Miller JA, DeLancey JOL. Does vaginal closure force differ in the supine and standing positions?

American J Obstet and Gynecol. May 2005; 192(5):1722-1728

Nichols DH, Randall CL. Vaginal surgery. 4th ed. Baltimore (MD): Williams & Wilkins; 1996.

Olsen AL, Smith VJ, Bergstrom JO, Colling JC, Clark AL. Epidemiology of surgically managed pelvic organ prolapse and urinary incontinence Obstet Gynecol. 1997 Apr;89(4):501-6

Paramore, R. H.: The uterus as a floating organ. In: The statics of the female pelvic viscera. H.K. Lewis and Co. Ltd, London: p. 12, 1918.

Reay Jones NH, Healy JC, King LJ, Saini S, Shousha S, Allen-Mersh TG. Pelvic connective tissue resilience decreases with vaginal delivery, menopause and uterine prolapse. Brit J Surg 2003;90:466-72.

Richardson AC, Lyon JB, Williams NL. A new look at pelvic relaxation. Am J Obstet Gynecol 1976;126:568–73.

Richardson AC, Edmonds PB, Williams NL. Treatment of stress urinary incontinence due to paravaginal fascial defect. Obstet Gynecol 1981;57:357–62.

Richardson AC. Paravaginal repair. In: Hurt WG, editor. Urogynecologic surgery. 2nd ed. Philadelphia (PA): Lippincott Williams & Wilkins; 2000. p. 71–80

Sze EH, Karram MM. Transvaginal repair of vault prolapse: a review. Obstet Gynecol 1997;89:466-75.

Shull BL, Bachofen C, Coates KW, Kuehl TJ. A transvaginal approach to repair of apical and other associated sites of pelvic organ prolapse with uterosacral ligaments. Am J

Obstet Gynecol 2000;183:1365-73.

Singh K, Jakab M, Reid WM, Berger LA, Hoyte L. Three-dimensional magnetic resonance imaging assessment of levator ani morphologic features in different grades of prolapse. Am J Obstet Gynecol 2003;188:910-915.

Tunn R, DeLancey JOL, Howard D, Thorp JM, Ashton-Miller JA, Quint LE. MR Imaging of levator ani muscle recovery following vaginal delivery. Int Urogynecol J 1999;10:300-7.

Weber AM, Walters MD, Piedmonte MR, Ballard LA. Anterior colporrhaphy: a randomized trial of three surgical techniques. Am J Obstet Gynecol 2001;185:1299-304; discussion 1304-6.

Chapter 2

Cross-sectional Area Measurement of Levator Ani Muscle in women with and without prolapse

2.1 Introduction

Despite the prevalence of the problem, the disease mechanism responsible for organ prolapse is still not fully understood. However injury and deterioration of muscle, nerve and connective tissue are believed to play a role in altering normal pelvic organ function and predicposing to prolapsed (for example, Boreham et al, 2002, Takano et al, 2002, Smith et al, 1989).

There is also a growing body of evidence that the levator ani muscles are important to pelvic organ support. Magnetic resonance (MR) imaging reveals levator ani muscle morphology. A visible defect in the pubic portion of the levator ani can be seen in 18% of primiparous women six months after vaginal delivery (DeLancey et al, 2003, Dietz et al, 2005, Kearney et al, 2006), and these types of defect have been found in women with pelvic floor dysfunction (Kirschner-Hermanns et al, 1993, Tunn et al, 1998, Hoyte et al, 2001, Singh 2003). The iliococcygeal portion is less commonly affected (in only 2% of women, DeLancey et al, 2003). The pubic portion contains muscle fibers that originate from the pubic bone and include the pubovisceral muscle and puborectal muscle (Kearney et al, 2004). Despite the association between prolapse and levator damage,

there are women with prolapse who do not have levator damage and women with normal support who do have levator damage. This has led some investigators to quantify levator ani muscle bulk to see if this explains the discrepancy.Several techniques have been used

to quantify muscle bulk and therby loss in muscle bulk. For example, Hoyte measured the distance from the pubic bone to the remaining muscle (Hoyte et al, 2001) as well as muscle thickness (Hoyte et al, 2004). Levator ani muscle volume has also been quantified (Fielding et al, 2000, Hoyte et al, 2001). Our group has assessed the degree of muscle damage visible in 2-D images (Kearney et al. 2006). This later technique focused on the amount of muscle missing but did not quantify how much muscle remains. Thus, despite a levator injury, a woman who started off with a larger muscle may end up with the same amount of muscle as a woman who inherently had smaller muscles. While comparing muscle volume provides useful information about muscle loss, muscle volume does not correlate as well with force because, although a longer parallel fibered muscle of a given cross-sectional area has a larger volume, it will not develop more force than a shorter muscle parallel-fibered muscle of the same cross-sectional area. The maximum force developed by striated muscle is related to its cross-sectional area measured perpendicular to muscle fiber direction and has been measured to be between 4 and 8 Kg/cm2 (Ikai et al, 1968, 1970). Therefore cross-sectional area measurement perpendicular to muscle fiber direction, rather than muscle volume, is the appropriate way to relate muscle morphology to function.

The levator ani muscle has a complex shape with fibers running in multiple directions. In particular, the muscle fibers in the pubic portion of the levator ani muscle run in a different direction than those in the iliococcygeal muscle (Lawson et al, 1974, Kearney et al, 2004, Singh et al, 2002). Therefore, the two regions must be separated prior to measurements of cross-sectional area perpendicular to the fiber direction. The muscle fibers in these regions also do not run perpendicular to standard axial, coronal or sagittal MR scan planes, so cross-sectional area measurements cannot be properly performed on

standard 2-D images.

2.2 Materials & Methods:

We first developed a method for quantifying the cross-sectional area of pubic portion of the levator ani muscle perpendicular to its muscle fiber direction. Then, the method was used to quantify the loss in cross-sectional area in women with unilateral levator ani defects where normal and abnormal muscle could be seen in the same individual. We then used this technique to investigate the extent of the muscle loss at different locations along the length of the muscle and also validate the technique's ability and sensitivity to detect muscle defects. The null hypotheses were tested that there would be no difference in (a) cross-sectional area between the defect and normal sides, nor (b) in the cross-sectional area along the length of the muscle.

Then we applied this 3-D technique to women with and without muscle defect and prolapse to test the hypotheses that levator ani cross-sectional area would not vary with defect severity as identified on MR scans. We also tested the hypothesis that these cross-sectional areas would not differ in women with normal support from those with pelvic organ prolapse.

2.2.1 Develop and validate measurement technique on women with unilateral levator ani muscle defect

2.2.1.1 Unilateral levator ani muscle defect study group

A convenience sample of twelve women with a unilateral levator ani muscle defect were selected from an IRB-approved study comparing muscle anatomy in women with prolapse and women with normal pelvic organ support. The prolapse patients were recruited through the University of Michigan Urogynecology Clinic. The controls were recruited through advertisements as well as through the Women's Health Registry; a list of women who expressed interest in participating in women's health projects. Patients

were excluded if they had previous surgery for prolapse or incontinence, genital anomalies, or had delivered in the past year. Patients were enrolled between June, 2001 and September, 2003. Women with visible unilateral defects in the pubic portion of the levator ani muscle on MR images were selected so that, within the same individual, normal muscle morphology on one side could be compared with abnormal muscle morphology on the other side (Figure 2-1). This circumvents inter-individual differences in muscle appearance and bulk. These women represented both individuals with prolapse and normal support.

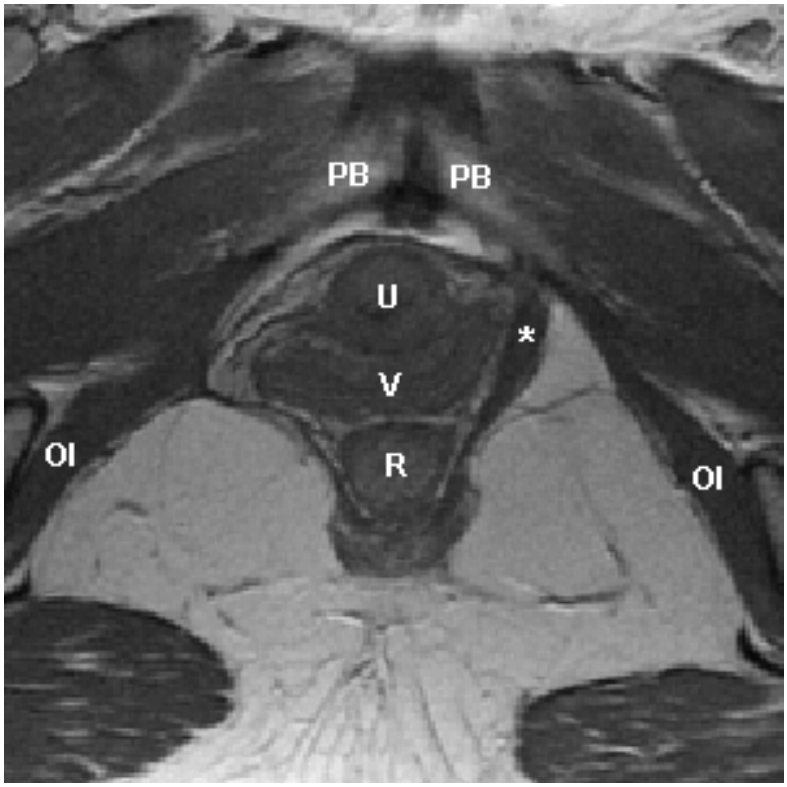

Figure 2-1: Axial proton density MR image of a woman with a right unilateral defect. The left levator ani muscle is intact (denoted by *) while the right side portion of the muscle is missing. PB denotes pubic bone; U: urethra; V: vagina; R: Rectum; OI: obturator internus muscle.

In the 12 women selected, five had prolapse of one vaginal wall or a cervix at least 1 cm below the hymen and seven had normal support of all pelvic structures with no vaginal wall lower than 1 cm above the hymen as assessed by clinic evaluation (POP-Q) (Bump et al, 1996). The average age was 56.2 ± SD 11.9 years and average BMI was 27.3 ± SD 4.0 Kg/m^2. Parity was 3.15± SD 1.77. Ten additional women with normal

intact levator ani muscle on MRI were selected as control group to validate the method. Five had prolapse and five had normal pelvic organ support. The average age was 62.5 ± SD 3.34 years and average BMI was 27.5 ± SD 5.0 Kg/m^2. Parity was 2.8± SD 1.75.

To compare the normal and defective sides, we first separated the levator ani in the midline. Each side was then designated as either "normal" or "defective". Within 12 women, five had defective muscle on left side and seven had defective right side muscle.

2.2.1.2 Model reconstruction

Multiplanar, two-dimensional, fast spin, proton density MR images (echo time 15 ms, repetition time 4000 ms) were obtained by use of a 1.5 T superconducting magnet (General Electric Signa Horizon LX) with version 9.1 software. The fields of view of axial and coronal images were both 16×16 cm and the field of view in sagittal images was 20×20 cm. All three views had slice thicknesses of 4 mm with a 1 mm gap between slices.

Axial, sagittal and coronal MR-images were imported into a three-dimensional (3-D) imaging program (3-D Slicer, version 2.1b1) and aligned using anatomic landmarks (arcuate pubic ligament, pubic bone, pubic symphysis, etc). To reduce modeling artifacts from partial volume averaging of oblique structures on a single scan plane, 3-D volume-rendering models were generated by combining models built from axial and coronal planes. The combined models were imported into I-DEAS version 9.0 (EDS, Plano, TX), an engineering graphics program (Figure 2-2A).

A mirrored model of the normal muscle (dashed outline) was superimposed on the contralateral defective side to visualize the area of missing muscle (Figure 2-2B). Volumes of the overall levator ani muscle including both the pubic portion and iliococcygeal portion on the normal and defective sides were calculated in I-DEAS ®.

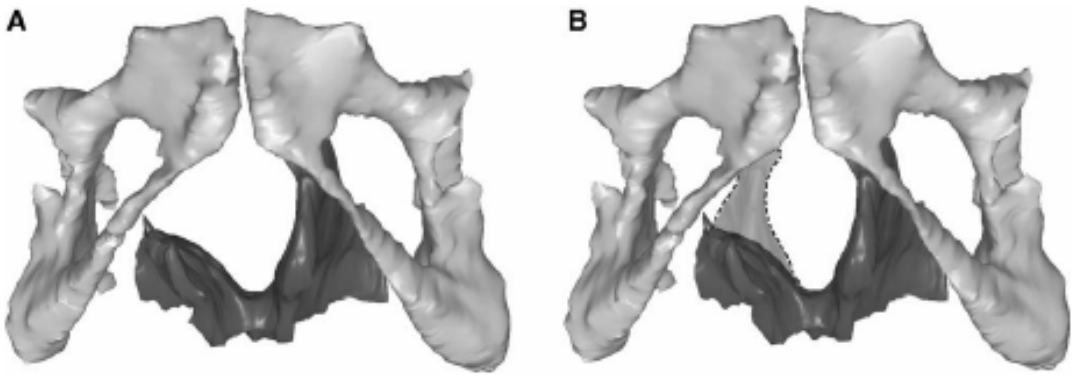

Figure 2-2. Reconstructed 3-D model showing the pubic bone and levator ani muscle with a right unilateral defect (A). In B, the dashed region shows the expected location of the missing muscle after reflecting the muscle from the normal across the midline side.

2.2.1.3 Separate pubic portion of levator ani muscle

The pubic portion of the levator ani muscle was separated from the iliococcygeal portion by establishing a dividing plane through three anatomical landmarks that could be identified independent of whether or not there was a defect in the levator ani. The middle landmark was defined as the upper aspect of the puborectalis "bump" on the mid-sagittal slice (Figure 2-3a). Two lateral landmarks for the plane were defined as the most medial origin of the iliococcygeus from the arcus tendineus levator ani (ATFP). As the ATFP directly overlies the obturator internus muscle, the point of connection of the iliococcygeal and the obturator internus on the left and the right sides was used as the landmark (Figure 2-3b & c). All landmarks were imported into the I-DEAS based model. The levator ani muscle was then divided into a pubic portion and an iliococcygeus portion on both normal and defective sides by a plane constructed using the landmarks described above (Figure 2-4). The volumes were calculated for each portion of the muscle.

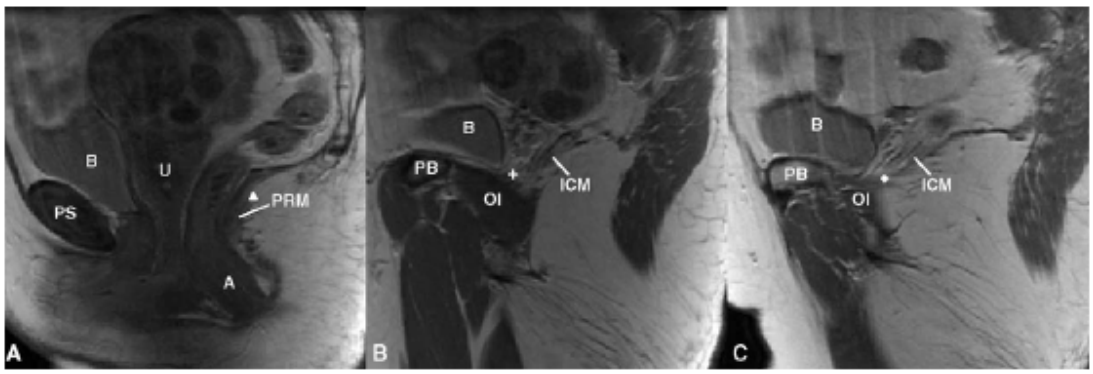

Figure 2-3. Separating the pubic portion of levator ani from the iliococcygeus portion on MR scans. a): identification of the middle point (triangle) on the mid-sagittal MR image; b & c): identification of the two lateral points on MR image (cross and diamond). The following structures were identified in MR image to help for orientation. PS: pubic symphysis; PB:pubic bone; B: bladder; A: anus; OI: oburator internus; U:uterus (with fibroids); PRM: puborectalis muscle. ICM: iliococcygeus muscle

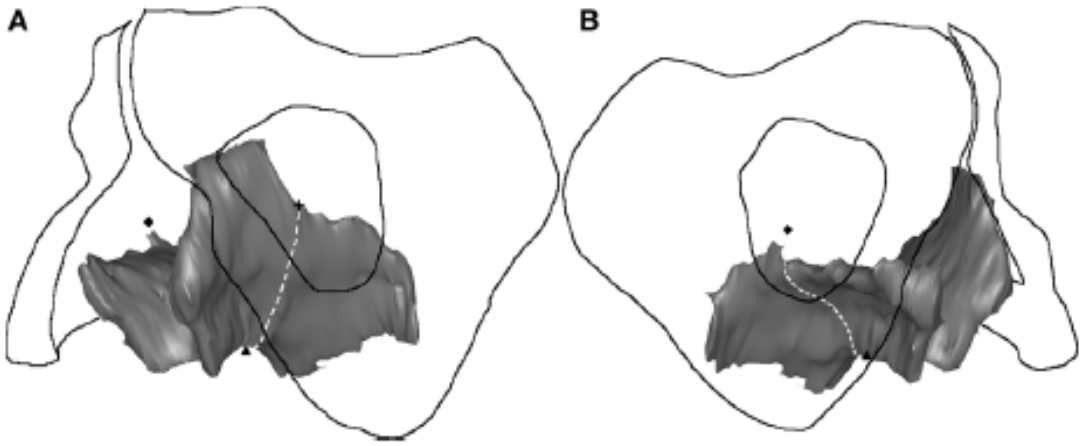

Figure 2-4: 3-D view of the separation of the pubic portion from the iliococcygeal portion of the levator ani. The dashed line represents the plane of separation, while the triangle, cross and diamond have the same meaning as in the preceding figure.

2.2.1.4 Identify muscle fiber direction

Although there is evidence that the pubic portion of the levator ani has a parallel-fibered morphology (Janda et al, 2003), its muscle fiber direction is not directly

observable on the MR scans, so it was approximated by establishing a line between the middle of the origin point and the center of the insertions using anatomic landmarks independent of muscle presence or absence. The muscle origins were defined in axial MR images as lying 1.5 cm above the arcuate pubic ligament, and 0.2 cm medial from the obturator internus insertion on the left and right pubic rami, based on the senior author's dissection and MR imaging experience (Strohbehn et al, 1996). The insertion points were defined in the sagittal plane as the center of the intersphincteric groove on slices 0.5 cm lateral to the mid-sagittal slice on either side (Figures 2-5 & 2-6).

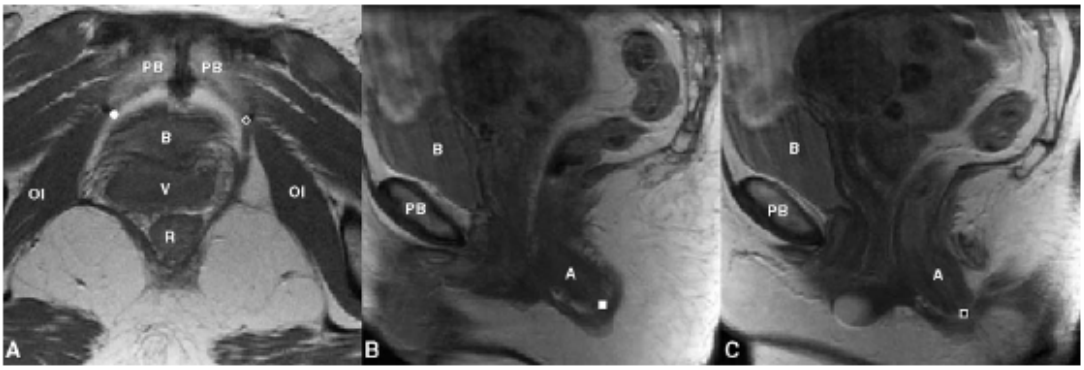

Figure 2-5. Reference points for determining fiber direction in the pubic portion of the levator ani. a) Origin points on axial MR image at its junction with obturator internus (OI) as open circle on patient's left and filled circle on patient's right; b&c) Right (filled square) and left (open square) insertion point on sagittal MR scans. The following structures are identified aid orientation. PB: pubic bone; B: bladder; V: vagina; R: rectum; A: anus

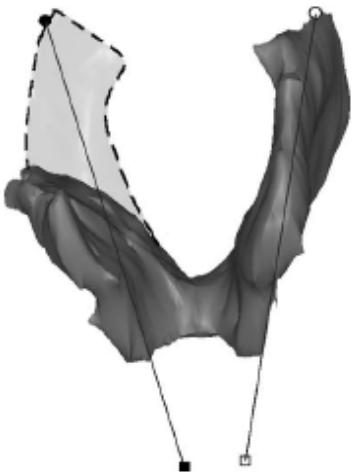

Figure 2-6. Lines connecting the origin and insertion points (see preceding figure) were used to estimate muscle fiber direction. The dashed region shows the expected location of the muscle on the defective side, were it intact.

2.2.1.5 Calculate muscle cross-sectional area

Using I-DEAS, five equally-spaced cross-sectional 'cutting' planes were passed perpendicular to the fiber direction line. The resulting cross-sections were numbered from '1' at the pubic origin to '5' at the insertion end (Figure 2-7). Since location 5 lay dorsal to the edge of the muscle with the defect, the cross-sectional areas were only calculated bilaterally from locations 1 to 4. Figure 2-7 shows a graphical demonstration of the sequence of steps used to quantify the unilateral levator ani muscle loss. Two-sided paired t-tests were used to compare for bilateral differences in cross-sectional area and volume.

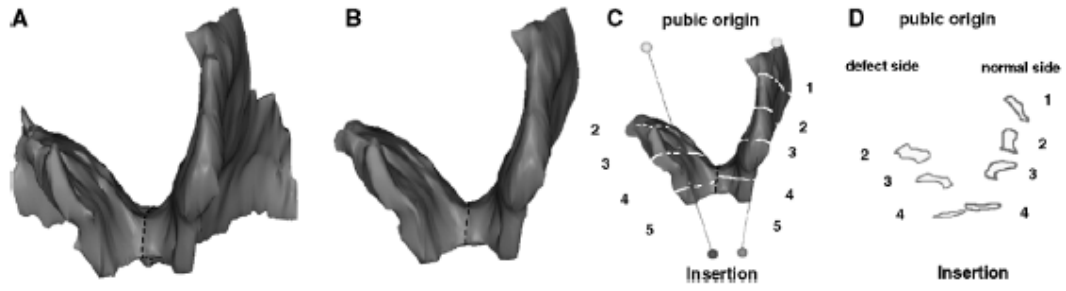

Figure 2-7. Steps to quantify levator ani muscle loss in a subject with a unilateral defect. A: Frontal view of the 3-D reconstruction model of levator ani was built. B: The pubic portion is separated from the iliococcygeal portion; here only the pubic portion is shown. C: The line of estimated fiber direction of the pubic portion was determined. Equally-spaced cutting planes perpendicular to the fiber direction line were placed. D: The resulting cross-sections are shown. Cross-sectional areas were then calculated. Due to the defect on the right, muscle is not present at location 1, therefore, it is not shown.

One might hypothesize that the fiber direction of the remaining muscle could change due to the presence of the defect and the use of the normal fiber direction may cause some error in estimation of the cross-sectional area of the remaining muscle. We therefore performed additional analysis by approximating the defect muscle direction by curving and rotating the normal muscle fiber direction line to best fit the remaining muscle model. We then estimated the degree of error by calculating the cross-sectional area perpendicular to remaining muscle fiber direction and comparing it with the normal fiber direction by using a paired t- test (Figure 2-8).

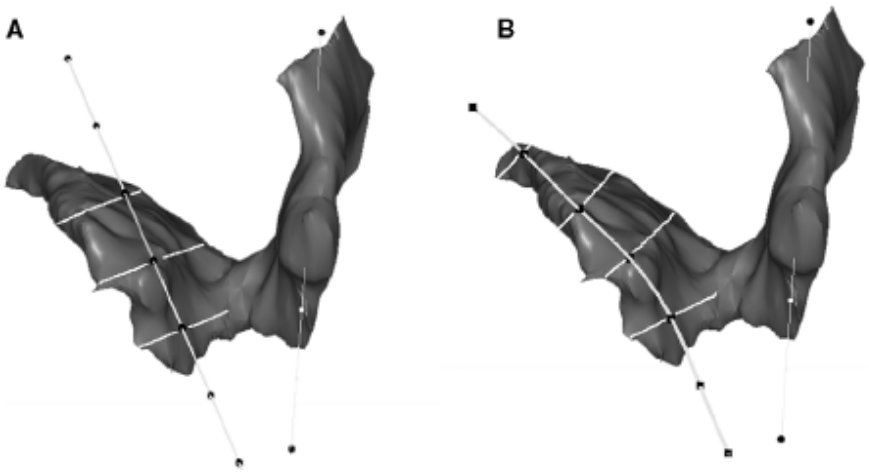

Figure 2-8 A: Cross-sectional area perpendicular to normal muscle direction; B: Cross-sectional area perpendicular to remaining muscle direction.

2.2.2 Quantify muscle cross-section loss in women with and without prolapse

To perform this analysis, sixty subjects were selected from an ongoing IRB-approved case-control study comparing findings in women with normal support to women with pelvic organ prolapse between November 2000 and April 2005. Of these, 30 women had pelvic organ prolapse as demonstrated by a vaginal wall or the cervix being at least 1 cm beyond the introitus upon supine examination during maximal Valsalva. Thirty controls, who had normal support with vaginal wall and cervix 1 cm or more above the hymen were also selected for analysis. In both the prolapse and control group, women were selected from the parent study with 10 having "no levator ani defects", 10 having "minor" defects and 10 having "major" defects (see below). Patients were selected such that the mean age of each group would be similar. Subjects were all Caucasian with the exception of one African-American woman. For the parent study, women with prolapse had been recruited from the University of Michigan Urogynecology Clinic while controls were women recruited through advertisements, as well as through the Women's Health Registry, a database of women who expressed interest in participating in women's health projects. Women were excluded if they had previous surgery for prolapse or incontinence, had genital anomalies, or had delivered in the past year.

The severity of the defect in the pubovisceral portion of the levator ani muscle

was determined using MR images and a visual scoring system 6. Defects were scored on each side as "0" = no defect, "1" = less than 50% loss, "2" = more than 50% loss and "3" = loss of all significant muscle (Figure 2-9). Scores from both sides were added together for a summed score ranging from 0 to 6. Summed scores were then grouped into three categories: 0 = no defect; 1-3 = minor defect; and 4-6 = major defects as previously described (Kearney et al, 2006).

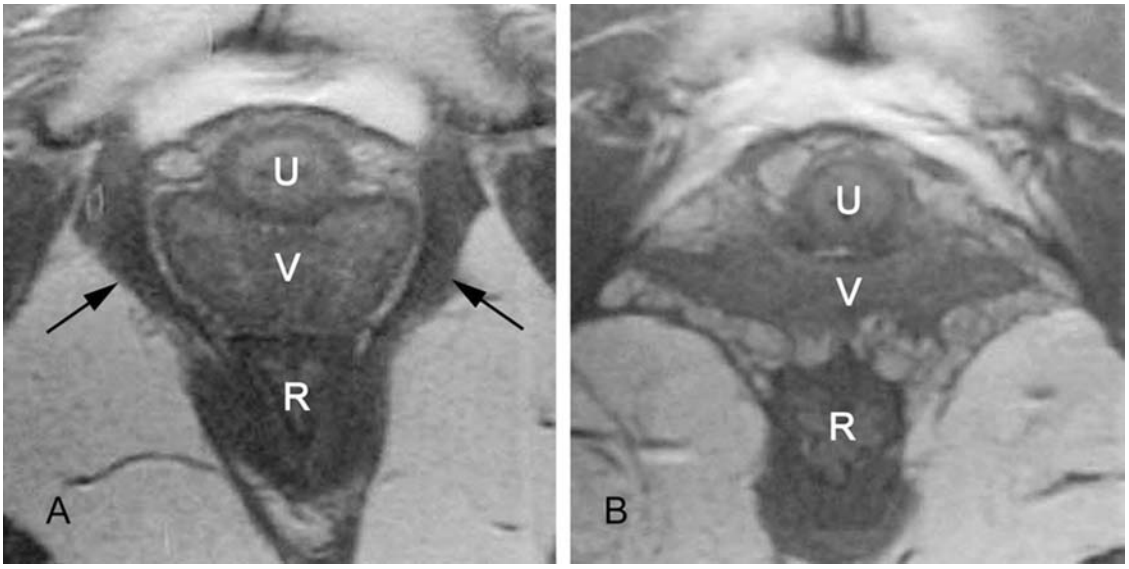

Figure 2-9 Axial MR images showing the levator ani. a: intact pubovisceral muscle bilaterally as demonstrated by arrows; b: complete loss of bilateral muscles. © DeLancey 2006

Using the same technique described earlier, axial, sagittal, and coronal MR images were imported into a 3-D imaging program (3-D Slicer, version 2.1b1, Brigham and Women's Hospital, Boston, MA) and aligned using anatomic landmarks. 3-D volume-rendering models were generated from axial and coronal planes (Figure 2-10) and then imported into I-DEAS® version 9.0 (UGS, Plano, TX), an engineering graphics program to perform measurements.

The muscle fiber direction was approximated by establishing a line between the middle of the origin point and the center of the insertions using anatomic landmarks described earlier. Using I-DEAS®, cross sectional areas of the pubic portion were calculated perpendicular to a fiber direction line from the pubic origin to the middle of the visceral insertion at 17 equidistant points (Figure 2-11). One-way ANOVA was performed; $P<0.05$ was considered significant. A power calculation was not possible at

the beginning of the study since no data were available concerning these measurements. Therefore, a post-hoc power calculation was performed.

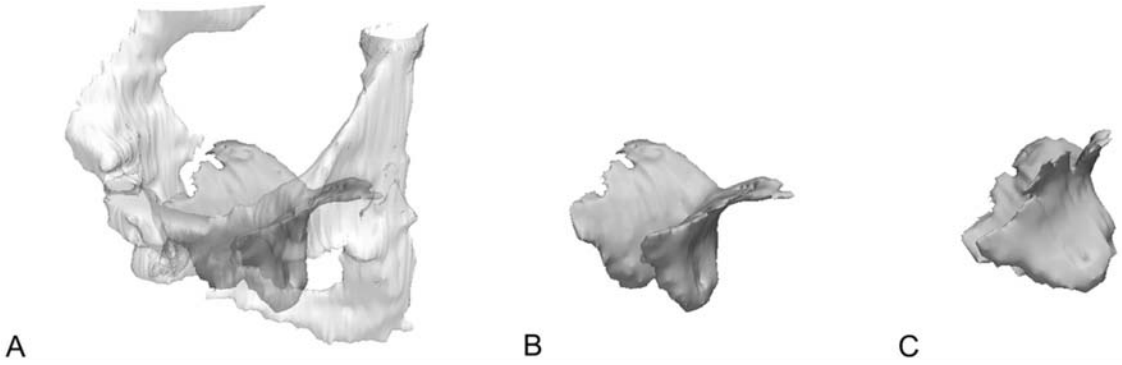

Figure 2-10 3-D Slicer models. a: ¾view of the levator ani muscle and pubic bone; b: levator ani with pubic bones removed; c: lateral view of muscle. © DeLancey 2006

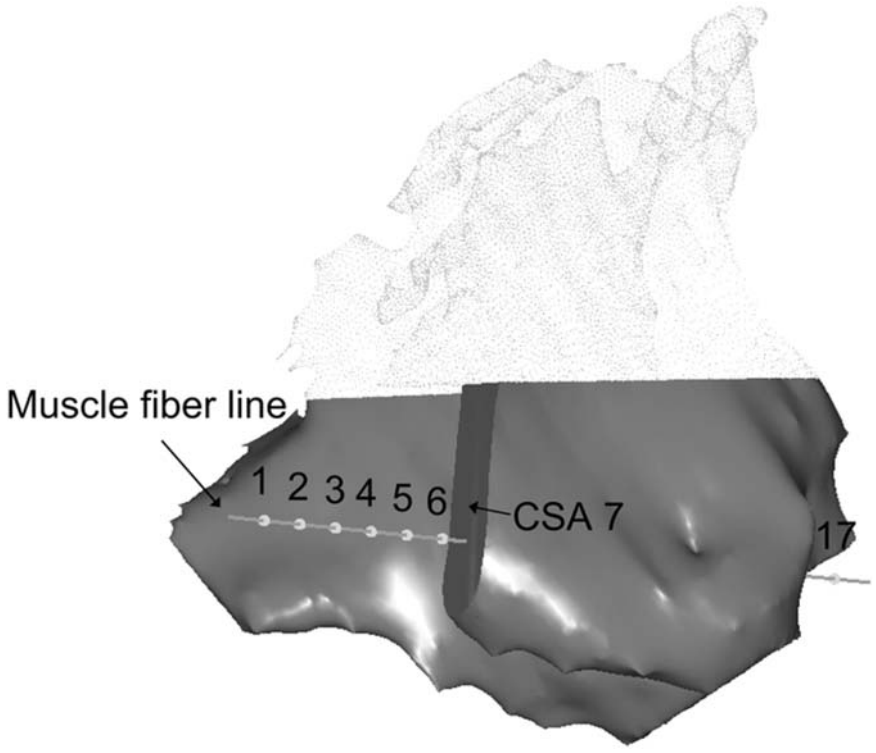

Figure 2-11: Levator model and cross-sections. Fiber direction line for the left side of pubic portion of levator ani muscle is shown. The locations of cross-section areas (CSA) are shown and numbered 1 (most ventral) to 17 (most dorsal). The model has been cut at CSA 7. CSA 8 to 16 are not numbered in the figure. © DeLancey 2006

2.3 Results

2.3.1 Results for women with unilateral levator ani muscle defect

In the women with normal levator ani muscle, there is no significant difference between left and right cross-sectional areas at any location (Table 2-1).

Table 2-1: Comparison of mean ± standard error cross-sectional area (CSA) in cm2 of left and right side in ten women with normal muscle.

	Locatio n 1	Locatio n 2	Locatio n 3	Locatio n 4
CSA of left side (cm^2)	1.30 ± 0.20	2.26 ± 0.15	2.84 ± 0.11	2.62 ± 0.21
CSA of right side (cm^2)	1.20 ± 0.25	2.23 ± 0.17	2.71 ± 0.14	2.74 ± 0.19
P-value	0.43	0.84	0.35	0.42

In the women with a unilateral defect, the defective side had a significantly smaller muscle cross-sectional area at each location in the pubic portion of the levator ani (Figure 2-12). However, the extent of the cross-sectional area loss differed depending on location. The largest mean cross-sectional area loss (81%, P=0.0002) was near the pubic origin (location 1), while near the insertion (location 4) the loss in mean cross-sectional area was not statistically significant (13.5%, P=0.1987).

There was not a statistically significant difference in the cross-sectional areas calculated using the “normal” fiber direction compared to the approximated remaining fiber direction (Table 2-2), thereby validating the use of the “normal” fiber direction on the defective side.

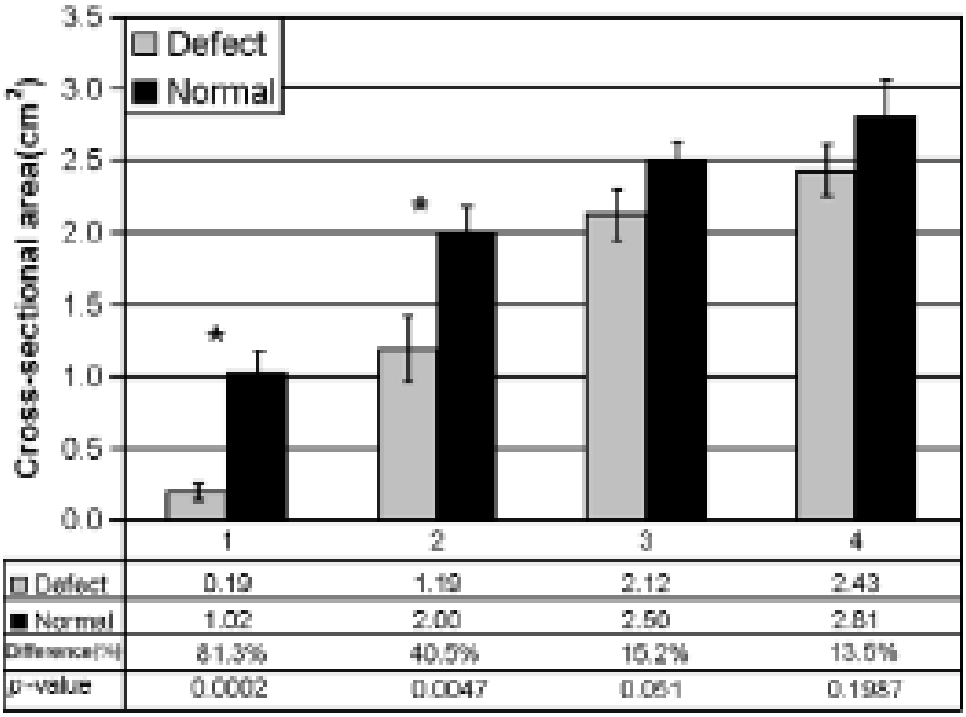

Figure 2-12. Bilateral comparison of muscle cross-sectional area of pubic portion of levator ani muscle perpendicular to its fiber direction. Bars are standard error and * denotes $p<0.05$.

Table 2-2: Comparison of mean ± standard error cross-sectional area (CSA) in cm2 calculated using "normal" fiber direction with that calculated using remaining fiber direction.

	Location 1	Location 2	Location 3	Location 4
CSA perpendicular to 'normal' muscle direction	0.19 ± 0.06	1.19 ± 0.23	2.12 ± 0.19	2.43 ± 0.18
CSA perpendicular to remaining muscle direction	0.24 ± 0.10	1.15 ± 0.20	2.09 ± 0.20	2.31 ± 0.20
P-value	0.24	0.33	0.60	0.42

The overall volume of the levator muscle was 13.69% smaller on the defective

side(17.96 ± 1.4 cm^3) than on the normal side (20.81± 1.35 cm^3 , P=0.0004). This was primarily attributable to a reduction in the pubic portion of levator ani muscle (defective side: 9.16 ± 0.83 cm^3 normal side: 12.19 ± 0.71 cm^3, a 24.6% volume reduction, P<0.0001), while the iliococcygeal portions were not significantly different (defective side: 8.80 ± 1.25 cm^3; normal side: 8.62 ± 1.12 cm^3, P<0.0001P=0.64).

2.3.2 Results for women with and with prolapse

Patient demographics are presented in Table 2-3. There was no significant difference in BMI between women with and without prolapse (mean BMI: prolapse=27.16 kg/m^2, controls=25.92 kg/m^2, P-value = 0.2689). The max POP-Q point is also shown which represents the most dependent vaginal wall point. All patients with prolapse were Stage II or greater. Of the 30 patients with prolapse, the majority had anterior compartment prolapse (N=25) while three patients had posterior compartment prolapse and two had apical prolapse.

Table 2-3: Patient demographics (mean ± SEM values).

Defect status	Group status	Age (year)	Vaginal parity	BMI (kg/m^2)	Max POP-Q(cm)
None	**Normal**	63 ± 2.4	2.8 ± 0.3	23.7 ± 0.6	-1.2 ± 0.1
	Prolapse	62 ± 3.1	2.7 ± 0.5	29.5 ± 1.4	+1.9 ± 0.4
Minor	**Normal**	60.6 ± 2.5	2.5 ± 0.6	25.9 ± 1.5	-1.5 ± 0.2
	Prolapse	61.5 ± 1.9	4.6 ± 0.7	25.3 ± 1.1	+2.6 ± 0.3
Major	**Normal**	60.4 ± 2.8	2.9 ± 0.5	28.2 ± 1.3	-1.2 ± 0.1
	Prolapse	62.3 ± 3.5	3.7 ± 0.7	26.7 ± 1.4	+2.5 ± 0.5

The mean cross-sectional areas at each location are shown in Figure 2-13. In locations (2 - 7), the women with major defects had the smallest cross-sectional area, followed by those with minor defects. These cross-section locations represent where the muscle originates from the pubic bone. We designated locations 2-10 as the ventral portion of the muscle based their locations on our 3-D models. The mean (± SEM)

cross-sectional area values for areas 2 – 10 taken as a group were as follows: no defects, 2.04 cm^2 ± 0.16; minor= 1.44 cm^2 ± 0.11; and major= 1.30 cm^2 ± .12 ($p < .001$). A post-hoc power calculation revealed that the current sample size had 96% power to detect a cross-sectional area difference between the different defect status groups in the ventral portion.

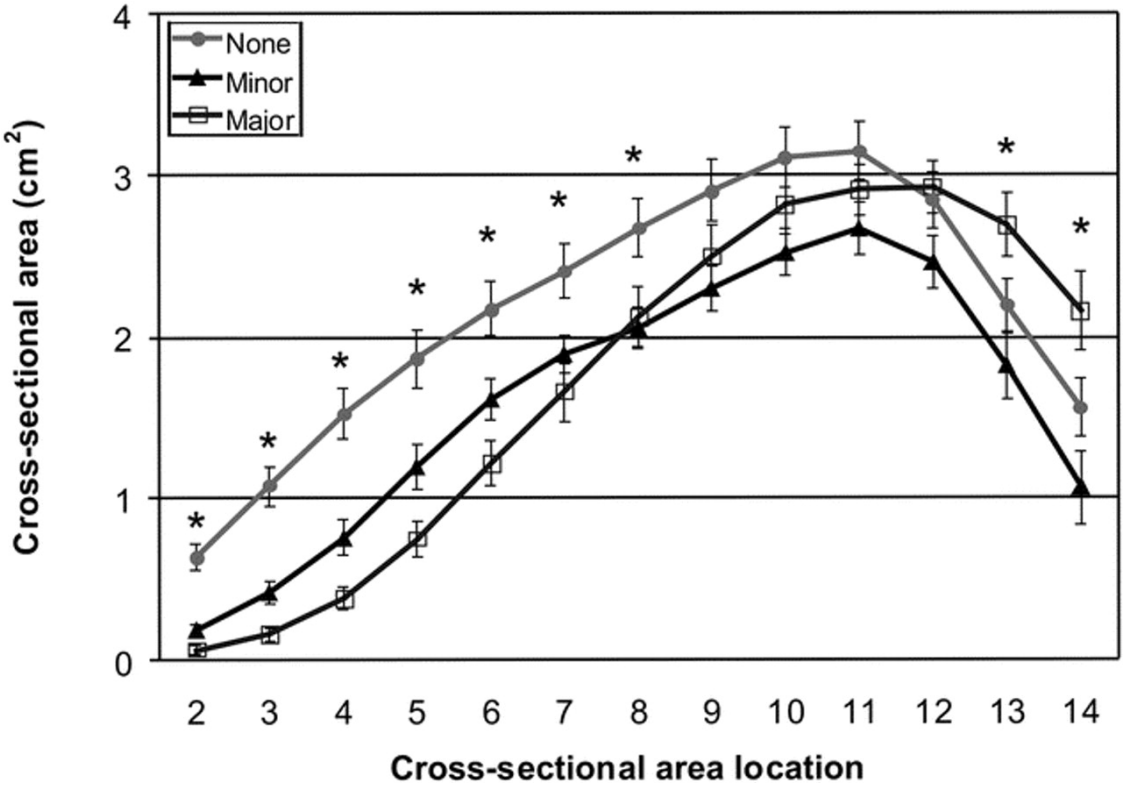

Figure 2-13: Levator cross-section areas at various locations (Mean ± SEM).

In the dorsal portion of the muscle, at cross-section locations 11 through 14, where the fibers of the sling of the puborectal muscle predominate behind the rectum, the women with major defects had the largest cross-sectional area compared to the minor or no defect groups (no defect group= 2.43 cm^2 ±. 0.13; minor= 2.00 cm^2 ±. 0.17; and major= 2.67 cm^2 ±. 0.20, p= 0.03).

The cross-sectional areas of the pubic portion of the levator muscle in women with prolapse and those with normal support in each defect grade are compared in Table 2-4. Within each group, (normal, minor, major) when the patients were divided according to prolapse status, there were no statistically significant differences in the cross-sectional

area in either the ventral or dorsal regions.

Table 2-4: Mean ± SEM cross-sectional areas (in cm2) in women with and without prolapse.

	Ventral			Dorsal		
	Prolapse	Normal	P-value	Prolapse	Normal	P-value
None	1.97 ± 0.29	2.11 ± 0.14	0.65	2.32 ± 0.25	2.55±0.11	0.40
Minor	1.51 ± 0.20	1.36 ± 0.09	0.52	2.00 ± 0.25	2.00±0.26	0.99
Major	1.34 ± 0.21	1.25 ± 0.12	0.73	2.67 ± 0.34	2.66±0.24	0.98

2.4 Discussion

In this chapter, a new technique was developed allowing levator ani muscle cross-sectional area to be measured perpendicular to muscle fiber direction. This is important for assessing the relationship between levator ani function and morphological changes in the muscle because muscle contractile force is proportional to cross-sectional area, not thickness or volume.

At first, we applied this technique to a group of women with unilateral levator ani muscle defect. Since there is no left and right difference in cross-sectional area in normal levator ani muscle, having a normal muscle on one side and a visibly defective muscle on the other side within the same individual offers a unique opportunity to validate the technique's capability to detect differences in cross-sectional area between the normal side and the side with defect.

Since the levator ani muscle damage usually appears in localized regions and more often in the pubic portion rather than in the iliococcygeal portion (Delancey et al, 2003), we focused on quantifying the cross-sectional area in the pubic portion to increase the

sensitivity of the method for identifying muscle defects. The finding of smaller volume in the pubic portion, but not in the iliococcygeal portion, shows that our method of separating the two parts of the muscle was effective in isolating the defective area.

Once the two parts of the muscle had been separated, muscle fiber direction for the pubic portion was determined independent of muscle presence by identifying muscle origin and insertion. A smaller cross-sectional area was detected in the defective muscle near the pubic origin corresponding to the anatomical location of the visible MR defect. Since no visible defects were evident in the iliococcygeus muscle, calculations of its cross-sectional area were omitted.

Several techniques have been used to quantify levator ani muscle morphology. Bernstein used perineal ultrasonography to visualize and measure the thickness of levator ani muscle (Bernstein et al, 1997). However, because image resolution is limited, it is not clear which portion of the levator ani muscle was measured or what angle of fiber direction was used. Aukee measured the thickness of the distal part of the pubococcygeal in static axial MR image and found it to be significantly correlated with EMG values during a maximal contraction (Aukee et al, 2004). This measurement only reflects one dimension of the muscle and the relationship of this dimension to fiber direction is not known. Hoyte et al quantified the levator ani muscle volume and levator ani angle using 3-D reconstructed models (Hoyte et al, 2004). Although volumetric techniques do provide a measurement of morphologic change, quantifying cross-sectional area of the intact muscle perpendicular to its fiber direction, as done in this study, is more appropriate from a biomechanical perspective because only then can the contractile force developed by the muscle be estimated. The smaller the cross-sectional area of residual muscle left by the defect, the smaller the contractile force it can develop.

Levator ani muscle shape is complex as evidenced in these 3-D reconstructions. This complexity precludes useful measurements of the muscle being made in standard MRI planes because slice angle variation in 2-D static MRI scans can cause measurement variations of up to 15% (Hoytel et al, 2001). Also, as stated earlier, fiber directions do not correspond to standard image acquisition planes and they can vary from subject to subject. Therefore we conclude that 3D reconstruction and establishment of fiber

direction in 3-D space is preferred for cross-sectional area measurements meant to reflect functional differences.

There were several challenges in developing this measurement method. The first was in the technique for levator ani separation. There are some small regions of the muscle where the iliococcygeal and the pubic portions overlap, for example, behind the rectum. Therefore separation of the pubic and iliococcygeal portions of the muscle does not preclude the possibility for inclusion of a small portion of the iliococcygeal muscle in the pubic portion, and vice versa. In addition, subdivisions in the pubic portion, such as the puborectalis and pubococcygeus, cannot be separated at the present time. Further refinements in the technique may allow more accurate separations to be made in the future.

Identification of muscle fiber direction is also a challenge. Although it is possible with MRI to see fiber direction in coarse grained muscles such as the gluteus maximus, it is not possible, at present, to consistently see individual fibers within the pubic portion of the levator. The straight line used to approximate muscle fiber direction from the muscle origin to insertion point allows us to circumvent this problem. However, some muscle fibers do not follow this approximate fiber direction. For example, cross-sectional areas calculated at location 4 are not strictly perpendicular to the fiber direction as some fibers cross the midline at this point. This problem does not affect locations 1, 2 or 3. We were concerned that a defect might also change the remaining fiber direction; however, our calculations showed that the differences in measurements were not statistically significant (Table 2-2).

Then we applied this technique to a larger group of women to investigate the muscle loss in women with and with prolapse and different degree of levator ani muscle defect.

It is noteworthy that women with major defects exhibited a 36 % reduction in cross-section area in the ventral portion of the levator ani muscle compared with women without defects, whereas in the posterior portion of the muscle, women with major defects exhibited a 9% larger cross-section area compared to those without defects. While women with minor defects similarly exhibited a 29% smaller cross-section area in the ventral portion of the muscle compared to those with no defects, they had a smaller

cross-section in the dorsal portion of the muscle.

The finding of smaller cross-section area in the ventral portion based on severity of visible defects on MR images reinforces the hypothesis that defects in the levator ani is localized to this area (DeLancey et al, 2003, Dietz et al, 2005). This region is where the pubovisceral or pubococcygeal muscle (pubovaginal muscle, puboanal muscle and puboperineal muscle) predominate. Comparing cross-sectional area of the muscle between the groups begins the process of using morphological differences to explain differences in muscle function. For a parallel-fibered, non-pennate muscle, the smaller the cross-sectional area, the smaller the maximal force a muscle can generate.

What might explain the paradoxical finding of increased muscle cross-sectional area in the dorsal region of the pubic portion in women with severe defects? In this region, the fibers of the puborectalis muscle predominate and form a sling behind the rectum (Kearney et al, 2004, Lawson et al, 1975). The increased cross-sectional area could represent compensatory hypertrophy. Alternatively this increased posterior cross-sectional area may represent disrupted muscle that has retracted dorsally; however, if this muscle has retracted because of detachment of its origin or insertion, atrophy should have occurred within months of the injury. Further research will be needed to clarify these newly-identified issues.

In both ventral and dorsal regions of the pubic portion of the levator ani muscle, cross-sectional area measurements did not show statistically significant differences when women with prolapse were compared with women having normal support for each level of defect. This does not mean that muscle defects are unimportant to the occurrence of prolapse because muscle defects happen more often in the ventral levator ani of women with prolapse 10 and differences in levator ani morphology have been observed between women with prolapse and normal support (Hoyte et al, 2001, Singh et al, 2003). However, when defects are present, the amount of muscle is the same regardless of whether there is prolapse or not. In other words, a woman with prolapse and a defect in the levator ani muscle had a similar levator cross-sectional area compared to a woman with a similar severity of levator defect, but normal support. This is logical because the pelvic organ support system consists of connective tissue, striated muscle, and smooth

muscle. Therefore, damage in any one of these systems will not explain all occurrences of prolapse.

This study quantified differences in levator ani muscle cross-sectional area perpendicular to the fiber direction in different patient populations. It should help investigators assess the biomechanical role of levator ani muscle loss in causing pelvic organ prolapse. The difference in cross-sectional area in the ventral and dorsal regions of the muscle indicates that the levator ani muscle is affected in a nonuniform manner, consistent with the fact that the levator ani is composed of several different component muscles that are differentially affected by damage. Specific patterns of damage to specific muscle elements may be important for the development of pelvic floor dysfunction.

References

Aukee P, Usenius JP, Kirkinen P. An evaluation of pelvic floor anatomy and function by MRI. Eur J Obstet Gynecol Reprod Biol. 2004; 112(1):84-8.

Bernstein IT. The pelvic floor muscles: muscle thickness in healthy and urinary-incontinent women measured by perineal ultrasonography with reference to the effect of pelvic floor training. Estrogen receptor studies.Neurourol Urodyn. 1997;16(4):237-75.

Boreham MK et al. Morphometric analysis of smooth muscle in the anterior vaginal wall of women with pelvic organ prolapse. Am J Obstet Gynecol 2002;187: 56-63.

Boreham MK et al. Morphometric properties of the posterior vaginal wall in women with pelvic organ prolapse. Am J Obstet Gynecol 2002; 187: 1501-1509.

Boyles SH, Weber AM, Meyn L. Procedures for pelvic organ prolapse in the United States, 1979-1997. Am J Obstet Gynecol 2003;188:108-15

Delete Boyles SH, Weber AM, Meyn L. Procedures for urinary incontinence in the United States, 1979-1997. Am J Obstet Gynecol 2003;189:·70-5.

Bump RC, Mattiasson A, Bo K, Brubaker LP, DeLancey JO, Klarskov P, Shull BL, Smith AR. The standardization of terminology of female pelvic organ prolapse and pelvic floor dysfunction. Am J Obstet Gynecol. 1996; 175(1):10-7.

Chen L, Hsu Y, Ashton-Miller JA, DeLancey JOL. Measurement of the pubic portion of the levator ani muscle in women with unilateral defects in 3D models from MR images. Int J Gynaecol Obstet. 2006 Mar;92(3):234-41.

DeLancey JO, Kearney R, Chou Q, Speights S, Binno S. The appearance of levator ani muscle abnormalities in magnetic resonance images after vaginal delivery. Obstet

Gynecol. 2003;101(1):46-53.

Dietz HP, Lanzarone V. Levator trauma after vaginal delivery. Am J Obstet Gynecol. 2005; 106(4): 707-12.

Fielding JR, Dumanli H, Schreyer AG, Okuda S, Gering DT, Zou KH et al. MR-based three-dimensional modeling of the normal pelvic floor in women: Quantification of muscle mass. Am J Radiology. 2000: 174; 657-60.

Hoyte L, Fielding JR, Versi E, Mamisch C, Kolvenbach C, Kikinis R Variations in levator ani volume and geometry in women: the application of MR based 3D reconstruction in evaluating pelvic floor dysfunction. Arch Esp Urol. 2001 Jul-Aug;54(6):532-9

Hoyte L, Schierlitz L, Zou K, Flesh G, Fielding JR. Two- and 3-dimensional MRI comparison of levator ani structure, volume, and integrity in women with stress incontinence and prolapse. Am J Obstet Gynecol. 2001; 185(1):11-9.

Hoyte L and Ratiu P. Linear measurements in 2-dimentional pelvic floor imaging: The impact of slice tilt angles on measurement reproducibility. Am J Obstet Gynecol 2001;185:537-544.

Hoyte L, Jakab M, Warfield SK, Shott S, Flesh G, Fielding JR. Levator ani thickness variations in symptomatic and asymptomatic women using magnetic resonance-based 3-dimensional color mapping. Am J Obstet Gynecol. 2004; 191:856-61.

Ikai M, Fukunaga T. Calculation of muscle strength per unit cross-sectional area of human muscle by means of ultrasonic measurement. Int. Z. angew. Physiol. Einschl. Arbeitsphysiol. 1968; 26(1):26-32.

Ikai M, Fukunaga T. A study on training effect on strength per unit cross-sectional area of muscle by means of ultrasonic measurement. Int. Z. angew. Physiol. Einschl. Arbeitsphysiol. 1970; 28(3):173-180

Janda S, van der Helm FC, de Blok SB. Measuring morphological parameters of the pelvic floor for finite element modelling purposes. J Biomech. 2003; 36(6):749-57.

Kearney R, Sawhney R, DeLancey JO. Levator ani muscle anatomy evaluated by origin-insertion pairs. Obstet Gynecol. 2004; 104(1):168-73.

Kearney R, Miller JM, Ashton-Miller JA, DeLancey JOL. Obstetric factors associated with levator ani muscle injury after vaginal birth. Obstet Gynecol. 2006; 107(1): 144-9.

Kirschner-Hermanns R, Wein B, Niehaus S, Schaefer W, Jakse G. The contribution of magnetic resonance imaging of the pelvic floor to the understanding of urinary incontinence. Br J Urol 1993;72:715–8.

Kris Strohbehn, James H. Ellis, Judith A. Strohbehn, John O.L. DeLancey. Magnetic resonance imaging of levator ani with anatomic correlation. Obstet Gynecol. 1996; 87(2):277-85.

Lawson JO. Pelvic anatomy. I. Pelvic floor muscles Ann R Coll Surg Engl 1974;54:244-52.

.

Smith ARD, Hosker GL, Warrell DW. The role of partial denervation of the pelvic floor in the etiology of genitourinary prolapse and stress incontinence of urine: a neurophysiologic study. Br J Obstet Gynaecol 1989;96:24-28 et al

Singh K, Reid WM, Berger LA. Magnetic resonance imaging of normal levator ani anatomy and function. Obstet Gynecol. 2002; 99(3):433-8

Singh K, Jakab M, Reid WM, Berger LA, Hoyte L. Three-dimensional magnetic resonance imaging assessment of levator ani morphologic features in different grades of prolapse. Am J Obstet Gynecol. 2003; 188(4):910-5.

Takano CC et al. Analysis of collagen in parametrium and vaginal apex of women with and without uterine prolapse. Int Urogynecol J 2002; 13(6):342-5.

Tunn R, Paris S, Fischer W, Hamm B, Kuchinke J. Static magnetic resonance imaging of the pelvic floor muscle morphology in women with stress urinary incontinence. Neurourol Urodyn. 1998;17(6):579-89.

Chapter 3 Geometrical Analyses of Anterior Vaginal Wall in Women With and Without Prolapse

3.1 Vaginal Thickness, Cross-Sectional Area, and Perimeter in Women With and Those Without Prolapse

ABSTRACT

OBJECTIVE: Use axial magnetic resonance imaging to test the null hypothesis that no difference exists in apparent vaginal thickness between women with and those without prolapse.

METHODS: Magnetic resonance imaging studies of 24 patients with prolapse at least 2 cm beyond the introitus were selected from an ongoing study comparing women with prolapse with normal control subjects. The magnetic resonance scans of 24 women with prolapse (cases) and 24 women without prolapse (controls) were selected from those of women of similar age, race, and parity. The magnetic resonance files were imported into an experimental modeling program, and 3-dimensional models of each vagina were created. The minimum transverse plane cross-sectional area, mid-sagittal plane diameter, and transverse plane perimeter of each vaginal model were calculated.

RESULTS: Neither the mean age (cases 58.6 years +/- standard deviation [SD] 14.4 versus controls 59.4 years +/- SD 13.2) nor the mean body mass index (cases 24.1 kg/m(2)+/- SD 3.3, controls 25.7 kg/m(2)+/- SD 3.7) differed significantly between groups. Minimum mid-sagittal vaginal diameters did not differ between groups. Patients with prolapse had larger minimum vaginal cross-sectional areas than controls (5.71 cm(2)+/-

standard error of the mean [SEM] 0.25 versus 4.76 cm(2)+/- SEM 0.20, respectively; P = .005). The perimeter of the vagina was also larger in the prolapse group (11.10 cm +/- SEM 0.24) compared with

controls (9.96 cm +/- SEM 0.22) P = .001. Subgroup analysis of patients with endogenous or exogenous estrogen showed

prolapse patients had larger vaginal cross-sectional area (P = .030); in patients without estrogen group differences were not significant (P = .099).

CONCLUSION: Vaginal thickness is similar in women with and those without pelvic organ prolapse. The vaginal perimeter and cross-sectional areas are 11% and 20% larger in prolapse patients, respectively. Estrogen status did not affect differences found between groups.

3.1.1 Introduction

Pelvic organ prolapse is a remarkably common problem, yet the disease mechanism resulting in its occurrence remains poorly understood. There are competing hypotheses that have been proposed to explain its cause. For example, 2 differing mechanisms have been used to explain the formation of a cystocele: vaginal wall stretching versus vaginal wall detachment. The first focuses on stretching of the fibromuscular vaginal tube (fascia) as the disease mechanism of prolapse. This has also been referred to as a distention cystocele (Nichols et al 1996). The distention cystocele implies that the vagina becomes thin and attenuated in the formation of a cystocele. The other focuses more on the connections of the vaginal tube relative to the pelvic sidewall(Richardson et al, 1976,1981). When these connections break, a paravaginal defect or a displacement cystocele occurs (Nichols et al, 1996, Richardson et al, 2000). Similar considerations have been voiced concerning support of the posterior vaginal wall (Hoyte et al, 2000).

Magnetic resonance imaging is a tool that can be used to study pelvic floor structures. On axial magnetic resonance images, the vagina is a discreet structure with visible boundaries. The outer border of the vagina is delineated by a dark line that represents the fibromuscular wall of the vagina. Because the vagina is a potential space that is not filled

with fluid or air, the structure inside the dark fibromuscular circumference is made up of the coapted walls of the vagina. This allows the overall thickness of the vaginal wall to be measured and quantified.

To help gain insight regarding the role of each of the above hypotheses in explaining pelvic organ prolapse, we used magnetic resonance imaging to test the null hypothesis that no difference exists in apparent vaginal thickness between women with and those without prolapse.

3.1.2 Materials and Methods

Axial magnetic resonance scans of 25 women with prolapse of a vaginal wall or cervix at least 2 cm beyond the introitus were selected from an ongoing institutional review board–approved study comparing women with prolapse with normal control subjects. The prolapse patients were recruited through the University of Michigan Urogynecology Clinic. The controls were recruited mainly through advertisements, as well as through the Women's Health Registry, a list of women who expressed interest in participating in women's health projects. Patients were excluded if they had previous surgery for prolapse or incontinence, had genital anomalies, or had delivered in the past year. Patients were enrolled between June 2001 and September 2003. The magnetic resonance scans of 25 women with prolapse (cases) and 25 women without prolapse (controls) were selected from those of women of similar age, race, and parity. One patient in whom the prolapse was protruding at the time of magnetic resonance was excluded because this created a double layer of vagina, which would have confounded results. A control subject was therefore also excluded to produce 24 patients in each group for analysis. Multiplanar 2-dimensional fast-spin proton density magnetic resonance images (echo time 15 ms, repetition time 4,000 ms) of all pelvises were obtained by use of a 1.5 T superconducting magnet (Signa Horizon LX, General Electric, Milwaukee, WI) with version 9.1 software. The fields of view in both axial and coronal images were 16 x 16 cm, and the field of view in the sagittal images was 20 x 20 cm. All 3 views had slice thicknesses of 4 mm, with a 1-mm gap between slices.

The outer margin of the vagina was traced to include the fibromuscular wall by using 3-dimensional computer graphics and modeling software (Slicer 2b1; Massachusetts Institute of Technology, Cambridge, MA). In subjects with a uterus and cervix, the vagina was traced until the cervix could be seen (Figure 3 -1-1) to avoid including the cervix in the vaginal wall measurements. The vagina was traced in all of the axial slices to the level of the introitus, noted by the visibility of the vestibular bulbs (Figure 3 -1-1). Blinding of the investigator was attempted but often not possible because of the visible nature of the prolapse in many of the magnetic resonance images. Three-dimensional models based on the axial magnetic resonance tracings were then constructed. The models were imported into I-DEAS 9.0 (EDS, Hook, UK), an engineering computer-aided analysis and design program (Figure 3-1-2), to make measurements perpendicular to the long axis of the vagina to avoid 2-dimensional measurement errors (Figure 3-1-3A). The longitudinal axis of the 3-dimensional vaginal models was determined as the midline of the vagina contours in the mid-sagittal plane (Figure 3-1-3B). Five equally spaced points were selected along the longitudinal axis of each model, and cross sections of the vagina perpendicular to the longitudinal axis were made (Figure 3-1-3C). The minimum diameter in mid-sagittal plane, cross-sectional area, and length of the perimeter of the vagina were calculated at each cross section (Figure 3-1-3D). The perimeter of the vaginal wall was measured as the circumferential length of the outer vaginal wall margin on each cross section.

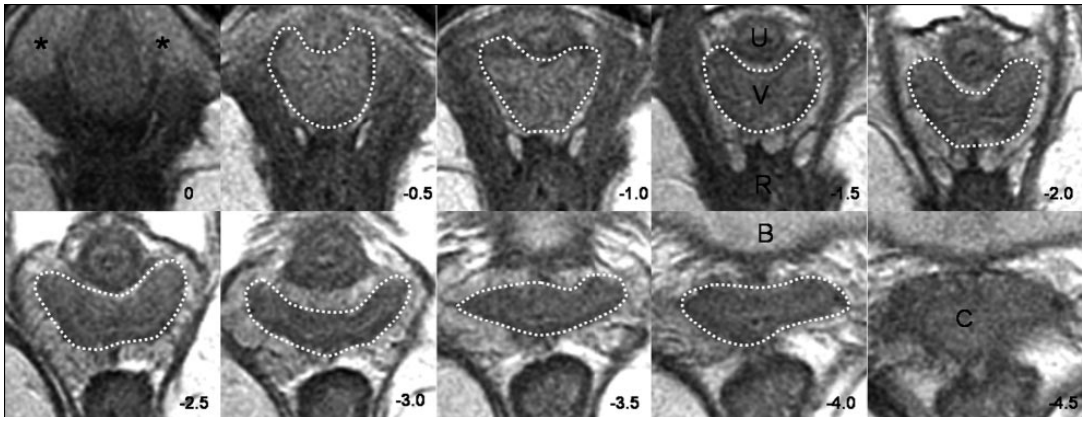

Figure 3-1-1. Axial slices at 5-mm intervals arranged caudal to cephalad starting from the image in the upper left (image 0). Vaginal tracings were made from above the level of the vestibular bulbs (VB), represented by asterisks (*), caudally (image 0) to below where the cervix (C) could be seen (image -4.0). U, urethra; V, vagina; R, rectum; B, bladder. © DeLancey 2004.

Descriptive statistics were generated, including the mean and standard error of the mean (SEM). The measurements at each cross section were summed for the groups, and an aggregated average was calculated. A repeated-measures analysis of variance was used to test for group and level effects. Two-sided, 2-group, t tests were used to test group differences. $P < .05$ was considered significant.

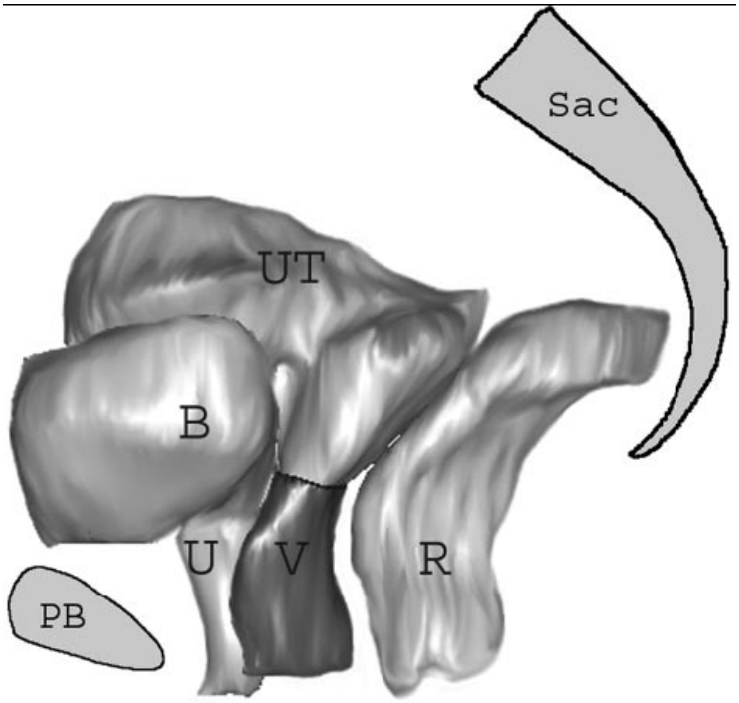

Figure 3-1-2. Selected 3-dimensional model as it appears in I-DEAS 9.0. The sacrum (Sac), pubic bone (PB), and pelvic organs have been shown for orientation. B, bladder; U, urethra; UT, uterus; V, vagina; R, rectum. © DeLancey 2004.

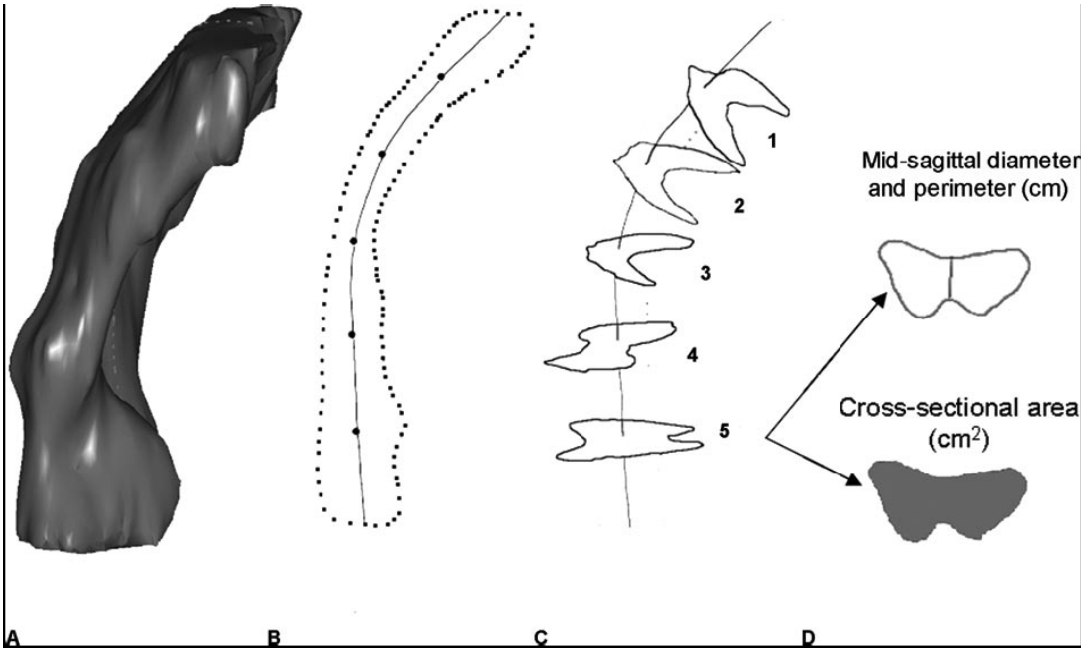

Figure 3-1-3. Steps in obtaining vaginal measurements: A. Threedimensional I-DEAS 9.0 vaginal model. B. Longitudinal axis determined in the mid-sagittal plane, with 5 equally spaced locations along the longitudinal axis marked. C.Sample cross sections: Location 1 is near the vaginal apex, and location 5 is near the hymen. D. Mid-sagittal diameter, perimeter, and cross-sectional area were calculated for each axial cross section. © DeLancey 2004.

3.1.3 Results

Subject groups had similar mean age and body mass index (Table 3-1-1). The analysis of variance showed that mid-sagittal vaginal diameters did not differ by group. There was, however, a significant difference by location (Table 3-1-2, Figure 3-1-4). The vaginal cross-sectional areas differed significantly by group but not by level (Table 3-1-2). The case group had mean cross-sectional areas that were 20% larger than those of controls (5.71 cm2± SEM 0.25 versus 4.76 cm2± SEM 0.20, respectively; P = .005; Figure 3-1-5). The perimeter of the vagina was significantly different by group as well as location (Table 3-1-2). The perimeter was significantly longer in the case group than in the controls (11.10 cm ± SEM 0.24 versus 9.96 cm ± SEM 0.22, respectively; P = .001; Figure 3-1-6). Post hoc tests of statistical power were calculated for group differences in

mid-sagittal diameter, cross-sectional area, and perimeter and were found to be 5%, 83%, and 92%, respectively.

Table 1. Patient Characteristics

	Prolapse (n = 24)	Controls (n = 24)
Age (y)*	58.6 ± 14.4	59.4 ± 13.2
Body mass index (kg/m^2)†	24.1 ± 3.3	25.7 ± 3.7
Estrogen		
Yes	16	14
No	8	10

Data are expressed as mean ±standard deviation or number.
* $P = .844$.
† $P = .12$.

Table 2. ANOVA Results in Terms of *F* Statistics and *P* Values

	Mid-Sagittal Diameter		Cross-Sectional Area		Vaginal Perimeter	
	F	*P*	*F*	*P*	*F*	*P*
Group	0.02	.88	8.91	.005	12.03	.001
Location	7.21	< .001	0.81	.52	5.52	< .001
Group × location	0.72	.58	1.12	.35	0.95	.44

ANOVA, analysis of variance.

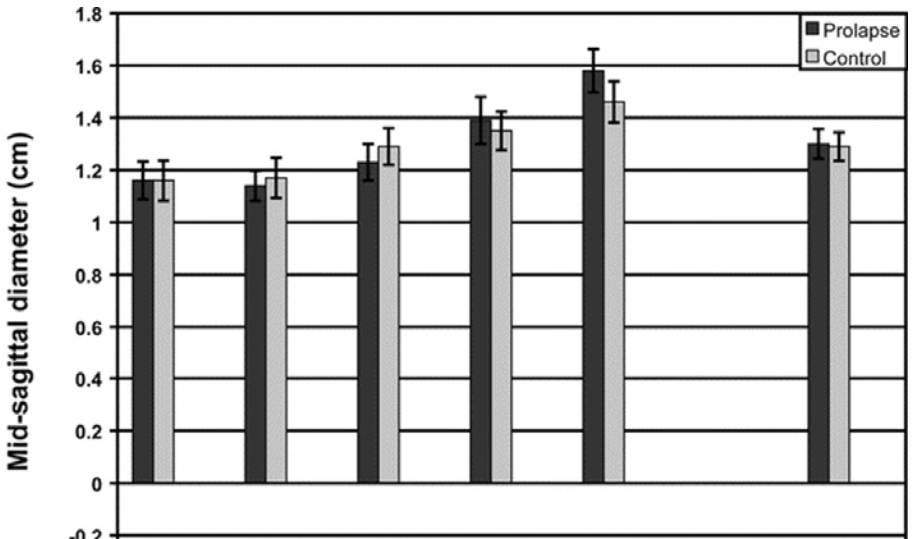

	1	2	3	4	5	Aggregate mean
Prolapse	1.16	1.14	1.23	1.39	1.58	1.3
Control	1.16	1.17	1.29	1.35	1.46	1.29
Difference (%)	0%	-2.56%	-4.65%	2.96%	8.22%	0.77%
P-value	0.931	0.753	0.56	0.768	0.295	0.928

Figure 3-1-4. Vaginal mid-sagittal diameter at each of the 5 vaginal locations. Refer to Figure 3-1-3 for vaginal locations. The aggregate mean of the 5 individual segments is also shown at right. Error bars indicate standard error of the mean.

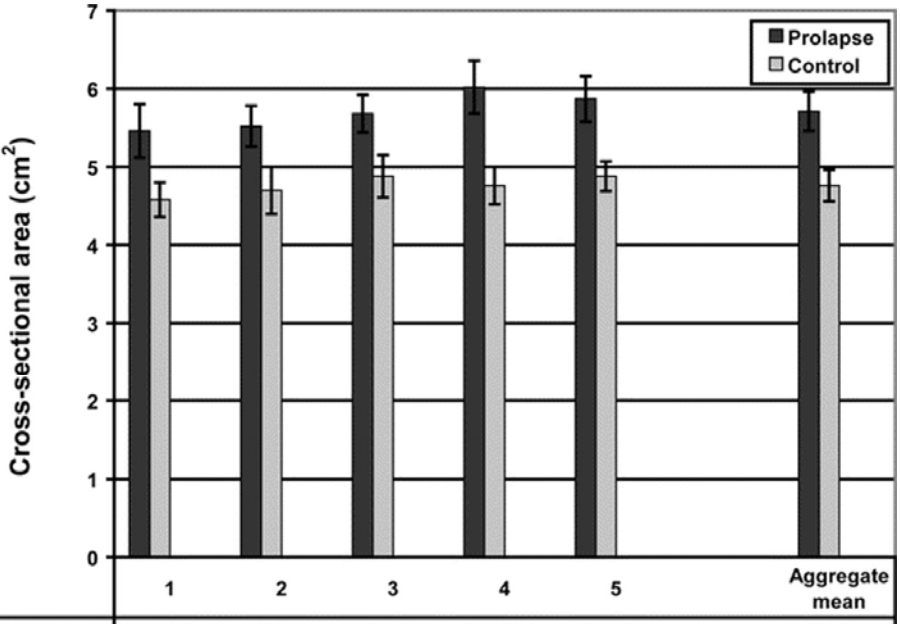

	1	2	3	4	5	Aggregate mean
Prolapse	5.46	5.52	5.68	6.02	5.87	5.71
Control	4.58	4.7	4.88	4.76	4.88	4.76
Difference (%)	19.21%	17.44%	16.39%	26.47%	20.29%	19.96%
P-value	0.04	0.044	0.031	0.005	0.007	0.005

Figure 3-1-5. Cross-sectional area at each of the 5 vaginal locations. The aggregate mean of the 5 individual segments is shown at right. Error bars indicate standard error of the mean.

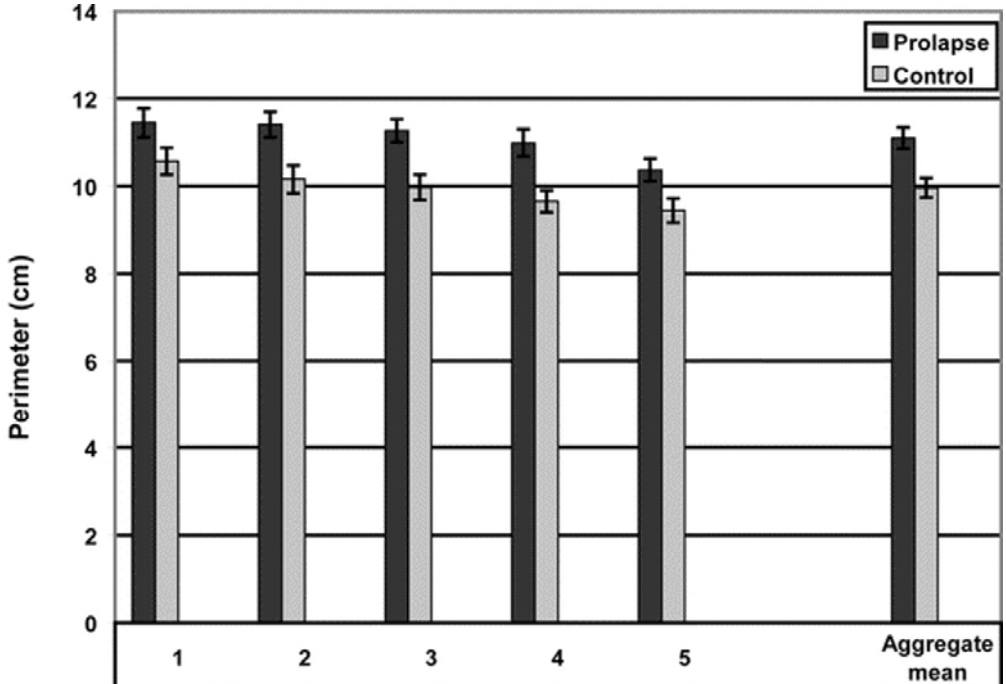

	1	2	3	4	5	Aggregate mean
Prolapse	11.45	11.41	11.27	10.99	10.37	11.1
Control	10.57	10.16	9.97	9.65	9.44	9.96
Difference (%)	8.32%	12.30%	13.04%	13.89%	9.85%	11.45%
P-value	0.058	0.006	0.002	0.001	0.019	0.001

Figure 3-1-6. Vaginal perimeter. The aggregate mean of the 5 individual segments is shown at right. Error bars indicate standard error of the mean.

A subanalysis was performed to examine the effect of estrogen status on vaginal cross-sectional area and vaginal thickness. In the case group, 16 patients were either premenopausal or on hormone replacement therapy, compared with 14 in the control group. Eight patients in the case group and 10 in the control group were postmenopausal and not on hormone replacement therapy. Comparing cases and controls who were estrogenized, the case patients had 19% larger mean cross-sectional areas (5.90 cm2± SEM 0.33) than the controls (4.96 cm2± SEM 0.25; P = .030). Among women without estrogen, there was a trend toward the case group having larger mean cross-sectional areas (case 5.33 cm2± SEM 0.34, controls 4.48 cm2± SEM 0.34; P = .099), but the difference was not statistically significant. When mean mid-sagittal diameter was examined based on hormonal status, there were no group differences in either women with estrogen (case 1.31 cm ± SEM 0.08, control 1.35 cm ± SEM 0.07; P = .699) or those without estrogen (case 1.28 cm ± SEM 0.09, control 1.21 cm ± SEM 0.09; P = .614). The mean mid-sagittal vaginal diameters in the controls with (n = 14) and those without (n = 10) estrogen were compared, but no significant differences were found.

3.1.4 Discussion

As judged by its appearance on magnetic resonance scans, vaginal thickness in women with prolapse was not different from that in women with normal support. There was less than a 1% difference in the mid-sagittal diameter between the groups. Because the mid-sagittal diameter is the sum of the anterior and the posterior vaginal walls, women with prolapse do not appear to have thinner vaginas.

Women with prolapse do have a 20% larger mean vaginal cross-sectional area. Because the mid-sagittal diameters of the 2 groups were similar, the larger cross-sectional area of the prolapse group must be due to a larger vaginal width, which is represented by the 11% larger vaginal perimeter. These data indicate that there is more vaginal tissue in women with prolapse than in women without prolapse. This contradicts the clinical assumption that the vagina in women with prolapse is thin.

The fact that the same trends in cross-sectional area and mid-sagittal vaginal diameter were maintained regardless of estrogen status confirms that hormonal status was not a confounding variable in this study. Although estrogen status did not change the trends in mean cross-sectional area and mid-sagittal diameter between the groups, it has been well established that the presence of estrogen positively affects vaginal maturation.(Blakeman et al, 2001, Vardy et al, 2003) Indeed, the 10% larger mid-sagittal vaginal diameter in control patients with estrogen compared with controls without estrogen suggests that, with a larger sample size, the difference in thickness might become statistically significant.

Historically, pelvic surgeons have focused on attenuation of the "endopelvic fascia" as the cause of prolapse. In 1954, Ricci performed definitive anatomical studies on pelvic connective tissue and provided an excellent review of the origin of the myth of the endopelvic fascia.(Vardy et al, 2003, Ricci et al, 1954) Repeated histologic examination has failed to demonstrate a clear "fascial" layer. After performing a literature review and performing their own histologic studies, Weber and Walters (Weber et al, 1997) described the vagina as being made up of 3 layers: mucosa, muscularis, and adventitia. The adventitial layer is a connective tissue layer of collagen and elastin that separates the muscular wall of the vagina and the paravaginal tissues. The adventitia is variably discrete and does not form a complete capsule surrounding the vagina as a true fascial layer.(Weber et al, 1997) Because of the lack of discrete fascial covering, our tracing outside the fibromuscular wall includes all the important structural layers of the vagina. In a study of (Boreham et al, 2002) women with enteroceles, vaginal wall muscularis was found between vaginal epithelium and peritoneum in all cases; this also suggests that it is not a site-specific defect in the fibromuscular wall that leads to prolapse.(Tulikangas et al, 2002)

Although the site-specific defect theory for prolapse has become less popular because of the lack of histologic evidence, a significant body of research remains focused on the vaginal tube as the source of the problem. Boreham et al (Boreham et al, 2002) found that the morphometry of anterior vaginal wall tissue obtained from women with prolapse was significantly altered compared with that from women with normal support. Women with

prolapse had decreased fractional area of smooth muscle and disorganized smooth muscle bundles with decreased α-actin staining.(Boreham et al, 2002) In a separate study,(Boreham et al, 2002) they found that the decreased fractional area of smooth muscle was also present in the posterior vaginal wall and that women with prolapse had smaller and fewer nerve bundles in the muscularis compared with controls. Boreham et al (Boreham et al, 2001) also found that caldesmon, a protein that inhibits smooth muscle contractility, had increased expression in the vaginal smooth muscle of women with prolapse. A number of other studies have focused on collagen differences in the vaginal tube of women with prolapse compared with controls. Although differences in collagen content have been found, it is difficult to determine whether these differences resulted in or are a result of prolapse.

The mechanical strength of the vaginal wall is determined by its composition, tissue architecture, and thickness, all of which influence its material properties. Few studies have examined the thickness of the vaginal wall in prolapse compared with controls. Tulikangas et al (Tulikangas et al, 2002) found that the muscularis layer was thicker in women with enteroceles compared with controls. Shrinkage due to formalin fixation and differences between excised tissue and in situ tissues may help explain why vaginal thickness in that study was approximately half that found in the present study. We are not aware of any other studies that have quantified vaginal wall thickness in patients with prolapse or controls. Our findings that vaginal wall thickness appears similar in both groups suggest that it is not the fibromuscular tube of the vagina that is defective. However, we are not able to comment on the vaginal tissue architecture or composition, both of which can influence the material properties of the vagina.

A strength of this study is the development of a method to quantitatively describe the anatomy of prolapse compared with normal women. Measurements done on 2-dimensional axial magnetic resonance images are inaccurate because they are not usually acquired perpendicular to the longitudinal axis of the vagina. This is due to the position of the patient in the magnetic resonance scanner as well as the natural sagittal curvature of the vagina. The variations in slice angle can lead to systemic errors in the measurements of the 2-dimensional magnetic resonance images.(Hoyte and Ratiul, 2001)

By varying the slice angle of magnetic resonance images, Hoyte and Ratiu (Hoyte and Ratiu, 2001)found that 2-dimensional measurements can differ by up to 15%. To circumvent this error, we created 3-dimensional models of the vaginas of our subjects. This allowed for accurate comparisons of the vaginal tube of women with prolapse and that of normal controls.

Although we found that the thicknesses of the vaginas between groups were not statistically different, we cannot preclude the possibility that the material properties of the vaginal wall might differ in their functional capacities. It has also been observed that women with prolapse have dilated venules in the vaginal wall. (Boreham et al, 2002) led to errors in measurements of vaginal wall thickness in the present study. In addition, the study was performed on women in the supine posture when the gravity vector acts posteriorly rather than caudally, a difference that may affect the tensile loading of the vaginal wall in women with prolapse. This might have led to an underestimation of group differences in the supine posture.

To date, a unifying theory explaining the cause of pelvic organ prolapse based on objective scientific data does not exist. Different theories have been proposed, but data to resolve these differences are not available. Magnetic resonance imaging allows us to gather data that can be used to test the hypotheses concerning these long-debated issues. Although the development of prolapse is likely the common end point of different disease mechanisms, our study suggests that more attention should be focused on the connections of the vagina to the pelvic sidewall rather than the vagina itself.

3.2 Anterior vaginal wall length and degree of anterior compartment prolapse seen on dynamic MR images

ABSTRACT

The objective of the study was to determine the relationship between midsagittal vaginal wall geometric parameters and the degree of anterior vaginal prolapse. We have previously presented data indicating that about half of anterior wall descent can be explained by the degree of apical descent present (Summers et al. 2006). This led us to examine whether other midsagittal vaginal geometric parameters are associated with anterior wall descent. Magnetic resonance (MR) scans of 145 women from the prior study were suitable for analysis after eight were excluded because of inadequate visibility of the anterior vaginal wall. Subjects had been selected from a study of pelvic organ prolapse that included women with and without prolapse. All patients underwent supine dynamic MR scans in the midsagittal plane. Anterior vaginal wall length, location of distal vaginal wall point, and the area under the midsagittal profile of the anterior vaginal wall were measured during maximal Valsalva. A linear regression model was used to examine how much of the variance in cystocele size could be explained by these vaginal parameters. When both apical descent and vaginal length were considered in the linear regression model, 77% ($R^2 = 0.77$, $p < 0.001$) of the variation in anterior wall descent was explained. Distal vaginal point and a measure anterior wall shape, the area under the profile of the anterior vaginal wall, added little to the model. Increasing vaginal length was positively correlated with greater degrees of anterior vaginal prolapse during maximal Valsalva ($R^2 = 0.30$, $p < 0.01$) determining 30% of the variation in anterior wall decent. Greater degrees of anterior vaginal prolapse are associated with a longer vaginal wall. Linear regression modeling suggests that 77% of anterior wall descent can be explained by apical descent and midsagittal anterior vaginal wall length.

Keywords Pelvic organ prolapse - Anterior prolapse - Cystocele - Apical descent - Vaginal length - Dynamic MR images

3.2.1 Introduction

The anterior vaginal prolapse is the most common form of pelvic organ prolapse (Hendrix et al, 2002) as well as the site with the highest rates of persistent and recurrent support defects (Shull et al, 2000). Blinded follow-up in a randomized prospective study of surgical techniques to correct anterior vaginal prolapse at an institution known for excellence in urogynecologic surgery found that only 30–45% of patients had satisfactory

or optimal results at 24 months (Weber et al, 2001). The high rate of suboptimal outcomes and the inability to predict which patients will fail surgery suggest a lack of knowledge regarding the disease mechanism of anterior wall prolapse.

Dynamic magnetic resonance (MR) imaging in the midsagittal plane has given us the ability to study the deformation of the anterior vaginal wall during Valsalva. Previous analysis using this approach found that about half ($R^2 = 0.53$) of anterior wall descent can be explained by the degree of apical descent present(Summers et al, 2006). The fact that apical descent only explains half of anterior wall descent raises the question of what other changes are involved. This led us to investigate the relationship of other midsagittal geometric factors, such as anterior vaginal wall length, displacement of the distal vagina, and anterior vaginal wall shape, to the degree of anterior wall descent. We hypothesized that these three factors would also predict a significant proportion of the variance in anterior wall descent.

3.2.2 Materials and methods

A secondary analysis was performed on the sample described in our original report (Summers et al, 2006). In brief, we recruited women representing varying degrees of pelvic organ support as part of an on-going study at the University of Michigan in Ann Arbor, MI. The original study is a case–control study where controls with vaginal points at least 1 cm above the hymen were matched to cases with prolapse at least 1 cm beyond the hymen (DeLancey et al, 2007). Pelvic support was determined using the pelvic organ prolapse quantification system on clinical exam. Women were selected from this pool to include women in whom the uterus was in situ, the cervix, bladder, and urethra were visible in the dynamic sagittal images, and a correct Valsalva maneuver was performed as judged by the movement of the abdominal wall and intestinal contents in a caudal direction. Women were recruited from the Urogynecology clinic at the University of Michigan and from advertisements. Women were excluded if they had a prior operation for pelvic organ prolapse or urinary incontinence. This resulted in a sample of 153 women for the original analysis. The relationship of the apex, as measured by the cervical

os location, and the anterior wall descent, as measured by the most dependent bladder point, was available in these women from the prior study (Summers et al 2006). Magnetic resonance (MR) scans of 145 women from the prior study were suitable for this study with good visualization of the anterior vaginal wall in the dynamic images (mean ± SD: age = 53.3 ± 12.5 years, parity = 2.7 ± 1.8, body mass index = 26.4 ± 4.5 kg/m^2). Eight scans from the original study were excluded because the complete vaginal wall could not be adequately seen in sufficient detail for accurate tracing. Although the original study included both cases and controls, our analysis concerned the relationship between cervix location, bladder descent, and vaginal length and did not depend on group status.

MRI was performed on a 1.5-T system (Signa, General Electric, Milwaukee, WI) using a four-channel torso-phased array coil with the subject in the supine position. Before starting the examination, the patient was instructed in regards to the straining maneuvers to be performed during the examination, starting from minimal to maximal straining. For dynamic imaging, a multiphase, single level image of the pelvis in the midsagittal plane was obtained approximately every second for 23–27 s using a T2-weighted single-shot fast spin-echo sequence (time at rest = 1,300 ms, time of excitation = 60 ms, slice thickness = 6 mm, field of view = 32–36 cm, matrix = 256 × 160, one excitation and half-Fourier acquisition). The time needed to acquire each of the images was determined by the patients' weight and was approximately a second. A set of 20 successive images were acquired in 23–27 s during rest and a graded Valsalva effort as follows: The operator instructed the subject to hold her breath in inspiration and initiated the scan and after 5 s of imaging during rest, the operator instructed the subject to strain minimally for 5 s, moderately for 5 s, and maximally for 5 s, then to breath normally and relax for another 5–7 s before ending the acquisition. Usually, three images were acquired at rest during suspended inspiration, 12 during the graded Valsalva effort, and five during post-Valsalva relaxation and normal breathing. These images were placed in a cine-loop using RadPix (Version 3.15, Weadock Software, LLC, Ann Arbor, MI) for display as a movie clip to evaluate the dynamics of prolapse.

The image at maximal Valsalva effort was selected for analysis (Figure 3-2-1). A local coordinate system was created using the inferior pubic point as the origin, the sacro-coccygeal inferior pubic point (SCIPP) line as the x-axis, and a line perpendicular to the SCIPP line through the inferior pubic point as the y-axis (Figure 3-2-1). The location of the external cervical os and the most dependent bladder point was previously determined using this coordinate system (Summers 2006). Degree of anterior wall and apical descent were determined by the location of the most caudal bladder point and external cervical os, respectively.

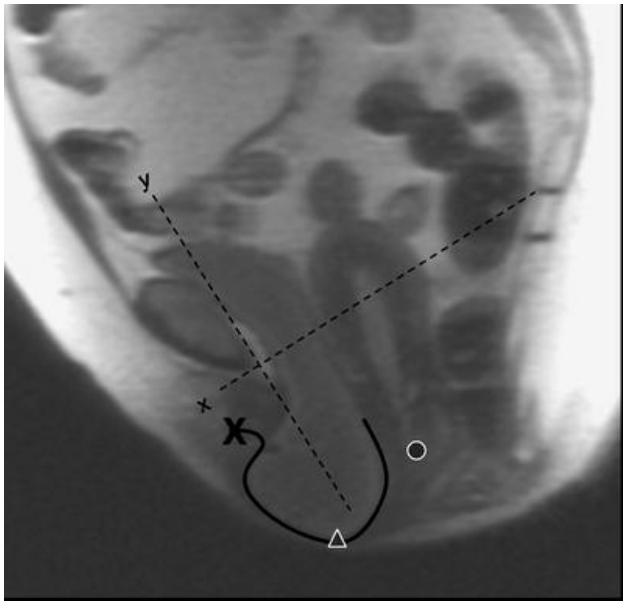

Figure 3-2-1 MR image at maximal Valsalva showing anterior vaginal wall tracing (solid black line), distal vaginal wall (x), bladder location (triangle), cervical os location (circle), and coordinate system (dotted lines)

To account for variability in patient size, we normalized all the subjects' pelvises to a SCIPP length of 10.5 cm, which was the mean SCIPP length for our sample. The anterior vaginal wall was traced from the anterior vaginal fornix to the external urinary meatus. A program was created using MatLab (the Mathwork, version 7.01 R14) to measure the length of the vaginal tracings and the SCIPP line. The location of the most distal vaginal point (the ventral end of the vaginal length tracing) and the area under the midsagittal profile of the anterior vaginal wall were also analyzed using MatLab. Finally, the area under the midsagittal anterior wall profile, from its proximal end to its distal end, was measured as the absolute area between the profile and a straight line connecting the two ends of the vaginal wall tracing (Figure 3-2-2). This parameter was a measure of the

complexity of the line shape of the vaginal wall tracing. Because these area calculations are a measure of vaginal wall shape rather than a quantification of actual area, non-normalized values were used.

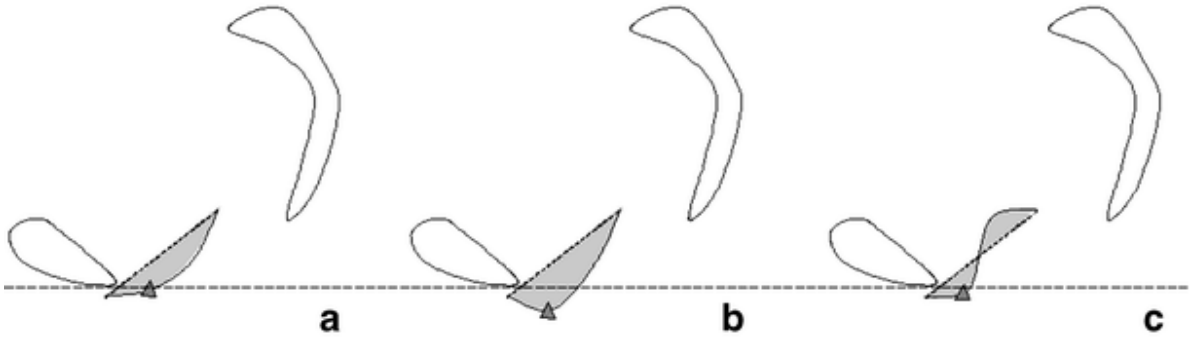

Figure 3-2-2 Area under the anterior vaginal wall profile. Pubic bone, sacrum, and coccyx are traced. The anterior vaginal wall tracings are shown. A line (small dotted) is used to connect the two ends of the vaginal wall tracing to create an area (shown in gray). Examples aligned using horizontal large dotted reference line. a Minimal descent of most caudal bladder point (triangle). b Greater descent of the bladder point with longer vaginal wall length and larger area. c Similar vaginal wall length to B but smaller area and lesser descent of bladder point

A linear regression model was performed with the dependent variable being prolapse size as measured by the most dependent bladder point and independent variables being the three geometric parameters. We calculated the Pearson correlation coefficient for the regression by comparing the previously obtained most dependent bladder point and the above vaginal wall parameters at maximum Valsalva: $p < 0.05$ was considered significant.

3.2.3 Results

Linear regression (Table 3-2-1) showed that 77% ($R^2 = 0.77$, $p < 0.01$) of midsagittal anterior wall descent can be explained by the combination of apical position and vaginal length. The exclusion of the five patients from the original study increased the correlation between cystocele and apical position from $R^2 = 0.53$ to 0.60. Increasing vaginal length was positively correlated with greater degrees of anterior vaginal prolapse during maximal Valsalva ($R^2 = 0.30$, $p < 0.01$; Figure 3-2-3). Thus, 30% ($R^2 = 0.30$) of the variation in anterior wall descent was determined by vaginal wall length alone. The area

under the vaginal wall profile and the distal urethral location were also investigated for regression modeling but were found not to contribute much to the degree of anterior wall descent.

Table 3-2-1 Linear regression modeling

	Cumulative R^2	*R^2 added*	*p value*
Apical	0.60	–	<0.001
+Vaginal length	0.77	0.17	<0.001
+Distal point	0.78	0.01	<0.001
+Area under vaginal profile	0.81	0.03	<0.001

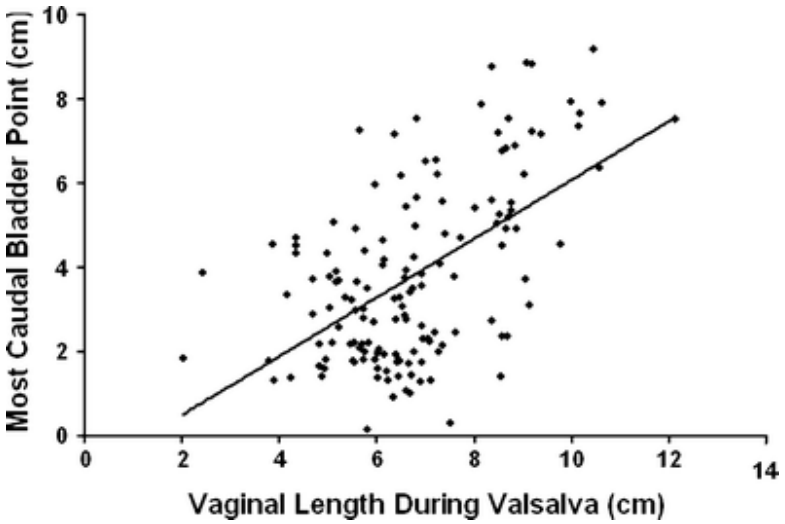

Figure 3-2-3 Vaginal length during Valsalva and distance of the most caudal bladder point below normal. There is a linear correlation $y = 0.69\ x - 0.85$, $R^2 = 0.30$

As would be expected from the correlation found between apical descent and anterior wall descent, there were subjects who had uterine descent and large cystoceles (Figure 3-2-4a). However, there were also subjects with relatively well-supported apical compartments who had large cystoceles with long anterior vaginal walls (Figure 3-2-4b). Other morphologic variants existed as well where there were examples of patients with cystoceles with normal and short vaginal wall lengths (Figure 3-2-4c, d, respectively).

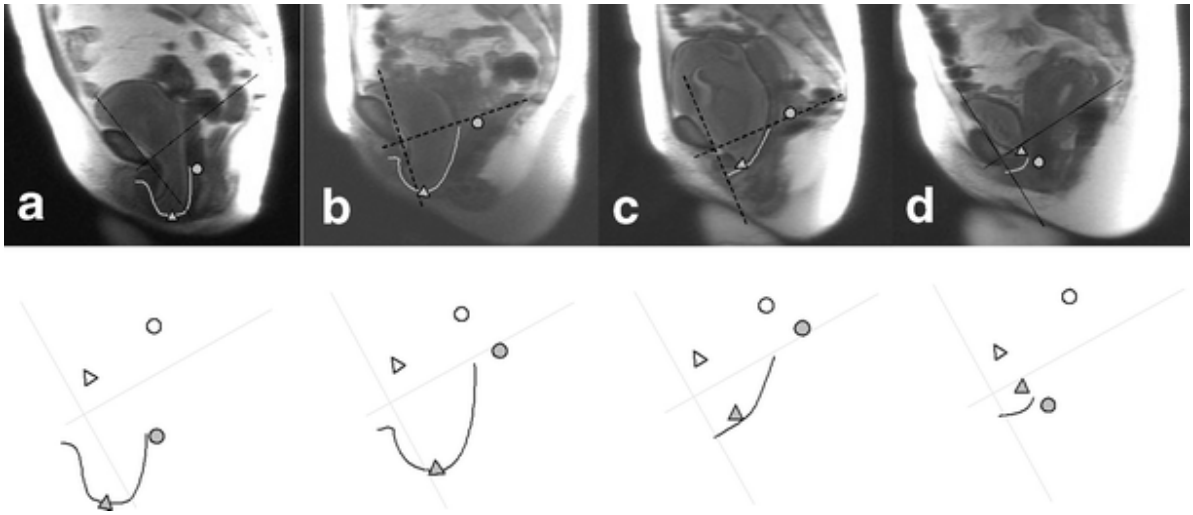

Figure 3-2-4 Subject examples showing relationship between apical support and vaginal length in determining the size of cystoceles. Top row: MR image with maximal Valsalva. Bottom row: Coordinate axis, vaginal tracings, as well as bladder and cervical locations. Images have been standardized for pelvic size and orientation. a Subject who had uterine descent and large cystocele. b Subject with relatively well-supported apical compartments who had large cystocele with a long anterior vaginal wall. c Subject with cystocele and a normal vaginal wall length. d Subject with cystocele with a short vaginal wall length

The relationship between apical descent and vaginal wall length was examined to see if apical descent resulted in longer vaginal length. The correlation was $R^2 = 0.36$, $p = 0.02$.

3.2.4 Discussion

Linear regression modeling shows that 77% of anterior wall descent can be explained by both vaginal length and apical descent measured on midsagittal dynamic MR images. A positive correlation was found between anterior wall descent and anterior vaginal wall length with 30% of variation in anterior wall descent being explained by the length of the vaginal wall. These relationships suggest that the disease mechanism of anterior wall prolapse is likely multifactoral resulting in different morphologic variants of cystocele. Anterior vaginal support has been simplified to a trapezoidal vaginal wall with connections at the top and laterally (DeLancey et al, 2002). Our previous work supports the hypothesis that defects of the apical support are related to cystocele formation (Summers et al, 2006). The weak correlation between apical descent and vaginal length

and the strong correlation between vaginal length and cystocele size suggest that alterations in the actual vaginal wall itself may be involved in cystocele development.

Vaginal wall characteristics have been previously evaluated. The fraction of smooth muscle in the anterior vaginal wall shows great variability among individuals (Morgan et al, 2003), and its contractility is significantly decreased in women with pelvic organ prolapse (Boreham et al, 2002, Boreham et al, 2002). Patients with prolapse have also been found to have alterations in collagen ratios and turn over of collagen (Chen et al, 2002, Moalli et al, 2004, Norton et al, 1992). Findings regarding the collagen content of these tissues have been inconsistent with some studies showing no change (Liapis et al, 2000, Liapis et al, 2001), and others increased content (Kokcu et al, 2002). Comparison of 3D vaginal models of patients with and without prolapse showed similar vaginal anterior–posterior thickness between groups suggesting that the vaginal wall of patients with prolapse is not attenuated (Hsu et al, 2005). The shear strength of vaginal wall specimens was lower in patients with pelvic floor dysfunction than normal controls (Kondo et al, 1994), and great variability in the tensile and bending strength of samples has also been observed (Cosson et al, 2004)

The vaginal apex has also been examined as the site of failure. One study reported that collagen content was similar between prolapse patients and controls at the vaginal apex but was lower in the parametrial tissue (Takano et al, 2002) . The resiliency of the apical support structures such as the uterosacral ligaments has also been found to be significantly reduced among women with symptomatic uterovaginal prolapse (Reay et al, 2003).

Dynamic MR imaging has been used for the evaluation and staging of pelvic organ prolapse (Etlik et al, 2005, Lienemann et al, 1997, Singh et al, 2001). Ozasa et al. (Ozasa et al, 1992) also used midsagittal dynamic MRI to asses changes in pelvic support in women with prolapse. They qualitatively compared descent using the relationship of a best-fit levator line and the pubic bone, however, did not perform quantitative measurements. The current study has the advantage of quantifying midsagittal changes

that occur during Valsalva. These quantifications deepen our understanding of anterior compartment prolapse mechanisms.

There are several limitations of this study. The dynamic sequence used is limited to a midsagittal view, thereby not allowing the study of changes that may occur in the lateral vaginal wall, which have been observed in anterior compartment prolapse (Richardson et al, 1981). Therefore, we cannot comment on the presence or effects of paravaginal defects. In addition, these sequences were acquired in the supine position, which may limit the descent of the pelvic structures. We minimized this limitation by careful coaching the woman to achieve the maximal prolapse and reviewed all the dynamic video clips to make sure that Valsalva was performed correctly. In the past, researchers have compared supine dynamic MR images with those performed in a sitting position in an open configuration scanner and found supine scans during straining to be comparable in documenting pelvic floor movement (Fielding et al, 1998, Bertsschinger et al, 2002). An additional limitation is represented by the example in Figure 3-2-4d. This woman has significant anterior wall prolapse and apical descent but yet has a short vaginal length. Although clinically, this woman does not have a shortened wall, she appears to on dynamic MR images because the anterior wall is folded in on itself like an accordion.

The association of increased midline vaginal length in anterior compartment prolapse provides objective data to be considered in the clinical thinking and treatment of cystoceles. Traditionally, anterior vaginal wall prolapse is attributed to either lateral detachment of the anterior vaginal wall at the pelvic side wall, referred to as a displacement “cystocele,” or as a central failure of the vaginal wall itself that results in a distension “cystocele.” Whether length changes are due to a paravaginal defect, midline defect, or are simply due to stretching of the vaginal wall once a cystocele becomes present will require further research. The association seen in this study nevertheless raises interesting clinical questions. For example, do traditional side-to-side plications address excess vaginal length associated with anterior compartment prolapse?

References

Bertsschinger KM, Hetzer FH, Roos JE, Treiber K, Marincek B, Hilfiker PR Dynamic MR imaging of the pelvic floor performed with patient sitting in an open-magnet unit versus with patient supine in a closed-magnet unit. Radiology 2002; 223(2):501–508

Blakeman PJ, Hilton P, Bulmer JN. Cellular proliferation in the female lower urinary tract with reference to oestrogen status. BJOG 2001;108:813–6.

Boreham MK, Wai CY, Miller RT, Schaffer JI, Word RA. Morphometric properties of the posterior vaginal wall in women with pelvic organ prolapse. Am J Obstet Gynecol 2002;187:1501–9.

Boreham MK, Miller RT, Schaffer JI, Word RA. Smooth muscle heavy chain and caldesmon expression in the anterior vaginal wall of women with and without pelvic organ prolapse. Am J Obstet Gynecol 2001;185:944–52.

Boreham MK, Wai CY, Miller RT, Schaffer JI, Word RA. Morphometric analysis of smooth muscle in the anterior vaginal wall of women with pelvic organ prolapse. Am J Obstet Gynecol 2002;187:56–63.

Chen BH, Wen Y, Li H, Polan ML. Collagen metabolism and turnover in women with stress urinary incontinence and pelvic prolapse. Int Urogynecol J Pelvic Floor Dysfunct 2002;13(2):80–87

Cosson M, Lambaudie E, Boukerrou M, Lobry P, Crepin G, Ego A A biomechanical study of the strength of vaginal tissues. Results on 16 post-menopausal patients presenting with genital prolapse. Eur J Obstet Gynecol Reprod Biol 2004;112(2):201–205

DeLancey JOL. Fascial and muscular abnormalities in women with urethral hypermobility and anterior vaginal wall prolapse. Am J Obstet Gynecol 2002;187:93–98

DeLancey JO, Morgan DM, Fenner DE, Kearney R, Guire K, Miller JM, Hussain H, Umek W, Hsu Y, Ashton-Miller JA. Comparison of levator ani muscle defects and function in women with and without pelvic organ prolapse. Obstet Gynecol 2007;109:295–302

Etlik O, Arslan H, Odabasi O, Odabasi H, Harman M, Celebi H et al. The role of the MR-fluoroscopy in the diagnosis and staging of the pelvic organ prolapse. Eur J Radiol 2005;53:136–141

Fielding JR, Griffiths DJ, Versi E, Mulkern RV, Lee MLT, Jolesz FA (1998) MR imaging of pelvic floor continence mechanisms in the supine and sitting positions. Am J Roentgenol 171:1607–1610

Gitsch E, Palmrich AH. Gynelogical operative anatomy. Berlin, Germany: De Gruyter; 1977.

Hendrix SL, Clark A, Nygaard I, Aragaki A, Barnabei V, McTiernan A. Pelvic organ prolapse in the women's health initiative: gravity and gravidity. Am J Obstet Gynecol 2002;186(6):1160–1166

Hoyte L, Ratiu P. Linear measurements in 2-dimensional pelvic floor imaging: the impact of slice tilt angles on measurement reproducibility. Am J Obstet Gynecol 2001;185:537–44.

Hsu Y, Chen L, DeLancey JOL, Ashton-Miller JA Vaginal thickness, cross-sectional area, and perimeter in women with and those without prolapse. Obstet Gynecol 2005;105(5):1012–1017

Kokcu A, Yanik F, Cetinkaya M, Alper T, Kandemir B, Malatyalioglu E Histopathological evaluation of the connective tissue of the vaginal fascia and the uterine ligaments in women with and without pelvic relaxation. Arch Gynecol Obstet 2002;266(2):75–78

Kondo A, Narushima M, Yoshikawa Y, Hayashi H. Pelvic fascia strength in women with stress urinary incontinence in comparison with those who are continent. Neurourol Urodyn 1994;13(5):507–513

Liapis A, Bakas P, Pafiti A, Hassiakos D, Frangos-Plemenos M, Creatsas G. Changes in the quantity of collagen type I in women with genuine stress incontinence. 2000;Urol Res 28(5):323–326

Liapis A, Bakas P, Pafiti A, Frangos-Plemenos M, Arnoyannaki N, Creatsas G. Changes of collagen type III in female patients with genuine stress incontinence and pelvic floor prolapse. Eur J Obstet Gynecol Reprod Biol 2001;97:76–9.

Lienemann A, Anthuber C, Baron A, Kohz P, Reiser M (1997) Dynamic MR colpocystorectography assessing pelvic-floor descent. Eur Radiol 1997;7(8):1309–1317

Moalli PA, Talarico LC, Sung VW, Klingensmith WL, Shand SH, Meyn LA, Watkins SC. Impact of menopause on collagen subtypes in the arcus tendineous fasciae pelvis. Am J Obstet Gynecol 2004;190(3):620–627

Morgan DM, Iyengar J, DeLancey JO. A technique to evaluate the thickness and density of nonvascular smooth muscle in the suburethral fibromuscular layer. Am J Obstet Gynecol 2003;188(5):1183–1185

Nichols DH, Randall CL. Vaginal surgery. 4th ed. Baltimore (MD): Williams & Wilkins; 1996.

Norton P, Boyd C, Deak S. Collagen synthesis in women with genital prolapse or stress urinary incontinence. Neurourol Urodyn 1992;11:300–1.

Ozasa H, Mori T, Togashi K (1992) Study of uterine prolapse by magnetic resonance imaging: Topographical changes involving the levator ani muscle and the vagina.

Gynecol Obstet Invest 34:43–48

Reay Jones NH, Healy JC, King LJ, Saini S, Shousha S, Allen-Mersh TG Pelvic connective tissue resilience decreases with vaginal delivery, menopause and uterine prolapse. Br J Surg 2003;90(4):466–472

Ricci JV, Thom CH. The myth of a surgically useful fascia in vaginal plastic reconstructions. Q Rev Surg 1954;11:253–61.

Ricci JV, Lisa JR, Thom CH, Kron WL. The relationship of the vagina to adjacent organs in reconstructive surgery: a histologic study. Am J Surg 1947;74:387–410.

Richardson AC, Lyon JB, Williams NL. A new look at pelvic relaxation. Am J Obstet Gynecol 1976;126:568–73.

Richardson AC, Edmonds PB, Williams NL. Treatment of stress urinary incontinence due to paravaginal fascial defect. Obstet Gynecol 1981;57:357–62.

Richardson AC. Paravaginal repair. In: Hurt WG, editor. Urogynecologic surgery. 2nd ed. Philadelphia (PA): Lippincott Williams & Wilkins; 2000. p. 71–80.

Richardson AC, DeLancey JOL. Anatomy of genital support. In: Hurt WG, editor. Urogynecologic surgery. 2nd ed. Philadephia (PA): Lippincott Williams & Wilkins; 2000. p. 21–35.

Shull BL, Bachofen C, Coates KW, Kuehl TJ .A transvaginal approach to repair of apical and other associated sites of pelvic organ prolapse with uterosacral ligaments. Am J Obstet Gynecol 2000;183:1365–1373

Singh K, Reid WM, Berger LA Assessment and grading of pelvic organ prolapse by use of dynamic magnetic resonance imaging. Am J Obstet Gynecol 2001;185(1):71–77

Summers A, Winkel LA, Hussain HK, DeLancey JOL. The relationship between anterior and apical compartment support. Am J Obstet Gynecol 2006;194:1438–1443

Takano CC, Girao MJ, Sartori MG, Castro RA, Arruda RM, Simoes MJ, et al. Analysis of collagen in parametrium and vaginal apex of women with and without uterine prolapse. Int Urogynecol J Pelvic Floor Dysfunct 2002;13:342–5.

Tulikangas PK, Walters MD, Brainard JA, Weber AM. Enterocele: is there a histologic defect? Obstet Gynecol 2001;98:634–7.

Vardy MD, Landsay R, Scotti RJ, Mikhail M, Richart RM, Nieves J, et al. Short-term urogenital effects of raloxifene, tamoxifen and estrogen. Am J Obstet Gynecol 2003;189:81–8.

Weber AM, Walters MD. Anterior vaginal prolapse: review of anatomy and techniques of surgical repair. Obstet Gynecol 1997;89:311–8.

Weber AM, Walters MD, Piedmonte MR, Ballard LA Anterior colporrhaphy: a randomized trial of three surgical techniques. Am J Obstet Gynecol 2001;185:1299–1304

Chapter 4

2D Conceptual Lumped Parameter Model

ABSTRACT

Objective: To use a biomechanical model to explore how impairment of the pubovisceral portion of the levator ani muscle and/or the apical vaginal suspension complex might interact to affect anterior vaginal wall prolapse severity.

Method: A lumped parameter biomechanical model of the anterior vaginal wall and its support system was developed and implemented in Matlab. The anterior vaginal wall and its main muscular and connective tissue support elements, namely the levator plate, pubovisceral muscle, cardinal and uterosacral ligaments were included and their geometry was based on mid-sagittal plane magnetic resonance scans. Material properties were based on published data. The change in the sagittal profile of the anterior vaginal wall during a maximum Valsalva was then predicted for different combinations of pubovisceral muscle and connective tissue impairment.

Results: Under raised intra-abdominal pressure, the magnitude of anterior vaginal wall prolapse was shown to be a combined function of both pubovisceral muscle and uterosacral and/or cardinal ligament ("apical supports") impairment. Once a certain degree of pubovisceral impairment was reached, the genital hiatus opened and a prolapse developed. The larger the pubovisceral impairment, the larger the anterior wall prolapse became. A 90% impairment of apical support led to an increase in anterior wall prolapse from 0.3 cm to 1.9 cm (a 530% increase) at 60% pubovisceral muscle impairment, and from 0.7 cm to 2.4 cm (a 240% increase) at 80% pubovisceral muscle impairment.

Conclusions: These results suggest that a prolapse can develop as a result of impairment of the muscular and apical supports of the anterior vaginal wall.

4.1 Introduction

Pelvic organ prolapse is a common disease that prevents women from enjoying a full and active life. In the US, approximately 200,000 women (Boyles et al, 2003) have surgery to repair prolapse annually with a cost to society that exceeds one billion dollars per year (Subak et al, 2001). Anterior vaginal wall prolapse, clinically known as cystocele, is the most common form of pelvic organ prolapse. (Hendrix et al, 2002)

At present, our understanding of anterior vaginal wall support mechanisms is focused primarily on paravaginal attachments. (Richardson et al, 1976,DeLancey et al, 1992) Recently two additional observations have been made. First, levator ani muscle damage is seen in women with prolapse (Tunn et al, 1998, Singh et al, 2003, Hoyte et al, 2001, Hoyte et al,2004). Second, anterior compartment prolapse is highly correlated ($r = 0.73$) with loss of apical support (Summers et al, 2006). How these observations help explain anterior compartment failure has been unclear and is a goal of the present paper.

A common approach to analyze how a complex biological system works is to represent the behavior of interest with a mathematical model. Such models yield can useful mechanistic insights and even predict system responses with reasonable accuracy (Alexander et al, 2003). One class of such models is the "lumped parameter" model in which the relevant features of the biological system are divided into relatively few subunits. Through simplifying assumptions, the overall properties of each subunit can be approximated by an equation. Hence, the relationship between the tensile force and length of the pubovisceral muscle can most simply be represented by a lumped parameter representing the development of active contractile force and another representing the passive resistance of the muscle to stretch. Overall system behavior is then predicted by assembling and solving the system of equations that represent the various subunits and how they physically interact with one another.

The aim of this study, therefore, was to develop and test a first-generation model to investigate how changes in pelvic floor muscle support and apical connective tissue

support interact to affect anterior vaginal wall prolapse under conditions of raised intra-abdominal pressure.

4.2 Methods

A sagittally-symmetric, lumped parameter, biomechanical model of the anterior vaginal wall and its support system was developed based on our previous anatomical work (DeLancey et al, 1992,DeLancey et al, 1994, DeLancey et al, 1999,DeLancey et al, 2002). As a first step, the dimensions and orientation of the anterior vaginal wall and its support system were measured from mid-sagittal plane magnetic resonance scans of 10 healthy volunteers. This sample size was judged sufficient, based on the authors' previous experience, to yield representative geometry. These women were recruited from 2001 to 2003 as controls in an case-control study, approved by University of Michigan IRBMED, comparing findings in women with normal support to women with pelvic organ prolapse. They denied having incontinence or prolapse symptoms and had demonstrated normal support on POP-Q examination (Bump et al, 1996) (no vaginal wall point lower than one centimeter above the hymen). These women had a mean age of 58.8 years ($\pm$ standard deviation of 12.2 years) and parity of 2.45 ($\pm$ 1.03). Axial, sagittal and coronal magnetic resonance images of the pelvic floor region were taken at 5 mm intervals as previously described (Chou et al, 2001). The dimensions and orientation of the anterior vaginal wall and levator plate were measured in the mid-sagittal plane at rest. The mean length of the vaginal wall was 7.0 ($\pm$ 1.0) cm, with a mean vaginal inclination angle of 62.4 ($\pm$ 7.8) ^{o}. The mean length of the levator plate was 10.4 $\pm$ 0.9 cm with a mean levator inclination angle of 47.9 ($\pm$ 4.8) ^{o}.

A 3-D model of the levator ani muscles, vagina, rectum, cardinal and uterosacral ligaments ("apical supports"), pubic bone and sacrum was created from a representative subject's MR images using 3-D-Slicer version 2.1b1, as previously described (Chen et al 2005,Hsu et al, 2005). The attachments of the levator ani muscle to the pubic bone and the lines-of-action of the apical supports were located based on 3-dimensional reconstructions. A two-dimensional (2-D), sagittally-symmetric, lumped parameter, biomechanical model was then created by projecting the 3-D geometry of anterior vagina

wall and its support system onto the mid-sagittal plane (Figure 4-1). The anterior vaginal wall was modeled as a deformable and stretchable membrane lying on the rectum, which was supported by the levator plate. The anterior vaginal wall was fixed at the perineal membrane which was assumed to be stationary during Valsava. For simplicity, the levator plate was modeled as a rigid "trapdoor" hinged on the sacrum (SAC). To isolate the anterior vaginal wall effects, no relative motion was assumed to occur between the rectum and the levator plate. The pubovisceral portion of the levator ani muscle (PVM) was considered to control levator plate inclination with respect to the pelvis and was modeled using both an active contractile element and a passive elastic spring element ($F_{pvm} = F_{active} + F_{passive}$)

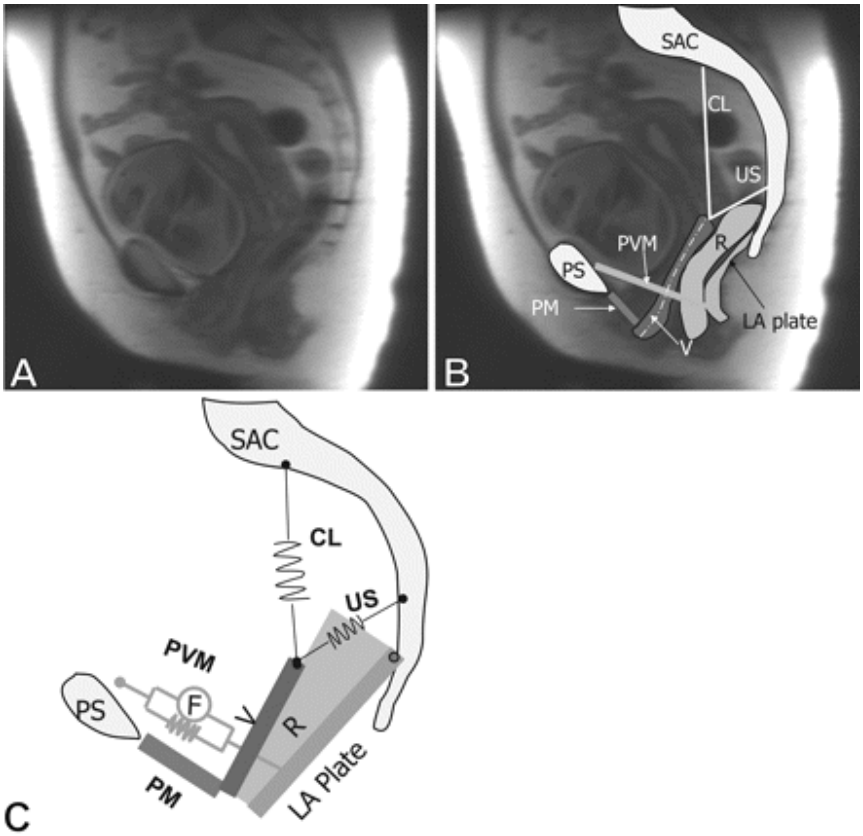

Figure 4-1 Model Development. *A:* mid-sagittal MR image. *B:* modeled element traced or projected on mid-sagittal MR image. *C:* lumped parameter biomechanical model. Pubovisceral muscle (PVM) is modeled as a spring in parallel with an active force generator. PS: pubic symphysis; SAC: sacrum; PM: perineal membrane; LA plate: levator plate; R: rectum; V: vagina; CL: cardinal ligament spring; US: uterosacral ligament spring; B: bladder; UT: uterus. © Biomechanics Research Laboratory, University of Michigan, 2006

Apical support, provided to the vagina in Level I by the cardinal ligament and the uterosacral ligament, was represented by two passive elastic springs (Figure 4-1) attached to the top of the vaginal wall. An exponential relationship between force and elongation for anterior vaginal wall membrane and all passive springs (including passive material property of pubovisceral muscle and the apical supports) was assumed to present the nonlinear (hyperelastic) material property of biological tissue, that is

$$F = C1 \times (e^{C2 \times (\frac{l - l_0}{l_0})} - 1)$$

where C1 and C2 are the material property parameters, l is the current length and l_0 is the initial length. The material property parameters of the vaginal wall were held constant through these simulations to focus on the interaction of apical supports and levator activity.

The vaginal wall, pubovisceral muscle and apical supports material properties used were based on values from existing literature (Yamada et al 1970, Bartscht et al, 1988). Table 4-1 shows the dimension and material property of each model element.

Table 4-1: Dimension and material property of each element of the 2-D biomechanical model (* R is modeled as rigid spacer allowing no movement relative to the model levator ani plate. LA: levator ani; PVM: pubovisceral muscle)

	Original length (cm)	Original inclination (relative to horizontal in degrees)	Equation representing material properties (F in Newton and l in cm)
Vaginal wall	7	62	$F = 1.00 \times (e^{5.6 \times (\frac{l - l_0}{l_0})} - 1)$
LA plate (R*)	10	48	Rigid plate
PVM	9.4	152	$F = 1.00 \times (e^{7 \times (\frac{l - l_0}{l_0})} - 1)$
Cardinal	7.6	81	$F = 4.27 \times (e^{0.61 \times (\frac{l - l_0}{l_0})} - 1)$
Uterosacral	4.8	25	$F = 4.27 \times (e^{0.61 \times (\frac{l - l_0}{l_0})} - 1)$

The model was implemented in Matlab^R (The MathWorks Inc., Natick, MA). To model a Valsalva maneuver, the model abdomen was pressurized with 70 cmH_2O of intra-abdominal pressure in order to represent a maximum Valsalva maneuver (Howard et al, 2000). In a woman with normal support, clinical observations show that a maximum Valsalva maneuver causes little displacement of the pelvic floor, if the pelvic floor muscles are actively contracted so as to equilibrate the downward intra-abdominal pressure acting on the levator plate (Shafik et al, 2003). Therefore, in our model we assumed that the intact pubovisceral muscle can increase its contractile force sufficiently above the baseline resting tone so as to maintain hiatus closure under increased intra-abdominal pressure, as observed in women with normal support. Therefore, the model anterior vaginal wall was considered to be completely supported by the rectum and levator plate, without tension on the cardinal and uterosacral ligaments. The mean maximum vaginal closure force was assumed to be 2.8 Newtons which is the average value reported in the literature (Morgan et al, 2005, Morin et al, 2004) (Figure 4-2a). Since the force exerted by the pubovisceral muscles holds the trap door or urogenital hiatus closed, intra-abdominal pressure cannot induce inferior-superior tension in the anterior vaginal wall because there is no pressure differential being generated.

To use the model to simulate the two mechanisms underlying prolapse, we modeled the pubovisceral impairment (indicated by *Defect%)* by simulating loss of both the pubovisceral muscle's active contractile force (F_{active}) and also its passive spring constant (derived its passive resistance to stretch in the uncontracted state), that is

$$F_{pcm}{}' = (1 - Defect\%) \times (C1 \times (e^{C2 \times (\frac{l - l_0}{l_0})} - 1) + F_{active})$$

Impairment of the connective tissue apical support (indicated by *Defect%)* was modeled as a decrease in their elastic properties, that is

$$F' = (1 - Defect\%) \times C1 \times (e^{C2 \times (\frac{l - l_0}{l_0})} - 1)$$

Model simulations were run with impairments of 0, 20, 40, 60, 80 % decrements in the maximal force that the pubovisceral muscle could generate and 0, 50, 90% increases in the elasticity of the apical support. Since we focused on the interaction between pubovisceral muscle and apical supports, the material property of the vaginal wall was held constant in all simulations. The primary outcome measure was the change in anterior vaginal wall curvature showing anterior vaginal wall deformation, and secondary outcome measures were the downward angular displacement of the levator plate and the downward translation of the top of the anterior vaginal wall under the action of 70 cmH_2O intra-abdominal pressure. We used the descent of the most dependent point of the vaginal wall as a measure of prolapse size, as shown in Figure 4-2b.

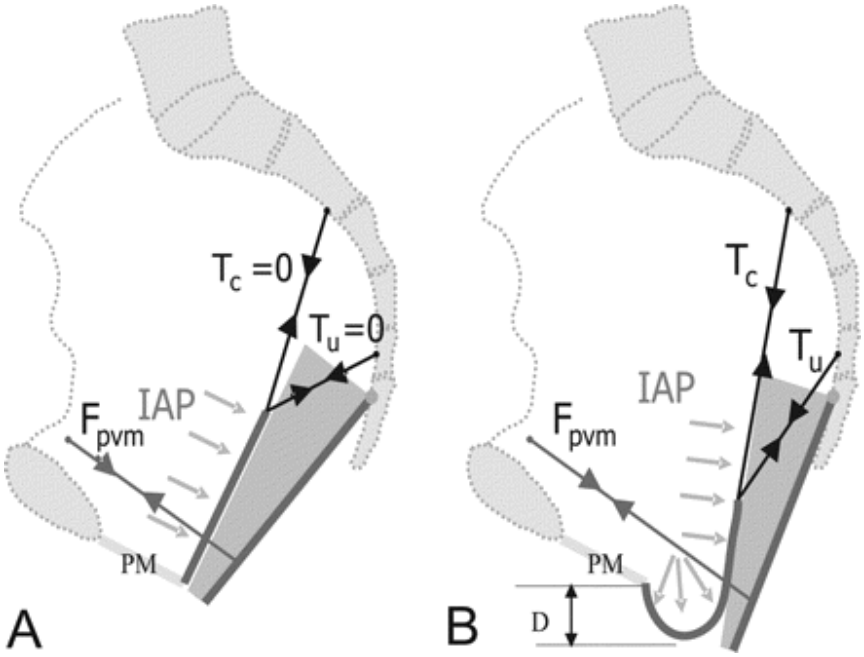

Figure 4-2. Force diagram showing the loading of the anterior vaginal wall and its support system.
A: loading anterior vaginal wall with normal muscular support ; B: loaded pelvic floor with defective muscular support and part of vaginal wall exposed to intra-abdominal pressure (light grey arrows). IAP denotes intra-abdominal pressure; Fpvm: tensile force generated by pubovisceral muscle between the projection of its origin on the pelvic side wall and insertion on the levator plate; Tc and Tu: tensile forces generated by the cardinal and uterosacral ligaments; D: the decent of the most dependent point of vaginal wall from end of perineal membrane (PM) which is used as the measurement of prolapse size in the simulation. Note descent of the vaginal apex as well as vaginal wall protrusion. © Biomechanics Research Laboratory, University of Michigan, 2006

4.3 Results

General model behavior under load is shown in Figure 2b. When the system with impaired muscle and connective tissue was loaded with maximum intra-abdominal pressure (Valsalva), downward rotation of the levator plate occurred when the defective pubovisceral muscle could no longer generate sufficient force to counterbalance the abdominal pressure increase. In this situation, the model trap-door begins to 'open' such that the lower part of the anterior vaginal wall is no longer supported by the levator ani plate. The unsupported distal region of vaginal wall becomes the tensile structure that separates a higher intra-abdominal pressure zone and a lower atmospheric pressure zone. This pressure differential causes the downward 'bulging' (deformation) of the distal anterior vaginal wall in the areas not supported by the levator ani muscle. This, in turn, induces a superior-inferior tension force in the upper anterior vaginal wall. The apical supports are now placed under tension as they resist the downward movement of the upper vaginal wall until a new mechanical equilibrium is achieved in the system.

The specific simulation results with different combinations of pubovisceral and apical support impairment are shown in Figure 4-3. Here, the degree of anterior vaginal wall descent is shown as the distance below the perineal membrane, which lies at the level of the hymenal ring. For the results in the top row (Figure 4-3 a, b, and c), the apical supports had the normal material parameter constants. The bottom row shows the results with 90% apical support impairment. In the first column (Figure 4-3 a and d), the pubovisceral muscle has normal active contractile function and normal passive material properties, while the second and third columns show the effects of increasing pubovisceral muscle impairment by 60% and 90%, respectively.

When the pubovisceral muscle has normal properties (Figure 4-3a), no anterior wall deformation is seen. With pubovisceral impairment (Figure 4-3b & c), some degree of anterior vaginal prolapse occurs. With normal muscles, but impaired apical support (Figure 4-3d), no displacement occurs because the vaginal wall is not subjected to a pressure differential.

The interaction between pubovisceral muscle defect and apical support impairment is shown in the bottom row (Figure 4-3e and f). When the apical support impairment was superimposed on the pubovisceral muscle impairment there was a loss of resistance to the descent of apical anterior vaginal wall, resulting in a much larger prolapse. The prolapse size, D, defined as the largest descent of the most independent point, is also shown in Figure 4-3. A 90% impairment of apical support led to an increase in anterior wall prolapse from 0.3 cm to 1.9 cm (a 530% increase) at 60% pubovisceral muscle impairment (Figure 4-3c vs. 3f), and from 0.7 cm to 2.4 cm (a 240% increase) at 80% pubovisceral muscle impairment (Figure 4-3b vs. 3e).

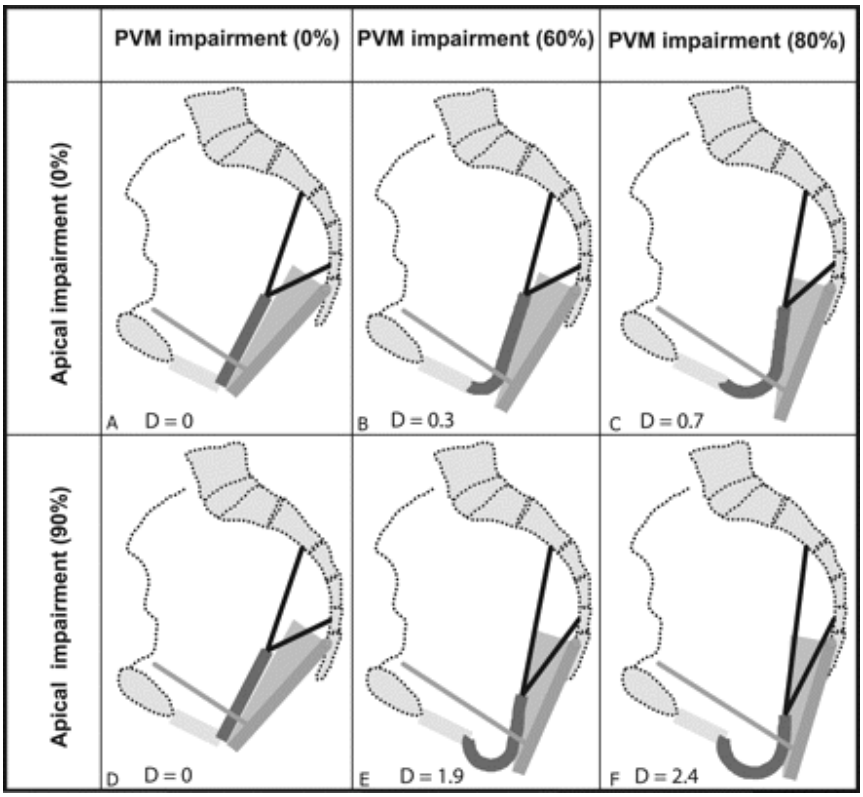

Figure 4-3. Simulated deformation of the model anterior vaginal wall, and its support system, under maximal Valsalva with various degrees of pubovisceral muscle (PVM) and cardinal and uterosacral ligament impairment (indicated in percent). D presents the size of prolapse measured as the decent of the most dependent point of vaginal wall from end of perineal membrane. © Biomechanics Research Laboratory, University of Michigan, 2006

The prolapse size is shown as a function of apical support impairment for different degree of pubovisceral impairment in Figure 4-4. The size of the prolapse

increased exponentially with increasing apical support impairment.

To verify that the simulation results were reasonable approximations of the interactions between connective tissue and muscular support of vaginal wall, these findings were compared to a typical magnetic resonance image of a patient with cystocele in both the resting state as well as under a maximum Valsalva (Figure 4-5). In the resting state, the patient has a relatively normal configuration. But with increasing intra-abdominal pressure associated with a Valsalva maneuver, the levator plate is pushed posteriorly and downwards to a more vertical orientation, the anterior vaginal wall is pushed inferiorly via the hiatus, while the uterus is pulled down by anterior vaginal wall. This scenario matches well with our model simulation thereby helping to validate the behavior of our model.

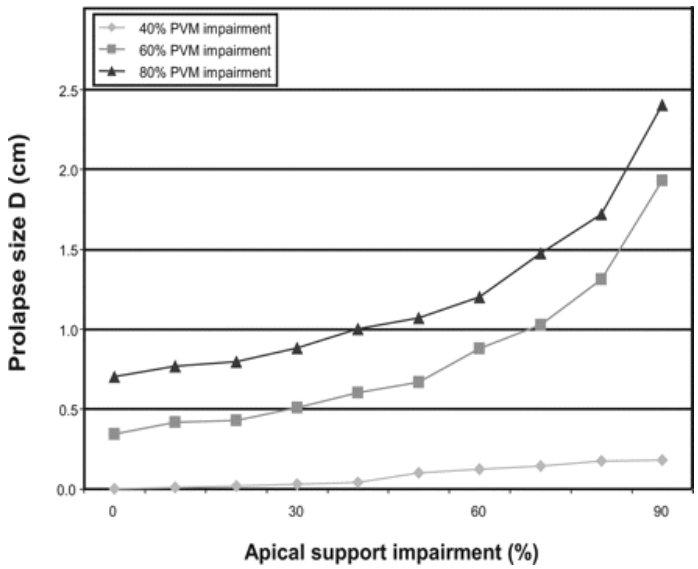

Figure 4-4: Prolapse size measured by the most dependent point on the vaginal wall as a function of apical support impairment for different degrees of pubovisceral muscle (PVM) impairment. © Biomechanics Research Laboratory, University of Michigan, 2006

4.4 Discussion

This paper presents the development of a simple 2-D model that was used to investigate how anterior vaginal wall muscular and connective tissue supports affect the size of anterior vaginal wall prolapse. The model is suitable for examining first-order effects of the interaction between these supportive elements in the presence of impairments in the pubovisceral muscle and apical support tissues. The model is

focused on anterior vaginal wall prolapse because it is the most common form of pelvic organ prolapse (Hendrix et al, 2002) and a form that can be used to initiate meaningful investigation into muscle/connective tissue interaction. We chose to focus on the apical connective tissue supports as a result of recent data (Summers et al, 2006) showing a strong correlation between apical descent and anterior compartment prolapse, recognizing that further work will be needed to add other elements of the support system. This model shows important qualitative results on how a combination of muscular and connective tissue impairments affects prolapse magnitude. The resulting anterior wall prolapses also mimic those seen clinically, thereby providing validity for our model.

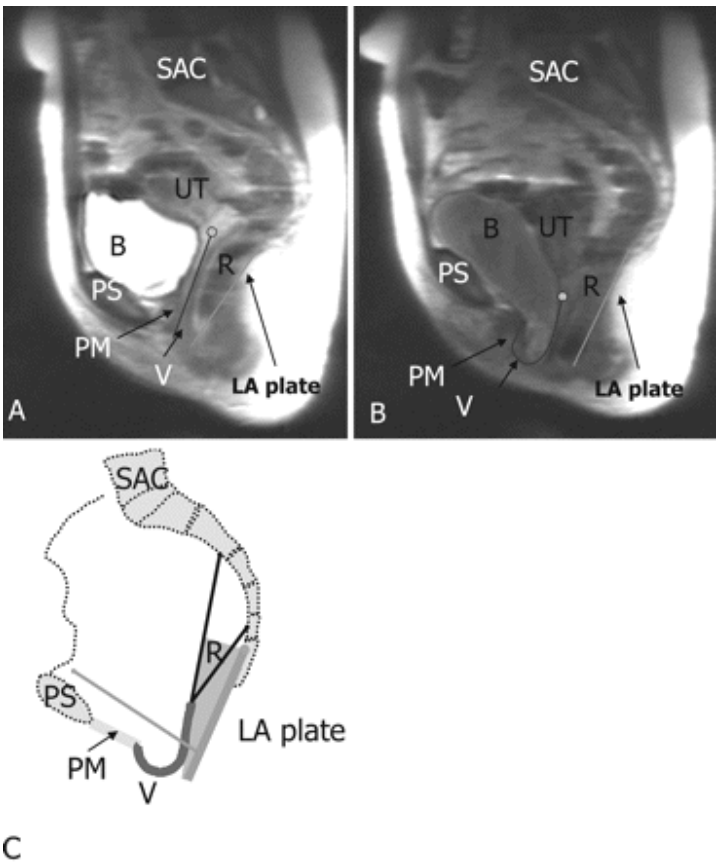

Figure 4-5. Validation of the model. *A:* mid-sagittal MR image of resting status; *B:* mid-sagittal MR image at maximum Valsava; *C:* sample model simulation result having a similar configuration as in (b). In this figure PS denotes pubic symphysis; SAC: sacrum; PM: perineal membrane; PVM: pubovisceral muscle; LA plate: levator plate; R: rectum; V: vagina; CL: cardinal ligament; US: uterosacral ligament; B: bladder; and UT: uterus © Biomechanics Research Laboratory, University of Michigan, 2006

The clinical significance of this article lies in its demonstration of the interaction between apical connective tissue support and the levator ani muscle impairments that result in anterior vaginal wall prolapse. This links research showing that the levator muscles are abnormal in women with pelvic organ prolapse (Tunn et al,1998, Singh et al, 2003, Hoyte et al, 2001, Hoyte et al, 2004) with observations of connective tissue abnormalities in pelvic organ prolapse (Richardson et al, 1976,DeLancey et al, 2002, Jackson et al, 1996). Our simulations also suggest that to some degree normal muscle and normal connective tissue function can compensate for injury to the other system. It is when both systems have impairments that the larger anterior vaginal wall prolapse is predicted. This can partly explain why women with levator ani muscle defect are more likely to have prolapse (Hoyte et al, 2004), but not all women with levator ani muscle defects have developed anterior vaginal wall prolapse.

When the intact pubovisceral muscle maintains urogenital hiatus closure, there is no tension in the vaginal wall because it is well supported inside the abdominal cavity by the levator plate and therefore no pressure differential acts across it. This assumption is based on clinical observations in nulliparous women that reveal minimal descent of the pelvic floor during Valsalva when the muscles are contracted. When the pubovisceral muscle is defective and its contractile force is reduced, then the model predicted that less hiatal closure force is generated, which agrees with clinical measurements showing a 30% reduction in force among women with stress incontinence (Morin et al, 2004). At a certain level of pubovisceral defect, the muscles are no longer able to maintain hiatal closure, and the distal vagina is now exposed to a pressure differential as it is interposed between the high abdominal pressure zone and lower atmospheric pressure. This pressure differential deforms the vaginal wall, driving it inferiorly towards the low pressure region. The behavior of our model extends previous theoretical work of the concept of the “pelvic valve” (Porges et al, 1960).

It is important to recognize that there are inherent limitations in this type of research. In this first simulation we chose to focus the analysis on the anterior vaginal wall and have made some simplifying assumptions. For example, it was assumed there is no deformation of levator plate or rectal movement relative to the levator plate. Second, this model is focused on the interaction between muscular support and apical suspension on anterior vaginal wall support. In this two-dimensional model, the paravaginal supports of the anterior vaginal wall that attach laterally to the pelvic sidewall were not specifically modeled because this requires a more complex, 3-dimensional, approach. From a structural mechanics point of view, paravaginal support adds a reinforcing element to the mid-portion of the vaginal wall which will reduce its descent through the hiatus. In our model, we found that we needed to adjust the property of the vaginal wall tissue to be ten times stiffer than published experimental results in order to obtain reasonable model results. This need may reflect the lack of paravaginal support. Also, stretch is not necessarily uniform along each element of the model as assumed; it can vary locally along and across the elements, especially if the thickness varies. The effect of non-uniform stretch in these structures requires further investigation, particularly if systematic regional variations in properties are found. Finally, the elements in the model were assumed to have hyperelastic material properties, with increasing resistance to stretch as is indeed found in many collagenous structures, but it is a limitation that no time dependent behavior was represented. Despite these simplifications, we believe this simple model captures the qualitative behavior of the system and yields useful predictions. In the future, distributed parameter models, such as finite element models, may prove to be more accurate and better for the three-dimensional analyses that are needed.

This is a first attempt to use biomechanical modeling to study the mechanics of pelvic organ support. The model offers an opportunity to analyze fundamental concepts related to how injury of levator ani muscle and impairment of connective tissue can lead to anterior vaginal wall prolapse.

References

Alexander RM. Modelling approaches in biomechanics. Phil Trans Roy Soc Lond B Biol Sci. 2003; 358(1437):1429-35.

Bartscht KD, Delancey JOL. A technique to study the passive supports of the uterus. Obstet Gynecol. 1988 Dec;72(6):940-3

Boyles SH, Weber AM, Meyn L. Procedures for pelvic organ prolapse in the United States, 1979-1997, Am J Obstet Gynecol 2003;188:108-15

Bartscht KD, Delancey JOL. A technique to study the passive supports of the uterus. Obstet Gynecol. 1988 Dec;72(6):940-3

Bump RC, Mattiasson A, Bo K, Brubaker LP, DeLancey JO, Klarskov P, Shull BL, Smith AR. The standardization of terminology of female pelvic organ prolapse and pelvic floor dysfunction. Am J Obstet Gynecol. 1996; 175(1):10-7.

Chen L, Hsu Y, Ashton-Miller JA, Delancey JO. Measurement of the pubic portion of the levator ani muscle in women with unilateral defects in 3-D models from MR images. Int J Gynaecol Obstet. 2006 92:234–41

Chou Q. DeLancey JO. A structured system to evaluate urethral support anatomy in magnetic resonance images. Am J ObstetGynecol 2001; 185(1):44-50

DeLancey JOL. Anatomic aspects of vaginal eversion after hysterectomy. Am J Obstet Gynecol 1992;166:1717-1728.

DeLancey JOL. Structural support of the urethra as it relates to stress urinary incontinence: The hammock hypothesis. Am J Obstet Gynecol 1994;170:1713-1720.

DeLancey JOL. Structural anatomy of the posterior pelvic compartment as it relates to rectocele. Am J Obstet Gynecol 1999;180:815-23.

DeLancey JOL. Fascial and muscular abnormalities in women with urethral hypermobility and anterior vaginal wall prolapse. Am J Obstet Gynecol, 2002;187:93-8.

Hendrix SL, Clark A, Nygaard I, Aragaki A, Barnabei V, McTiernan A. Pelvic organ prolapse in the Women's Health Initiative: gravity and gravidity. Am J Obstet Gynecol. 2002 Jun;186(6):1160-6.

Howard D, Miller JM, DeLancey JOL, Ashton-Miller JA. Differential Effects of Cough, Valsalva, and Continence Status on Vesical Neck Movement. Obstet Gyenecol 2000; 95: 535-540.

Hoyte L, Schierlitz L, Zou K, Flesh G, Fielding JR. Two- and 3-dimensional MRI comparison of levator ani structure, volume, and integrity in women with stress incontinence and prolapse. Am J Obstet Gynecol. 2001 Jul;185(1):11-9.

Hoyte L, Jakab M, Warfield SK, Shott S, Flesh G, Fielding JR. Levator ani thickness variations in symptomatic and asymptomatic women using magnetic resonance-based 3-dimensional color mapping. Am J Obstet Gynecol. 2004 Sep;191(3):856-61.

Hsu Y, Chen L, Delancey JO, Ashton-Miller JA. Vaginal thickness, cross-sectional area, and perimeter in women with and those without prolapse. Obstet Gynecol. 2005;105:1012-7.

Jackson SR, Avery NC, Tarlton JF, Eckford SD, Abrams P, Bailey AJ. Changes in metabolism of collagen in genitourinary prolapse. Lancet 1996;347:1658-61.

Morgan DM, Kaur G, Hsu Y, Fenner DE, Guire K, Miller J, Ashton-Miller JA, Delancey JO, Does vaginal closure force differ in the supine and standing positions? Am J Obstet Gynecol. 2005 May;192(5):1722-8.

Morin M, Bourbonnais D, Gravel D, Dumoulin C, Lemieux MC. Pelvic floor muscle function in continent and stress urinary incontinent women using dynamometric measurements. Neurourol Urodyn. 2004;23(7):668-74.

Porges R, Porges J, Blinick G. Mechanisms of Uterine Support and the Pathogenesis of Uterine Prolapse. Obstetrics and Gynecology 1960 Jun; 15(6):711-726

Richardson AC, Lyon JB, Williams NL. A new look at pelvic relaxation. Am J Obstet Gynecol. 1976 Nov 1;126(5):568-73

Shafik A, Doss S, Asaad S. Etiology of the resting myoelectric activity of the levator ani muscle: physioanatomic study with a new theory. World J Surg. 2003 Mar;27(3):309-14.

Singh K, Jakab M, Reid WM, Berger LA, Hoyte L. Three-dimensional magnetic resonance imaging assessment of levator ani morphologic features in different grades of prolapse. Am J Obstet Gynecol. 2003; 188(4):910-5.

Subak LL, Waetjen LE, van den Eden S, Thom DH, Vittinghoff E, Brown JS, Cost of pelvic organ prolapse surgery in the United States. Obstet Gynecol 2002; 98:646-51

Summers A, Winkel LA, Hussain H, DeLancey JOL. The Relationship between Anterior and Apical Compartment Support. Am J Obstet Gynecol 2006, 194:1438–43

Tunn R, Paris S, Fischer W, Hamm B, Kuchinke J. Static magnetic resonance imaging

of the pelvic floor muscle morphology in women with stress urinary incontinence and pelvic prolapse. Neurourol Urodyn. 1998;17(6):579-89.

Yamada H. Strength of Biological Materials. Waverly Press, INC. Baltimore, Maryland, 21202, USA. 1970. p. 205-270

Chapter 5

Development of a 3-D Finite Element Model of Anterior Vaginal Wall Support to Evaluate Mechanisms Underlying Cystocele Formation

ABSTRACT

Objectives: To use biomechanical computer modeling to study the complex structural mechanics of anterior wall support. The first aim was to develop a 3D computer model of the anterior vaginal wall and its supports. The second aim was to validate it and then use it to determine which combinations of muscle and connective tissue defects could result in formation of a cystocele similar to those observed on dynamic magnetic resonance imaging (MRI).

Methods: A subject-specific 3D model was developed based on MRI scans from a healthy nulliparous woman using 3D Slicer (v. 2.6). An engineering graphics program, I-DEAS^{TM}, was then used to simplify model geometry and include: 1) anterior vaginal wall, 2) levator muscle, 3) cardinal ligament, 4) uterosacral ligament, 5) arcus tendineus fascia pelvis, 6) arcus tendineus levator ani, 7) paravaginal attachments, and 8) the posterior compartment. The 3D model was then imported into ABAQUS^{TM}, a finite element analysis program. Tissue properties were assigned from literature values. The effect of different combinations of connective tissue and muscle impairments on cystocele formation were studied as abdominal pressure was increased from rest to a maximum of 168 cmH_2O. An iterative process was used to refine anatomical assumptions until convergence was obtained between model behavior and deformations observed on dynamic MRI.

Results: The resulting 3D finite element model predicted realistic cystocele formation in the presence of impairment in levator ani muscle apical and/or mesenteric connective tissue, including apical and paravaginal support. Simulated cystocele size was sensitive to both the magnitude of abdominal pressure and the degree of impairment assigned to the connective tissue and muscle. Simulated cystocele morphology was similar to that observed on dynamic MRI. Larger cystocele formed in the

presence of both muscular and mesenteric connective tissue support impairment compare to impairment in either support element alone. Apical

impairment resulted in a larger cystocele compared to paravaginal impairment given the same intra-abdominal pressure loading and levator ani muscle impairment. The results suggest that the levator ani muscle is the key element; impairment in levator ani muscle caused larger hiatus size, longer exposed vaginal length, larger apical descent and resulted in a larger cystocele size.

Conclusions: This 3D finite element model simulated the formation of a cystocele as seen on dynamic MRI. Presence of a cystocele required a levator muscle impairment, an increase in abdominal pressure, and apical and paravaginal support defects.

5.1 Introduction

The anterior vaginal wall prolapse, clinically known as cystocele, is the most common form of pelvic organ prolapse (Hendrix et al., 2002). It is also the site with the highest rate of persistent and recurrent support defects (Shull et al., 2000).

A growing number of studies have sought to improve our understanding of normal anterior vaginal support mechanisms as well as how these supports ordinarily prevent cystocele. Early studies were focused primarily on the anatomy of paravaginal attachments and their failure (Richardson, 1976, DeLancey et al., 1992, 2002). Subsequent investigations have revealed levator ani muscle damage in women with anterior vaginal wall prolapse specifically (DeLancey et al., 2002) and prolapse in general (Tunn et al., 1998, Singh et al., 2003, Hoyte et al., 2001,2004, DeLancey et al., 2002). Recently dynamic MRI studies have revealed that anterior compartment prolapse is also highly correlated (r=0.73) with loss of apical support (Summers et al., 2006).

Each of these observations concerns a particular aspect of anterior vaginal wall support

and failure. To begin to integrate these observations into a single disease model，we developed a first generation, 2D lumped parameter model (Chapter 4 and Chen et al., 2006). This model simulated realistic anterior vaginal wall deformation in mid-sagittal plane and provided an important insight on the interaction between muscular support to the anterior vaginal wall provided by the levator ani and apical connective tissue support provided by the cardinal and uterosacral ligaments. However this 2D mid-sagittal model had inherent limitations, most notably that the model did not include the paravaginal attachments to the pelvic side wall, as well as the effects of geometries of these bilateral attachments. Furthermore, the levator plate and rectum were modeled as rigid body.

To address those limitations, in this chapter we develop a more complex 3D finite element model to investigate how different effects, such as muscular support, apical defect, paravaginal defect and vaginal dead band effect, affect cystocele formation.

5.2 Methods

The first step was to select MR scans as a part of an institutional review board-approved study of nulliparous pelvic anatomy. The subject happened to be a 34-year-old nulliparous Caucasian woman. Axial, sagittal and coronal photon density magnetic resonance images of the pelvic floor region were taken at 5-mm intervals, as previously described (Strohbehn et al., 1996). The geometry of the woman's bony pelvic floor attachment points lay within one standard deviation of the mean size and shape of a group of 278 women: this included a 75th percentile sagittal diameter (measured from the midline of the arcuate pubic ligament to the center of the sacrococcygeal junction) and a 44th percentile lateral diameter (ischial spine separation distance) (Lien et al., 2003)

A 3-D volumetric model was rendered by lofting serial 4 mm-thick axial magnetic resonance sections to establish the geometry of the anterior vaginal wall and surrounding support tissues using 3D Slicer 2.1b1 (Slicer 2b1; Massachusetts Institute of Technology, Cambridge, MA), as described by Hsu et al., 2005 & Chen et al., 2006. The geometric model included the following anatomic structures:1) anterior vaginal wall (AVW), 2) levator muscles (LA), 3) cardinal ligaments (CL), 4) uterosacral ligaments (US), 5) arcus

tendineus fascia pelvis (ATFP), 6) arcus tendineus levator ani (ATLA), 7) paravaginal support (PS), and 8) the posterior compartment (PC) as shown in Figures 1A and B.

The volumetric model was imported into I-DEAS (Version 9.0, EDS, Hook, UK), an engineering modeling software program, and the model geometry was simplified, principally by smoothing the surfaces of the structures (Figure 5-1C). The simplified model was then imported into ABAQUS (Version 6.6-1 ABAQUS, Inc), an engineering finite element modeling program that allows one to create the finite element mesh that is used to represent the anterior vaginal wall, levator ani muscles and posterior compartment, and then to predict how the structures will deform under increases in abdominal pressure. The program also predicts the resulting distributions in tissue stresses and strains (Figure 1D). The anterior vaginal wall and levator ani muscles were modeled in the program as deformable shell elements. The posterior compartment including posterior vaginal wall and rectum were modeled as a deformable solid. Lastly, the elements used to represent the ligamentous connections (CL, US, PS, ATFP, ATLA) to the vaginal wall were 2D truss elements.

The soft tissue attachments to pelvis and stationary structures (known as "boundary conditions") are shown in Figure 1D. The origin of levator ani muscle from the pubic bone and ATLA, and the points of attachments of the ligaments to the pelvic sidewall, and distal end of the vagina were each assumed to allow rotational, but not translational, movements.

All the model elements were assigned hyperelastic material properties based on values from existing literature (Yamada et al., 1970, Bartscht et al., 1988) (Figure 5-2). Because this model was only used to simulate cystocele development during straining, when patients were asked to increase abdominal pressure with their pelvic muscles relaxed, the levator ani muscles were only considered to exhibit passive stretch and therefore passive stiffness, without active contractile behavior.

An iterative process was used to refine anatomical assumption based on senior author's

extensive dissection, clinical examination and surgical experience and dynamic MR imaging observation (DeLancey et al., 1994, 2002, Summers et al., 2006). The deformation behavior of the model under increasing abdominal pressure was then examined and compared to that observed on dynamic MRI during Valsalva (Summers et al., 2006). When the model behavior did not match with observed behavior, then iterative changes were made to anatomical connections, boundary conditions, material properties, and/or element type within the constraints of existing knowledge until the model behaved in a reasonable manner (Figure 5-1C, D).

To simulate cystocele formation, we set model parameters to simulate impairments in the various supportive components (i.e., CL, US, PS and PCM). An impairment was simulated as an decrease in material property stiffness in ligaments, a strategy used previously by Chen, et al (Chen et al., 2006). To simulate a impairment in levator ani muscle, their stiffness was considered to be decreased by 60% from normal values, consistent with the 60% decrease in maximum muscle strength observed in women with prolapse and muscle impairment compared to those who have normal support and intact muscle in the OPAL study (DeLancey et al., 2007). This assumption was made because Blanpied et al. (Blanpied et al., 1993) showed a linear relationship between the contractile force in a muscle and its tensile stiffness. Tissue adaptation is another important factor. When a structure undergoes sustained stress over time, it can generate either additional tissue and/or better quality tissue in order to reduce tissue stress. Clinically we found that women with prolapse have a larger vaginal cross-sectional area (Hsu et al., 2005). Loaded tissues can also change their properties over time, as in the case of hysteresis and creep. To begin to simulate the effect of these types of changes we simply shifted the stress and strain curve for vaginal properties incrementally to the right, as shown in Figure 5-3, and re-executed the simulations.

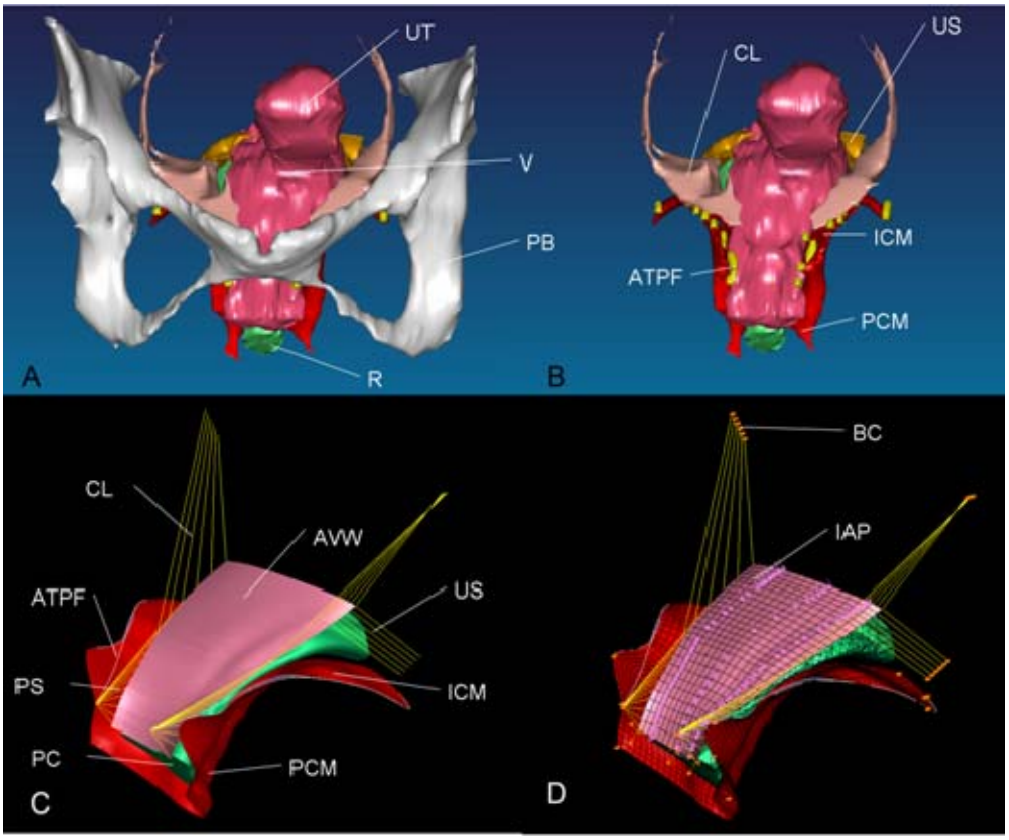

Figure 5-1 Model development. A: 3D volume rendered model of anterior support system including pubic bone； B: 3D volume-rendered model without pubic bone; C: Geometry simplified surface model; D: 3D finite element model with mesh, boundary condition (orange pin representing ligaments and muscle origin is pinned to pubic bone and pelvic sidewall), and abdominal pressure loading. PB: pubic bone; UT: uterus; V: vagina； R: rectum; CL: cardinal ligament; US: uterosacral ligament; ATFP: arcus tendineus fascia pelvis; ICM: iliococcygeus muscle; PCM: pubococcygeus muscle; AVW: anterior vaginal wall; PC: posterior compartment; PS: paravaginal support; IAP: abdominal pressure

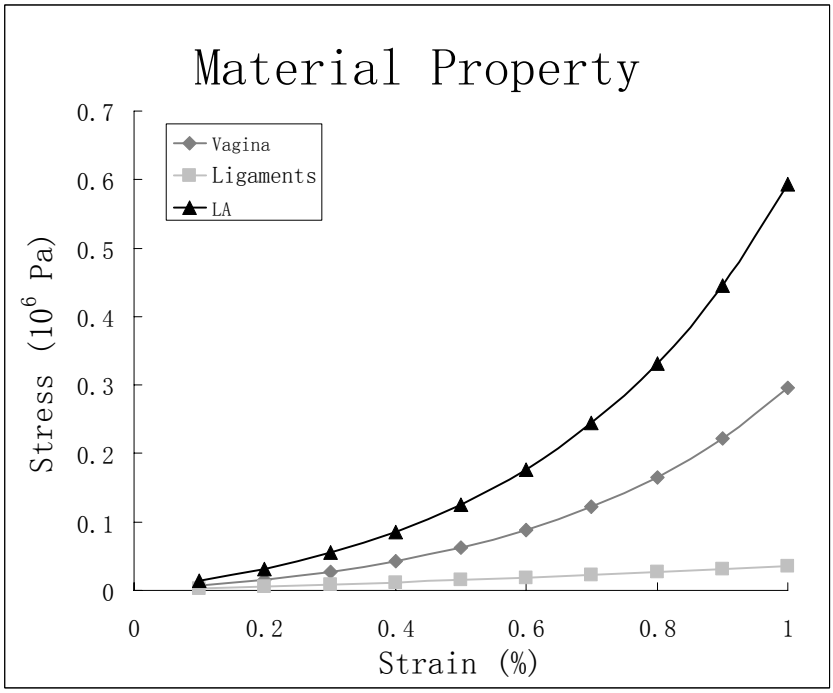

Figure 5-2 The material property of vagina, ligaments and levator ani muscle used in the model simulation,

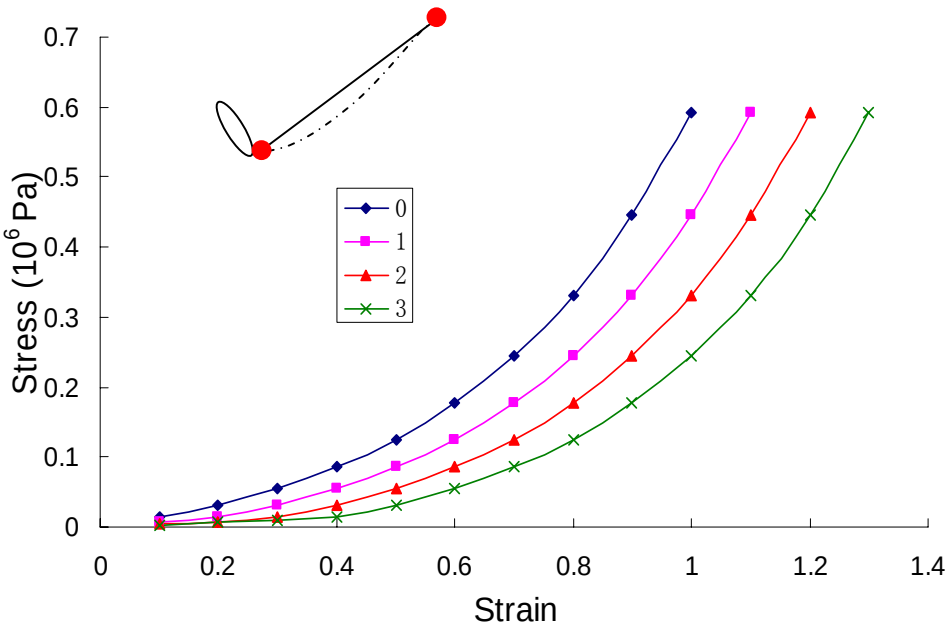

Figure 5-3 Vaginal wall tissue material properties at different stage of tissue adaptation. The curve on the left most (status 0) is the original data from Yamada (Yamada, 1976) which is assigned as status 0. Status 3, vaginal tissue has the longest dead band.

Simulations of the effects of abdominal pressure on model structures were handled in the following manner. The abdominal pressure was considered to act perpendicular to the surface of the anterior vaginal wall. In a previous study of 314 patients with prolapse, the 5th percentile, 50th and 95th percentile values of maximum Valsalva pressure were determined to be 60, 99 and 168 cmH_2O respectively (DeLancey et al., 2007). Therefore, the increase in abdominal pressure was simulated with the 20 increments of the pressure time relationship shown in Figure 5-6 .

The outcome measurements from the model include the descent of the most dependent point of the anterior vagina wall (d), apex descent (a) and hiatus size (h) as well as exposed vaginal length at the maximum intra-abdominal pressure (Figure 5-4). The maximum stress in the levator ani muscle and vaginal wall were also calculated.

The model was validated by comparing the mid-sagittal anterior vaginal wall deformation under increasing abdominal pressure with that in the dynamic MRI of a patient with Stage III cystocele performing the same maneuver, Figure 5-5. Under current assumptions underlying the model's functional anatomy, it not only correctly predicted cystocele formation, but also correctly predicted the increase in size that occurs with straining on midline dynamic MRI.

5.3 Results

When the intact model (without defects in the levator ani muscle, apical and paravaginal support) was loaded with up to 100 cmH_2O (50th percentile), a slight cystocele occurred (Figure 5-6 A). This can be compared with a more typical simulated cystocele formation (Figure 5-6B), in which cardinal, uterosacral ligament, and paravaginal support was set to 50% impairment and the PCM was set to have a 60% impairment. The sequential development of this cystocele with increasing abdominal pressure is shown in Figure 5-7. Figure 5-8 shows the relationship between simulated cystocele size and intra-abdominal pressure for this simulation. The best fit line for the

non-zero cystocele size data points was estimated. The compliance of anterior support system was estimated to be 0.49 mm/cmH_2O from the slope of the line.

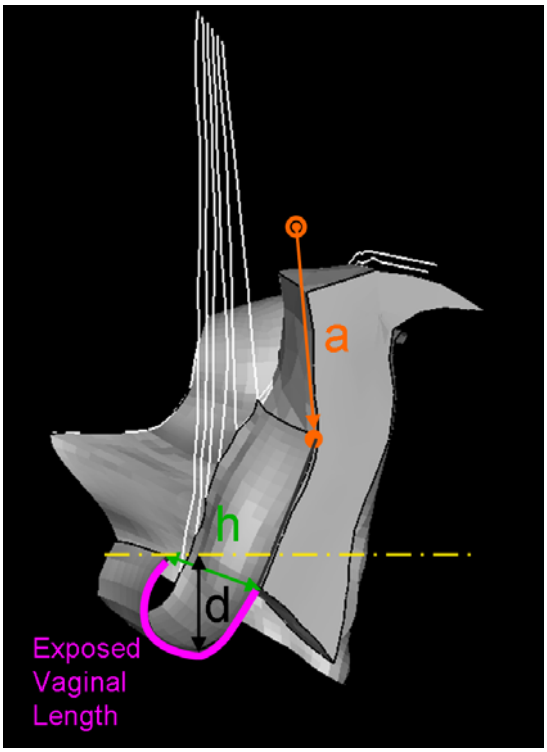

Figure 5-4 Outcome measurements. The illustration is the model configuration at maximum abdominal pressure and shows the four outcome measurements: a: apical descent, middle of vagina apex displacement from its position at rest; h: hiatus size at maximum loading, measured as tip of posterior vaginal compartment to distal end of vaginal wall (fixed); d: Prolapse size, measured as the vertical descent of the most dependent point of the vagina to distal end of vagina; Exposed Vaginal Length measured as the length of vaginal wall unsupported by the posterior vaginal compartment (and therefore exposed to the pressure differential with intra-abdominal pressure acting on the proximal surface and atmospheric pressure acting on its distal surface).

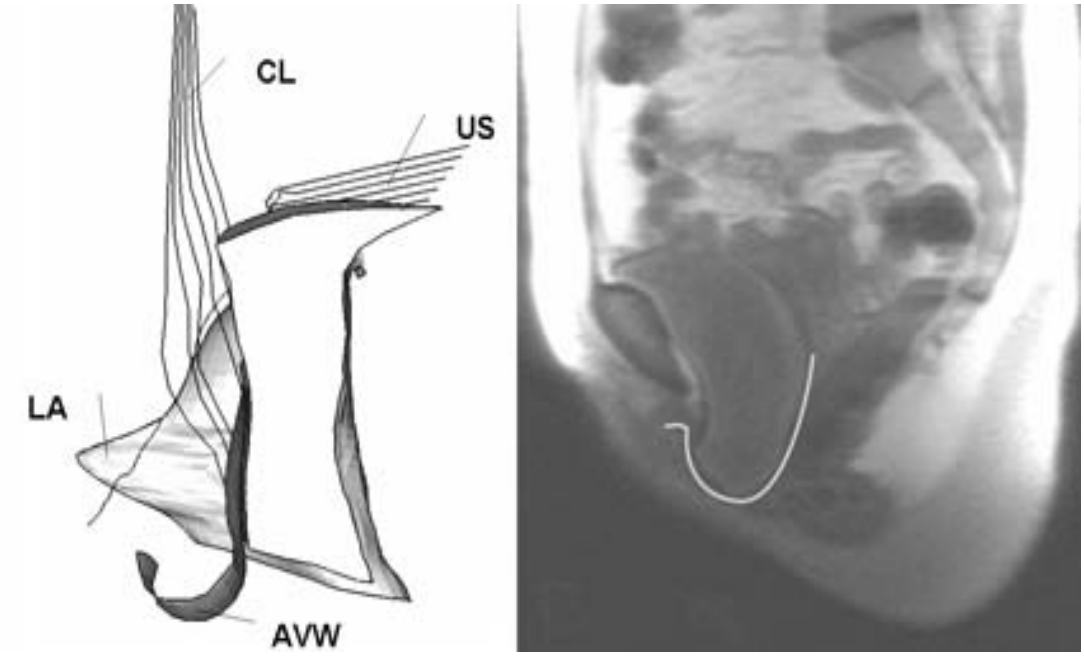

Figure 5-5. Model validation. At left side is one model-generated simulation result with a similar cystocele formation to that seen clinically in the dynamic MRI on right side of the figure.

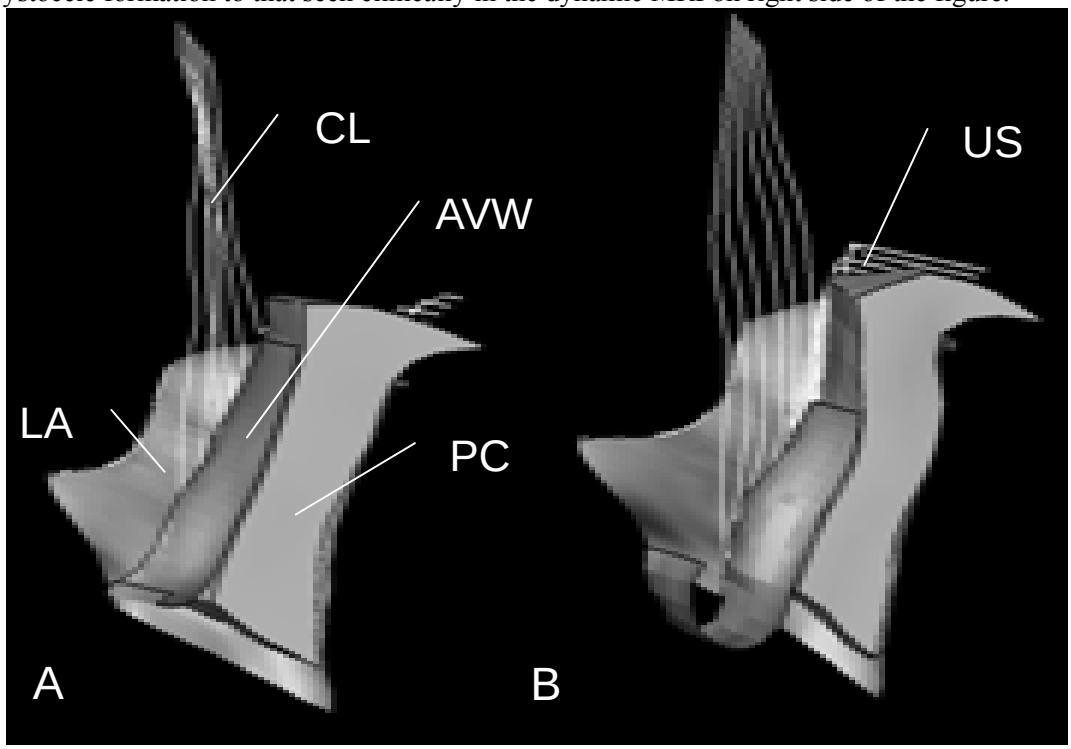

Figure 5-6 Lateral view of a mid-sagittal plane section of the 3D finite element model. Panel A: In this simulation, all support elements (levator ani muscle, cardinal uterosacral ligament, paravaginal support) have normal material properties. Panel B: In this simulation, the levator ani muscle was set to have a 60% reduction in its properties, and a 50% reduction in cardinal and uterosacral ligament and paravaginal support properties. LA denotes levator ani, CL: cardinal ligament, AVW: arterial vaginal wall, PC: posterior compartment, US: uterosacral ligament

The size of the cystocele was found to vary depending on the maximal abdominal pressure applied to the model (Figure 5-9). Cystocele size is sensitive to structure impairments. At a 168cmH_20 maximum intra-abdominal pressure, a levator ani muscle impairment alone resulted in slightly larger cystocele than a mesenteric connective tissue impairment alone. The model with the combined impairment had the largest simulated cystocele size, as hypothesized.

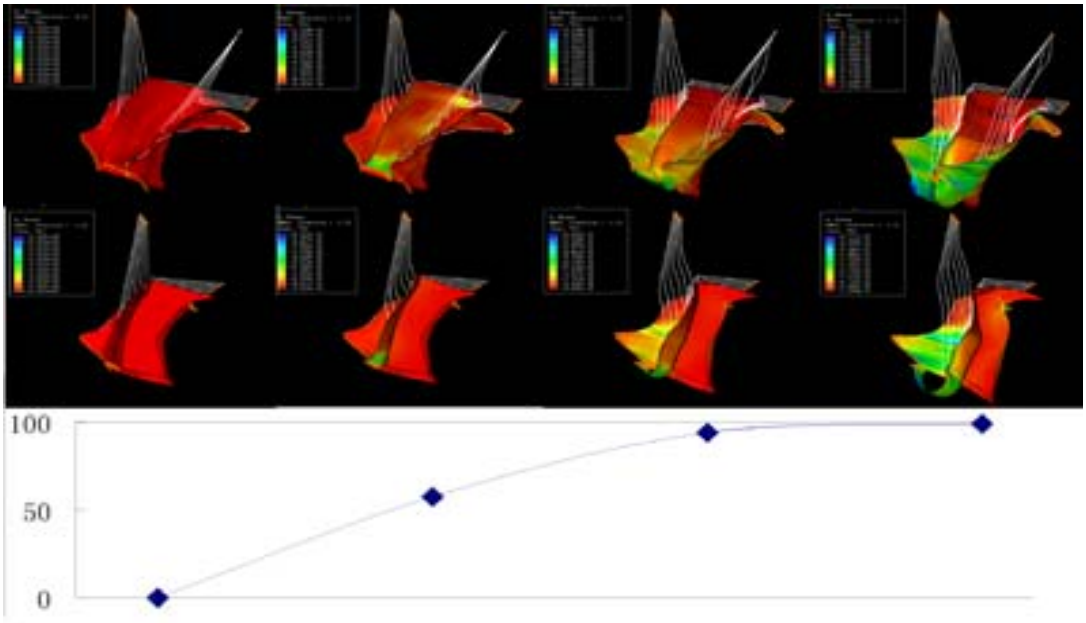

Figure 5-7. Sequential development of a typical simulated cystocele. In this simulation, the levator ani muscle had a 60% impairment, apical and paravaginal support properties were set to having a 50% impairment,,. The abdominal pressure was then increased from zero to 100 cmH_2O over time course (plotted on the vertical axis of the bottom illustration) at four different time points (seen on the horizontal axis of the bottom plot). The first row shows the three-quarter view, while the second row shows a sagittal section. The color map shows the stress distributions in the different regions, with red indicating a low stress region and blue indicating a high stress region.

Figure 5-10 shows the effect of levator ani muscle impairment alone on the cystocele formation. The models with normal mesenteric connective tissue support and varying degree of impairments in the pubic portion of the LA were loaded with 168 cmH_2O intra-abdominal pressure. With increasing muscle impairment, there is a systematically increase in hiatus size, which allows a longer length of the vaginal wall to be exposed to a pressure differential (high intra-abdominal pressure on the "upper" side and (low)

atmosphere pressure on the "lower" side). A larger stress builds up in the vaginal wall and caused a larger apical descent (Figure 5-10). A larger cystocele size then results.

Investigations into effects of apical or paravaginal impairment to cystocele formation are shown in Figure 5-11. Predominant apical impairment (varying apical impairment at 0%, 20%, 40%, 60%, 80% but with normal paravaginal support), predominant paravaginal impairment (varying paravaginal impairment at 0%, 20%, 40%, 60%, 80% but with normal apical support) are shown for 168 cmH_2O maximal abdominal pressures and 60% levator ani muscle impairment. All cystocele sizes were normalized to cystocele size at normal apical and normal paravaginal support. The cystocele size was sensitive to the degree of apical impairment with 20% remaining apical support stiffness; the cystocele size increased 33% compared to the scenario with normal apical support. However there was only a slight change in cystocele size with increasing degrees of paravaginal impairment.

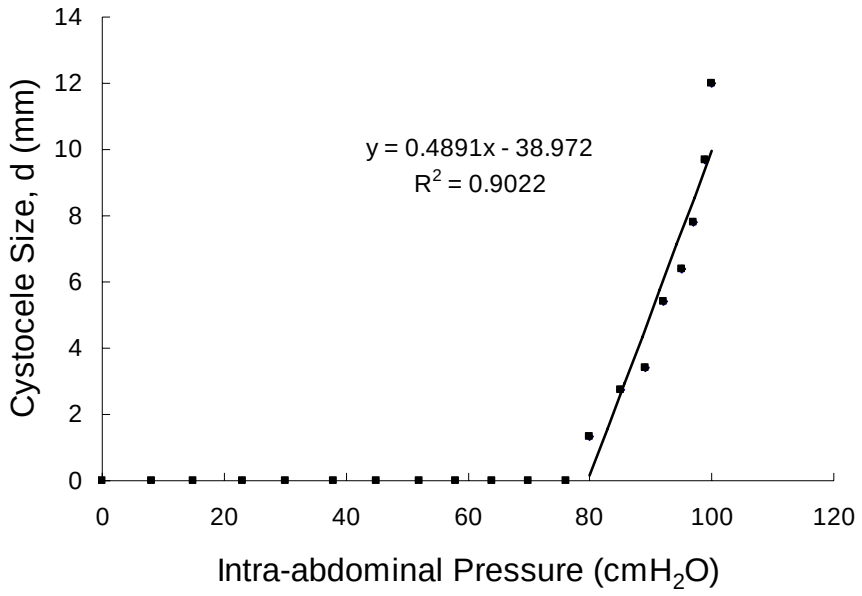

Figure 5-8 Relationship between cystocele size and intra-abdominal pressure in a simulated cystocele. In this simulation, the levator ani muscle had a 60% impairment, apical and paravaginal support were set to having a 50% impairment. The best fit line for non-zero cystocele size data points is plotted. The linear regression equation and coefficient of determination are shown in the illustration.

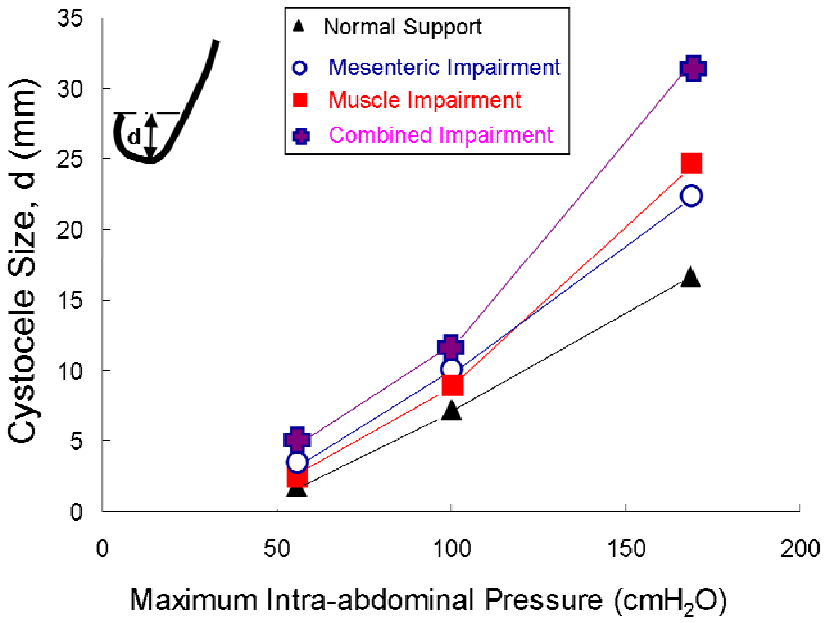

Figure 5-9 Simulated cystocele size for models with different impairment patterns at increasing values of maximum intra-abdominal pressure loading.

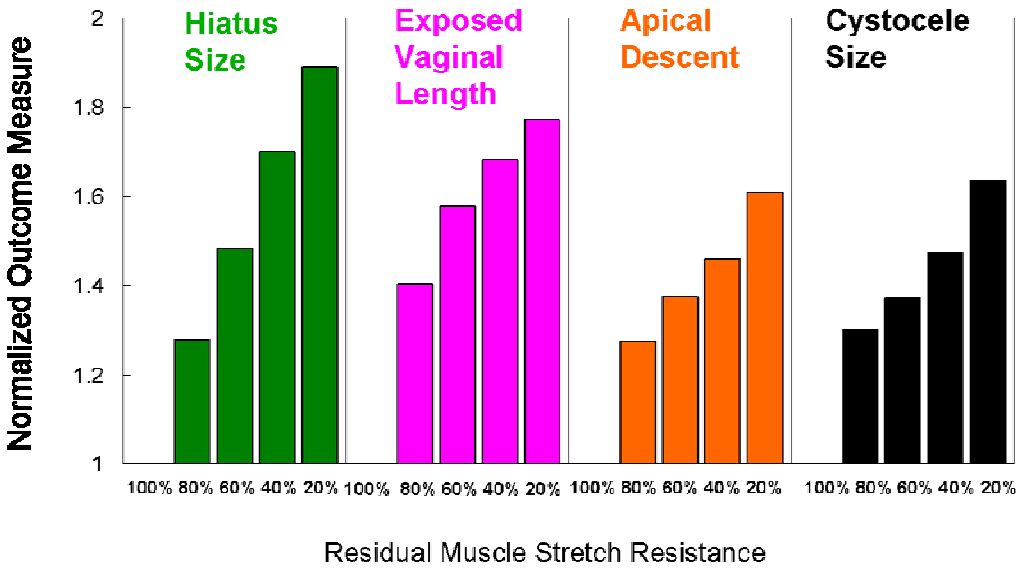

Figure 5-10 Effects of muscle impairment on cystocele formation. The outcome measurement was normalized to model outcome with intact LA muscle resistance to stretch.

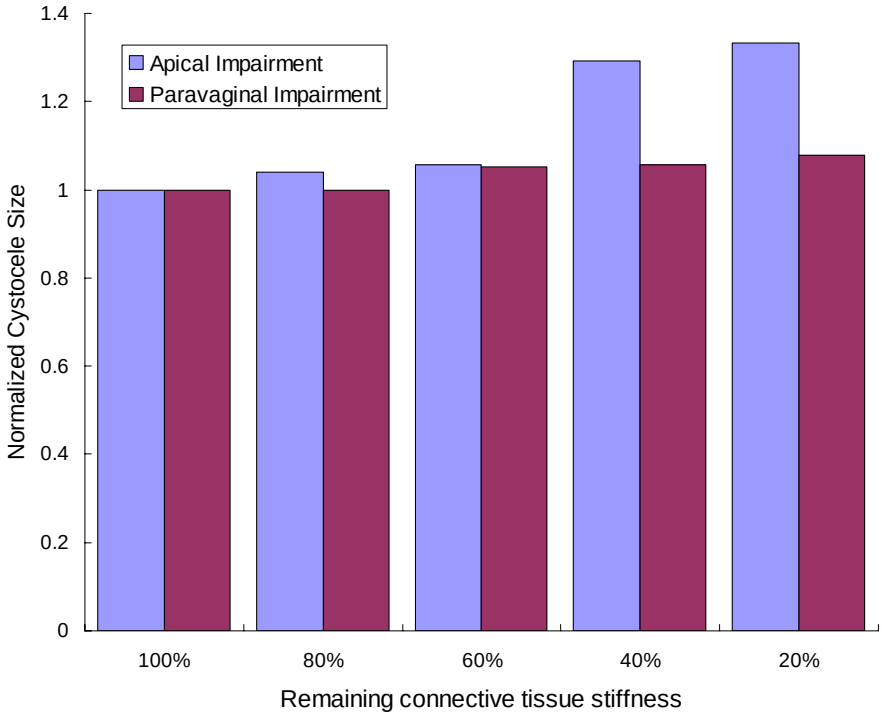

Figure 5-11 Effects of apical and paravaginal impairments on cystocele formation. Simulations had 60% levator ani muscle impairments and were loaded with 168cmH_2O maximum intra-abdominal pressure. For apical impairment simulations, models had normal paravaginal support, but a varying degree of apical support impairment with remaining apical connective tissue stiffness ranging from from 20% to 100% of the normal value. For paravaginal impairment simulations, models had normal apical support but varying degree of paravaginal support impairment with remaining paravaginal connective tissue stiffness ranging from 20% to 100% of normal values.

Simulated cystocele sizes were also sensitive to the vaginal tissue properties (Figure 5-12). A longer dead band resulted in a larger cystocele size. The relationship between cystocele size and vaginal tissue dead band status exhibited a non-linear (exponential) relationship, especially for models with combined defects.

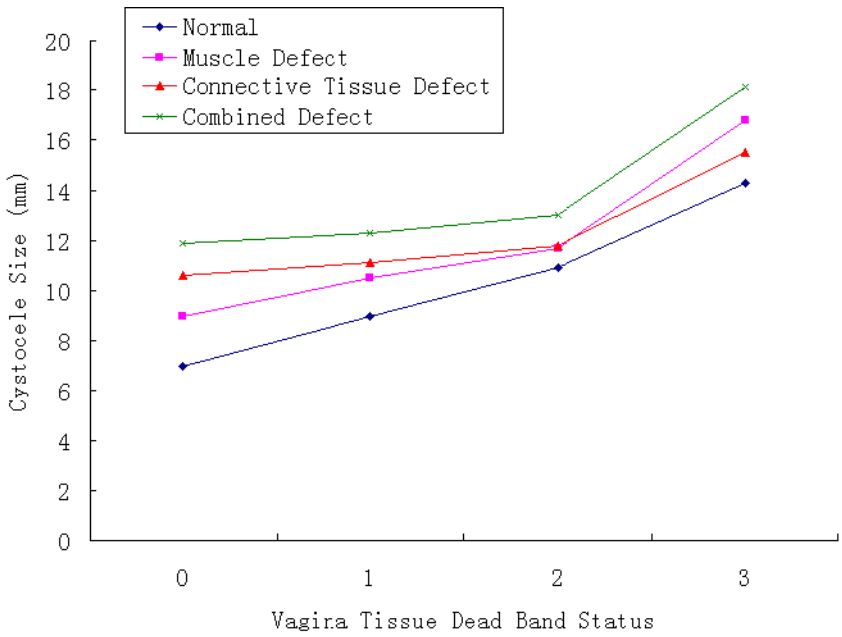

Figure 5-12 Relationship between vaginal tissue status and cystocele size. Vaginal tissue dead band status 0, 1, 2, 3 were as shown in figure 5-3.

5.4 Discussion

The significance of this study lays in its being the first 3D simulation of cystocele formation. The model has realistic anatomical geometry from a living normal woman with both connective tissue and muscular supports. It reproduces realistic cystocele similar to those seen clinically, under physiological abdominal pressure loading (Figure 5-5). Also the estimated anterior compartment compliance from model simulation was about 0.49 mm/cmH_2O which is close to that measured in living women with prolapsed (Chapter 6). By varying one parameter at a time, this validated finite element model allows theoretical "what-if" analyses to be performed on the effect of specific parameter variations on model behavior in a way that is impossible in living women.

The simulated cystocele size was found to be sensitive to maximum intra-abdominal pressure, the presence of impaired structures (levator ani muscle, apical connective tissue, paravaginal connective tissue, vaginal wall) and single vs multiple site impairments. The finding that impairments in multiple domains (muscle impairment and mesenteric

connective tissue impairment, including both apical and paravaginal) result in larger cystocele is similar to the result we found in the first generation model (Chapter 4, Chen et al., 2006) where we noted that when both muscle and connective tissue impairments were implemented in the model, larger cystoceles resulted than when only one or the other impairment was present.

The model suggests that levator ani muscle impairment played a very important role in cystocele formation. A decreasing in LA muscle resistance to stretch caused a larger hiatus size, and allowed a longer length of vaginal wall to be exposed to the pressure differential between high intra-abdominal pressure and low atmosphere pressure. This caused tension to build up in the vaginal wall tissue, dragged the apex down and thereby resulted in larger cystocele size.

The apex of vaginal wall was supported by apical connective tissue, including cardinal and uterosacral ligament. Impairment in apical support is another important factor of cystocele formation. An 80% impairment in apical support can result in a 33% larger cystocele size than that with normal apical support. This agrees with our earlier clinical findings that variation in apical support explained 60% of variation in prolapse size in a group women with a wide spectrum of pelvic floor support (Summer et al., 2006).

Restoring normal anatomy and function are common goals of reconstructive surgery. At present, our ability to specifically determine the location and type of impairment responsible for cystocele has been limited. By providing a specific analysis of regional impairments in support the findings of this study can form the framework for new imaging studies in women using ultrasound or magnetic resonance scans to make similar observations in living women. It also provides the unique ability to experimentally induce specific impairments and see what their effects are in ways that would not be ethical in humans. This should help direct targeted investigations into anatomical changes seen in women with cystourethrocele. Eventually, once we can determine the exact nature of structural impairments, targeted operations customized for each patient

might be developed that maximize surgical success while minimizing compensating distortion that can lead to postoperative problems with function.

It is important to recognize that there are still some inherent limitations in this model. First, active contraction of levator ani muscle was not represented in this model. Even though the subjects were asked to relax their LA muscles while performing Valsalva, because the LA have a postural function they have a constant level of active muscle tone. So the present model essentially the situation with a very low level of muscle activity in this muscle. Second, this model still has simplified anatomic structures and geometry. At the present time, there is no perineal body in the model, so the model constraint placed at the distal end of vagina did not permit movement of the perineal body during Valsalva. This might have tended to overconstrain the model and therefore resulted in a conservative model prediction of cystocele size. Therefore the quantitative values of tissue stresses predicted by the simulation are likely not accurate. However, the qualitative behavior should be reasonable. The model simulations also showed that cystocele size is not sensitive to paravaginal impairment, which might have resulted from a poor understanding of paravaginal support anatomy and/or unrealistic model assumption. The study of more detailed functional anatomy will provide more insights on how to better model it in the future. Third, the model has simplified material properties in that all elements were assumed to be hyperelastic. Any viscous, plastic or remodeling changes in material properties that can occur over a longer period of time were not considered in detail (except for the deadband simulation). In addition, the model was loaded with a single loading cycle. To study how the loading rate and number of loading cycles affect cystocele formation, more sophisticated visco-hyperelastic material properties should be used. Finally, the model was set up based on our best understanding of the essential nature of this highly complex anatomy. At present, we have based our observations on the anatomy of an average woman with normal pelvic floor support. How abnormal starting geometry and geometric variation in pelvic size and shape among normal population would affect cystocele formation needs to be further explored.

References

Bartscht KD, Delancey JO. A technique to study the passivesupports of the uterus. Obstet Gynecol 1988;72:940–3.

Blanpied, P., Smidt, G.L.. The difference in stiffness of the active plantarflexors between youngand elderly human females. J Gerontol 1993; 48, M58–M63.

Chen L, Hsu Y, Ashton-Miller JA, Delancey JOL. Measurement of the pubic portion of the levator ani muscle in women with unilateral defects in 3-D models from MR images. Int J Gynaecol Obstet 2006;92:234–41.

DeLancey JOL. Anatomic aspects of vaginal eversion after hysterectomy. Am J Obstet Gynecol 1992;166:1717–24.

DeLancey JOL. Structural support of the urethra as it relates to stress urinary incontinence: the hammock hypothesis, Am J Obstet Gynecol. 1994 Jun;170(6):1713-20.

Delancey JOL. Fascial and muscular abnormalities in women with urethral hypermobility and anterior vaginal wall prolapse. Am J Obstet Gynecol. 2002 Jul;187(1):93-8.

DeLancey JOL, Morgan DM, Fenner DE, Kearney R, Guire K, Miller JM, Hussain H, Umek W, Hsu Y, Ashton-Miller JA. Comparison of levator ani muscle defects and function in women with and without pelvic organ prolapse. Obstet Gynecol. 2007 Feb;109:295-302.

Hendrix SL, Clark A, Nygaard I, Aragaki A, Barnabei V, McTiernan A. Pelvic organ prolapse in the Women's Health Initiative: gravity and gravidity. Am J Obstet Gynecol 2002;186:1160–6.

Hsu Y, Chen L, Delancey JOL, Ashton-Miller JA. Vaginal thickness, cross-sectional area,

and perimeter in women with and those without prolapse. Obstet Gynecol 2005;105:1012–7.

Hoyte L, Schierlitz L, Zou K, Flesh G, Fielding JR. Two- and 3-dimensional MRI comparison of levator ani structure, volume, and integrity in women with stress incontinence and prolapse. Am J Obstet Gynecol 2001;185:11–9.

Hoyte L, Jakab M, Warfield SK, Shott S, Flesh G, Fielding JR. Levator ani thickness variations in symptomatic and asymptomatic women using magnetic resonance-based 3-dimensional color mapping. Am J Obstet Gynecol 2004;191:856–61.

Hoyte L, Thomas J, Foster RT, Shott S, Jakab M, Weidner AC. Racial differences in pelvic morphology among asymptomatic nulliparous women as seen on three-dimensional magnetic resonance images. Am J Obstet Gynecol. 2005 Dec;193(6):2035-40.

Hsu Y, Summers A, Hussain HK, Guire KE, Delancey JOL. Levator plate angle in women with pelvic organ prolapse compared to women with normal support using dynamic MR imaging, Am J Obstet Gynecol. 2006 May;194(5):1427-33

Lien KC, Mooney B, DeLancey JOL, Ashton-Miller JA. Levator ani muscle stretch induced by simulated vaginal birth. Obstet Gynecol. 2004 Jan;103(1):31-40

Richardson AC, Lyon JB, Williams NL. A new look at pelvic relaxation. Am J Obstet Gynecol 1976;126:568–73.

Shull BL, Bachofen C, Coates KW, Kuehl TJ. A transvaginal approach to repair of apical and other associated sites of pelvic organ prolapse with uterosacral ligaments Am J Obstet Gynecol. 2000 Dec;183(6):1365-73.

Singh K, Jakab M, Reid WM, Berger LA, Hoyte L. Three-dimensional magnetic resonance imaging assessment of levator ani morphologic features in different grades of prolapse. Am J Obstet Gynecol 2003;188:910–5.

Strohbehn K, Ellis JH, Ashton-Miller JA, DeLancey JOL. Magnetic resonance imaging of the levator ani with anatomic correlation. Obstet Gynecol 1996;87:277–85.

Summers A, Winkel LA, Hussain HK, DeLancey JOL. The Relationship between Anterior and Apical Compartment Support. Am J Obstet Gynecol 2006;194:1438–43.

Tunn R, Paris S, Fischer W, Hamm B, Kuchinke J. Static magnetic resonance imaging of the pelvic floor muscle morphology in women with stress urinary incontinence and pelvic prolapse. Neurourol Urodyn 1998;17:579–89.

Yamada H. Strength of Biological Materials. Baltimore (MD): Williams & Wilkins; 1970. p. 205–70

Chapter 6

In Vivo Assessment of Anterior Compartment Compliance and Its Relation to Prolapse

ABSTRACT

Objective: We tested the null hypothesis that anterior compartment compliance does not differ between women with and without prolapse and explored factors predicting variation in cystocele size.

Methods: Nineteen parous women with normal support (N=10) and varying degrees of anterior compartment prolapse (N=9) were taken from an ongoing study [mean ± SD Age: controls = 62±10 yrs, cases = 53±12 (p=.101) Parity: controls = 3±2, cases = 3±1, (p=.565)]. A bladder catheter was placed to measure abdominal pressure (Datascope®). Mid-sagittal pelvic MR images were obtained in the supine position from rest to maximum Valsalva over a 20 second interval at approximately a 1 Hz sampling rate. In each image, the distance from the most dependent bladder point to the average bladder location in 20 nullipara was measured. The relationship between bladder descent and abdominal pressure was examined for each subject using linear regression. The slope of the best-fit line is a measure of the anterior compartment compliance. The hypothesis was tested using an independent t-test. Multivariate analyses of the data from all subjects was also performed.

Results: Mean compliance was higher for cases (0.5 mm / cm H_2O ± 0.06 SEM) than controls (0.3 mm / cm H_2O ± .07, p=.039). Mean resting bladder point was lower in cases (2.4 ± 0.5 cm H_20) than controls (0.9±0.1 cm H_2O, p= .024). Maximum bladder displacement correlated best with compliance (R^2=.75, p<.01), less well with resting bladder location (R^2=.55, p<.01) but not with abdominal pressure (R^2=.15, p=.102). Linear regression modeling showed that resting bladder point explained 55% of the variation of maximum bladder displacement (p<.001). Adding the effect of compliance increased it to 86% (p<.001) and adding maximum abdominal pressure increased it further to 93%

(p=.001).

Conclusion: The *null* hypothesis was rejected. Women with cystocele have 67% greater compliance of their

support system compared to controls. However, resting bladder location was also an important predictor of cystocele size. *Comment:* The anterior vaginal wall support system has been shown to depend on the combined action of muscle and connective tissue. To our knowledge, these are the first *in vivo* MR-based compliance measurements of this system in women, and especially those with and without cystocele.

6.1 Introduction

The deterioration and weakening of anterior vaginal wall and/or its connective tissue support have been hypothesized to underlie the development of anterior vaginal prolapsed (Chapters 4 & 5).

The material properties of the anterior vaginal wall and its supportive connective tissue have been studied in women with and without prolapse. For example, the shear strength of vaginal wall specimens was found to be lower in patients with pelvic floor dysfunction then normal controls (Kondo et al, 1994) and great variability in the tensile and bending strength of samples has also been observed (Cosson et al, 2004). Women with prolapse had more extensible vaginal skin and a lower stiffness index compared to age-matched controls (Lei et al, 2006, Epstein et al, 2008). The resiliency of the apical support structures such as the uterosacral ligaments has also been found to be significantly reduced among women with symptomatic uterovaginal prolapse (Reay et al, 2003). However, those results contain a systematic bias in that the mechanical tests were all conducted *in vitro* when the tissue samples already had lost their smooth muscle tone.

As we know, the pelvic floor organs, when removed from the body, exist only as a limp and formless mass. Their shape and position in living women is determined by their tensile attachments to the pubic bones, through the muscles, and the connective

tissues of the pelvis. The interactions of levator ani muscles, apical connective tissue in the form of the cardinal and uterosacral "ligaments", and the connective tissues forming the anterior vaginal wall combine to form the anterior compartment support system. The word ligaments is here placed in inverted commas because these are not ligaments in the orthopedic sense of the word, but instead are comprised of mesenteric attachments involving smooth muscle, nerve and vascular tissue, in addition to connective tissue.

Clearly, given the relative complexity of the anterior vaginal wall support structures and the fact that *in vitro* tests may not really represent their behavior adequately, it would be better to evaluate their load-displacement behavior *in vivo* if possible.

Previous biomechanical models have demonstrated how the combined action of muscle and connective tissue contribute to anterior compartment support (Chapter 4 and Chen et al 2006). The simulated model can reproduce a similar size and shape of cystocele to that seen clinically under moderate intra-abdominal pressure. However, a more sophisticated model requires validation using *in vivo* compliance measurements as well.

Intra-abdominal pressures during cough and Valsalva have been measured during clinical exam (Howard et al, 2000, DeLancey et al, 2007), and displacements were measured during these activities have been quantified *in vivo* using ultrasound (Howard et al, 2000, Peng et al, 2007). However, no simultaneous measurements of intra-abdominal pressure and prolapse development have ever been made. So the relationship between load and displacament remains to be elucidated. It is tempting to use an inexpensive imaging modality such as clinical ultrasound to make such measurements. But it is simply not feasible because contact pressure between the ultrasound probe and the prolapse would distort the very measurements being made.

Dynamic MR imaging allows superior visualization of soft tissue movement without direct contact pressure. As such it is ideal for looking at displacement of the anterior compartment during abdominal loading or Valsalva. If we now add a novel method for measuring intra-abdominal pressure synchronously to the dynamic MR images being made, this permits simultaneous measurements of both abdominal pressure and anterior wall shape and displacement. The ability to determine the amount of anterior compartment displacement under a known level of intra-abdominal pressure loading

allows a calculation of compliance to be made.

It was therefore our objective to test the null hypothesis that anterior compartment compliance does not differ between women with and without prolapse and to explore biomechanical factors predicting variation in cystocele size.

6.2 Methods

Nineteen parous women with normal support (N=10) and varying degrees of anterior compartment prolapse (N=9) were taken from an ongoing study [mean ± SD Age: controls = 62 ± 10 yrs, cases = 53 ± 12 (p=.101) Parity: controls = 3 ± 2, cases = 3 ± 1, (p=.565). A catheter was placed in the bladder and connected to a pressure monitoring device (Datascope, Montvale, N.J.) to measure abdominal pressure. MRI was performed on a 1.5-T system (Signa, General Electric, Milwaukee, WI) using a four-channel, torso phased-array coil with the subject in the supine position. Before starting the examination, the patient was instructed in regards to the straining maneuvers to be performed during the examination, starting from minimal to maximal straining. For dynamic imaging, a multiphase, single level image of the pelvis in the mid-sagittal plane was obtained approximately every second over an interval 23 – 27 s using a T2-weighted, single-shot, fast spin-echo sequence (Repetition time (TR) = 1,300 ms; Echo time (TE) = 60 ms; slice thickness = 6 mm; field of view = 32 – 36 cm; matrix = 256 × 160; one excitation and half-Fourier acquisition). The time needed to actually acquire each of the images was determined by the patient's weight and was approximately one second. A set of 20 successive images were acquired in 23 – 27 s during rest as well as a graded Valsalva effort in the following manner. The operator instructed the subject to hold her breath in inspiration and initiated the scan. After 5 s of imaging with the subject at rest the operator instructed the subject to strain minimally for 5 s, moderately for 5 s, and maximally for 5 s, then to breath normally and relax for another 5 – 7 s before ending the acquisition. Usually, three images were acquired at rest during suspended inspiration, 12 during the graded Valsalva effort, and five during post-Valsalva relaxation and normal breathing. The most dependent bladder point was plotted on each image (Figure 6-1). The mean location of the normal resting bladder point has been previously determined in 20

nulliparous women (Summers et al, 2006). The displacement of the dynamic MR bladder point relative to the normal location in nullipara was determined using MATLAB v7.0 (MathWorks, Natick,MA). Abdominal pressure and bladder displacement was plotted for each subject and best-fit lines for the loading portion of the curve to the maximum displacement were obtained using linear regression (the line slope is a measure of compliance)(Figure 6-1). Bivariate analysis (Student t-test) comparing cases and controls and multivariate analysis of all subjects (correlation coefficients and linear regression modeling) were performed.

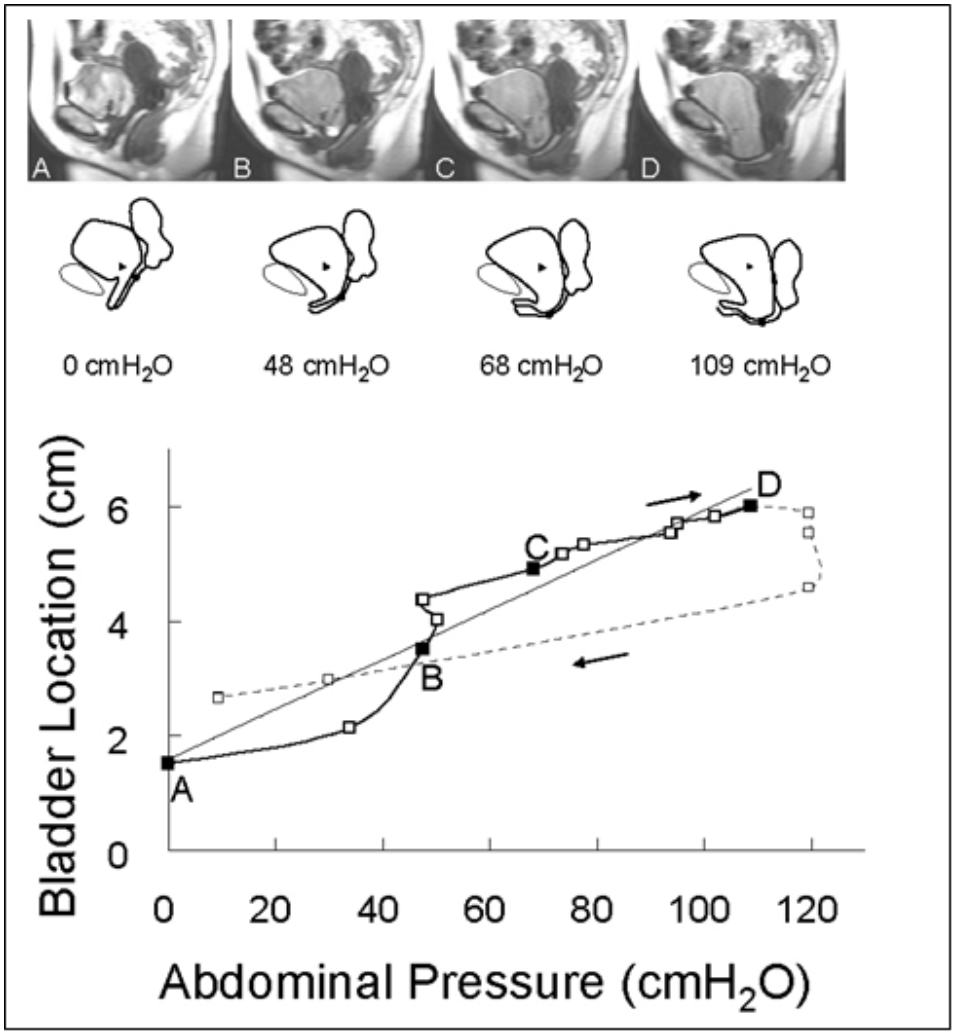

Figure 6-1 The upper tracings were constructed from dynamic mid-sagittal images of the subject whose lines is marked with an asterix. Black dots represent the most dependent bladder point and black triangles the location of the normal bladder point in nullipara. The graph showed the relationship between intra-abdominal pressure and bladder location during loading (solid tracing) and unloading (dashed tracing) cycle. Straight line is the best fitted line for the loading curve.

6.3 Results

The mean (± SEM) compliance was higher for cases (0.5 ± 0.06 mm/cmH_2O) than controls (0.3 ± .07 mm/cmH_2O, p=.039). The linear relationship of the loading curve was demonstrated by coefficients of determination (R^2) ranging from 0.21 to 0.98. There was, however, variability in compliance (line slope) between subjects (range: 0.005 to 0.097 cm/cmH_2O, Figure 6-2). The mean maximum displacement for the bladder was 4.6 cm. The mean resting bladder point in cases (2.4 ± 0.5 cm) was more displaced relative to the nullipara than controls (0.9 ± 0.1 cm, p= .024). The mean maximum pressure for controls (70.0±23) was not significantly different than that for cases (87.0 ± 27) (p=.154). Pearson correlation coefficient between maximal bladder displacement and 1) compliance was 0.86 (R^2=.75, p<.001), 2) resting bladder point was 0.74 (R^2=.55, p<.001), 3) maximum abdominal pressure was 0.39 (R^2=.15, p=.102). Linear regression modeling showed that resting bladder point helps to explain 55% of the variation of maximum bladder displacement (p<.001). Adding compliance of anterior compartment support increased it to 86% (p<.001) and adding maximum abdominal pressure increased it further to 93% (p=.001).

6.4 Discussion

We have developed a novel approach which allows us to quantify the compliance and behavior of the anterior compartment support system under physiologic load. Using this dynamic MR-based strategy, we were able to determine that patients with prolapse do have a more compliant anterior compartment support system compared to controls. Since compliance has an inverse relationship to stiffness, this corroborates earlier data suggesting that women with prolapse have less stiff vaginal tissues (Lei et al, 2007, Epstein et al, 2007). When we performed an analysis to determine the contribution of factors to the development of anterior compartment prolapse, as expected we found that compliance and abdominal pressure correlated strongly with descent of the anterior vaginal wall.

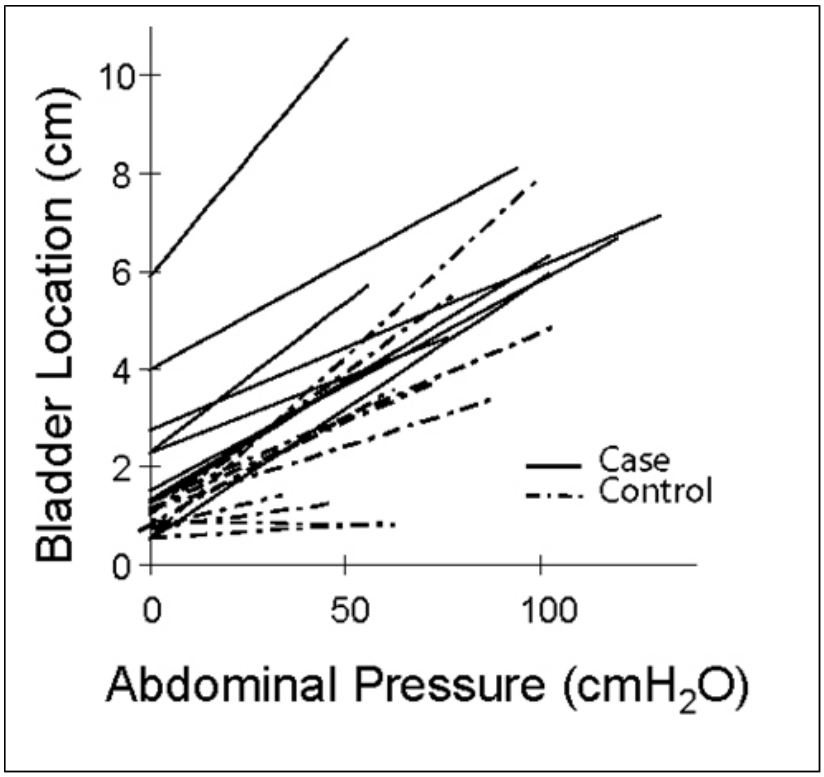

Figure 6-2 Best fit lines for the loading curves for all subjects. Solid lines present data for women with prolapse, dashed line were the data for women with normal support.

This study extends the existing literature on the biomechanics of pelvic organ prolapse in two important ways. The first is that it uses an in vivo material property testing method to compare women with and without prolapse. Numerous investigators have used in vitro testing method using uni-axial tensiometer to test the property of vaginal biopsy specimens (Lei et al, 2007, Rubod et al, 2008), however those specimens are lack of smooth muscle tone which exists in living women, also the loading applied to those specimens during uni-axial testing is not resemble the physiological loading in living women. Second, we were surprised to find that resting bladder point alone explained 55% of the variation bladder wall descent. This finding that prior to loading, the starting state of the bladder in women with prolapse differs from those with normal support is intriguing. This may represent long term adaptation of the anterior support

system which we currently are not able to quantify. For example, stretching and elongation of the connective tissue supports of the anterior compartment which has occurred over time.

We encountered several challenges during this study. There tends to be variation in a woman's levator muscle activity during a Valsalva maneuver, despite similar instructions being given. For example, during a pelvic examination women tend to contract their muscle during Valsalva when they are afraid to pass gas, instead of relaxing their muscle as instructed. Some may be less inhibited in the MR scanner since no one else is in the room with them. Also the effort that women develop during Valsalva can vary from one time to the next. The size of the cystocele may vary from one trial to another, even in the same subject, despite careful coaching and training during an office visit that was always conducted before the visit at which the dynamic MR exam was conducted. Lastly, the 1 Hz data collection rate for the dynamic MR images precluded any meaningful measurements from being made during a cough (during which the peak intra-abdominal pressure can be reached in half a second). For this reason, we only studied Valsalva.

We used the displacement of the most dependant bladder point and the value of intra-abdominal pressure required to achieve that displacement to estimate overall support system compliance. Even though it is simple to measure and easy to interpret, one landmark measurement hardly tells the whole story about system support properties and using this technique we tend to lose any insights about how compliance varies from one region to another. To address this limitation, we explored the feasibility of using a non-rigid image registration method to estimate anterior vaginal wall deformation, thereby assessing its support system compliance (see Appendix 'B'). However, time did not permit the full development of this technique for this application. However, the preliminary results were promising and this is direction that future research might follow.

References

Cosson M, Lambaudie E, Boukerrou M, Lobry P, Crépin G, Ego A. A biomechanical study of the strength of vaginal tissues. Results on 16 post-menopausal patients presenting with genital prolapse. Eur J Obstet Gynecol Reprod Biol. 2004 Feb 10;112(2):201-5.

DeLancey JOL. Fascial and muscular abnormalities in women with urethral hypermobility and anterior vaginal wall prolapse. Am J Obstet Gynecol, 2002;187:93-8.

Epstein LB, Graham CA, Heit MH. Systemic and vaginal biomechanical properties of women with normal vaginal support and pelvic organ
prolapse. Am J Obstet Gynecol 2007;197:1-165.

Kondo A, Narushima M, Yoshikawa Y, Hayashi H. Pelvic fascia strength in women with stress urinary incontinence in comparison with those who are continent. Neurourol Urodynam 1994;13:507-13.

Hendrix SL, Clark A, Nygaard I, Aragaki A, Barnabei V, McTiernan A. Pelvic organ prolapse in the Women's Health Initiative: gravity and gravidity. Am J Obstet Gynecol. 2002 Jun;186(6):1160-6

Howard D, Miller JM, Delancey JO, Ashton-Miller JA. Differential effects of cough, valsalva, and continence status on vesical neck movement. Obstet Gynecol. 2000 Apr;95(4):535-40.

Lei L., Song Y., Chen R. Biomechanical properties of prolapsed vaginal tissue
in pre- and postmenopausal women. Int Urogynecol J, 2007;18:603–607

Peng Q, Jones R, Shishido K, Constantinou CE. Ultrasound evaluation of dynamic responses of female pelvic floor muscles. Ultrasound Med Biol. 2007;33(3):342-52.

Reay Jones NH, Healy JC, King LJ, Saini S, Shousha S, Allen-Mersh TG. Pelvic connective tissue resilience decreases with vaginal delivery, menopause and uterine prolapse. Brit J Surg 2003;90:466-72.

Rubod C & Boukerrou M & Brieu M et al Biomechanical properties of vaginal tissue: preliminary results Int Urogynecol J. 2008;19:811–816

Sze EH, Karram MM. Transvaginal repair of vault prolapse: a review. Obstet Gynecol 1997;89:466-75.

Shull BL, Bachofen C, Coates KW, Kuehl TJ. A transvaginal approach to repair of apical and other associated sites of pelvic organ prolapse with uterosacral ligaments. Am J Obstet Gynecol 2000;183:1365-73.

Singh K, Jakab M, Reid WM, Berger LA, Hoyte L. Three-dimensional magnetic resonance imaging assessment of levator ani morphologic features in different grades of prolapse. Am J Obstet Gynecol 2003;188:910-915.

Chapter 7

General Discussion

Anterior vaginal prolapse (AVP), clinically referred to as "cystocele," is the most common form of pelvic organ prolapse. Despite its common occurrence, its pathomechanics remains poorly understood. This dissertation is a first attempt to understand the mechanisms underlying an anterior vaginal wall prolapse from a biomechanics point of view.

The approach was to first use advanced magnetic resonance (MR) imaging to establish the normal geometry of anterior vaginal wall support system and compare morphological differences between women with and without prolapse. Therefore, in Chapter 2 a technique was developed to quantify levator ani muscle cross-sectional area in women with and without visible muscle defect, and with and without prolapse. A localized cross-sectional area decrease was found in the ventral pubic portion of the levator ani muscle in women with defects. Surprisingly, in the dorsal pubic portion, women with major defect had a slightly larger cross-sectional area compared to women with intact muscle, which may imply compensational tissue hypertrophy in this region. However muscle cross-sectional areas were not different between women with and without prolapse when controlling for muscle status. This suggests that the muscle impairment is an important factor associated with anterior vaginal wall prolapse, but not the only factor.

In Chapter 3, we investigated how vaginal thickness and vaginal length associate with prolapse. We found that women with prolapse have thicker and longer vaginal walls -- in contrast to the common prevailing belief that it is a deterioration and thinning of vaginal tissue that is the cause of anterior vaginal wall prolapse. We found that descent of the apex of the vaginal wall and
vaginal wall length are two strong predictors for prolapse size; in fact they explained 77% of variation among prolapse size. This provides the clinical evidence that apical support and the vaginal wall itself are important support elements as well.

Therefore, the disease model we proposed is that the occurrence and magnitude of AVP is not explained by any single mechanism, but involves a combination of connective tissue support failure at one or more sites (including apical and/or paravaginal support) and also involves an interaction with pubococcygeal muscle impairment.

We tested this idea using biomechanical computer models, including both a theoretical 2D lumped parameter model (Chapter 4) and an anatomically more accurate, 3D, subject specific finite element model (Chapter 5). Those validated models allow us to analyze the pathomechanics of anterior vaginal wall prolapse by examining "what-if" scenarios, which include situations that are not amenable to experimentation in live individuals for obvious ethical reasons.

Our simulation results suggest why the levator ani muscle plays an important role in pelvic floor organ support, thus helping to explain the clinical observations of levator ani muscle impairments in these patients. For example, Delancey and colleagues found that women with prolapse have a larger hiatus on average (DeLancey et al. 1998), but why this might be so was not understood at the time. Later they found that women with prolapse are four times more likely to have levator ani muscle defect (DeLancey et al. 2007). Our MRI measurements (Chapter 2) showed that visible muscle defects on MR

images are directly associated with decreasing of muscle cross-sectional area. This in turn has been associated with a decrease in the isometric force that this muscle can generate and therefore the muscle's ability to resist stretch. This can help to explain why the hiatus may be larger in prolapsed women, but did not really explain why prolapse occurs. Our model simulations suggest that the impairment in pubic portion of levator ani muscle causes the enlarged hiatus which observed in these women. This allows a longer length of vaginal wall to be exposed to the action of a pressure differential between high intra-abdominal pressure (during physical activities such as straining, coughing, lifting, etc) and low atmosphere pressure, resulting in an increase in larger vaginal tissue stress and placing more load on connective tissue support. This increase stress drags down the apex and results in cystocele formation. Our model (Chapters 4 and 5) provided mechanistic insight in the relationship between muscle impairment and cystocele formation helping to link the clinical findings reviewed above.

The models also help to explain the importance of apical support. With muscle impairment present and the anterior vaginal wall subjected to a pressure differential loading, with intraabdominal pressure acting on its superior surface, and atmospheric pressure acting distally on its inferior surface, this tensile load has to be resisted by both apical and paravaginal connective tissue supports. Our model suggested that apical impairment resulted in a larger cystocele size compared to paravaginal impairment, a result which agrees with Summers' clinical finding (Summers et al. 2005).

This dissertation therefore extends the existing literature on pelvic organ prolapse mechanism. We can see this by examining Figure 7-1 which shows the extant understanding supported by scientific data at the time this dissertation research was started in 2002. In this understanding intra-abdominal pressure loaded on anterior compartment causes the tension in paravaginal support and vaginal wall itself. Impairments in paravaginal connective tissue and/or the weakening of anterior vaginal wall were thought to result in an abnormal vaginal elongation and in turn cause vaginal bulging based on the action of its geometric constraints, such as at the apex, paravaginal attachments and the distal location of vaginal wall. The biomechanical studies had

concentrated on the material properties changes observed in the vaginal wall and its supporting connective tissue.

This dissertation is the first time the interaction between muscle, connective tissue and anterior vaginal wall structures has been systematically investigated in the presence and absence of structural defects. Figure 7-2 shows a conceptual (systems analysis) model of our current understanding of the biomechanical mechanism underlying cystocele formation. The black portion shows the existing understanding at the time this dissertation started. The dark grey portion shows the contribution of this dissertation work. The light grey portion shows hypotheses yet to be investigated in the future.

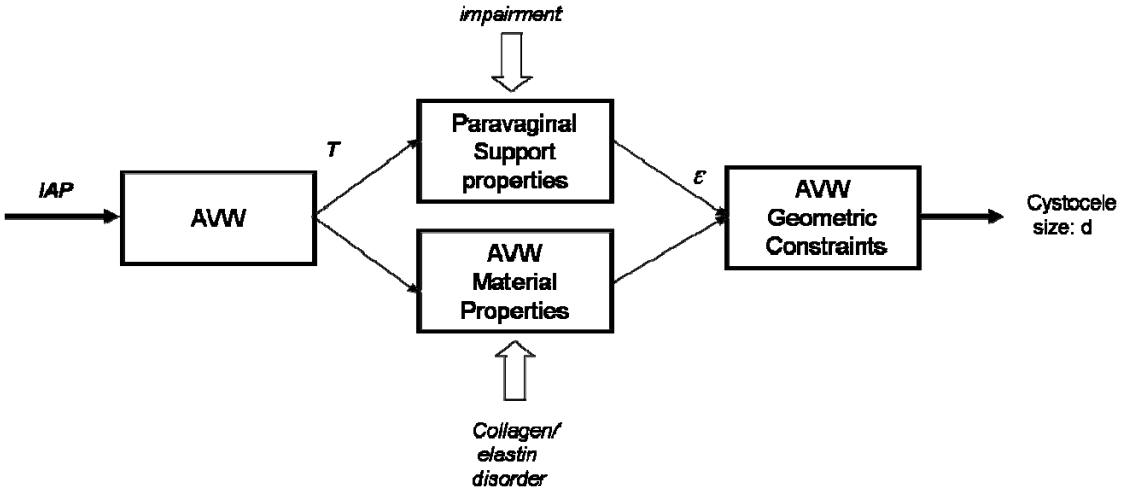

Figure 7-1 The understanding of cystocele formation supported by scientific data extant at the time this dissertation work started in the year 2002. IAP denotes intra-abdominal pressure; AVW: anterior vaginal wall; T: tension; and ε : strain.

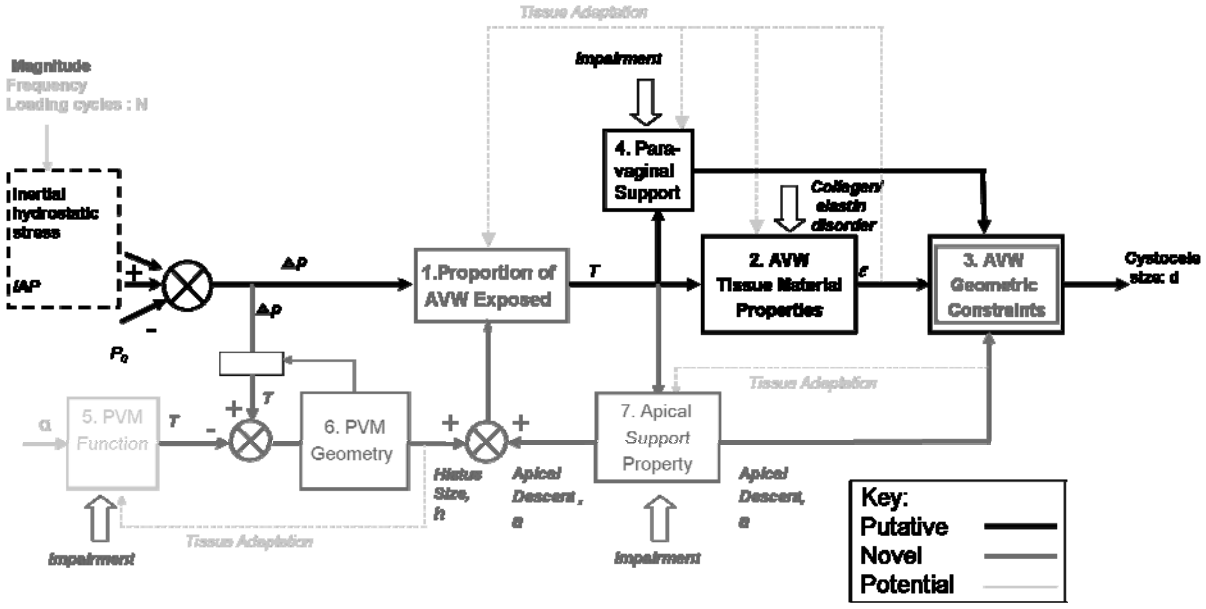

Figure 7-2 A new conceptual (systems analysis) model for the mechanism of anterior vaginal wall prolapse showing the factors leading to the development of a cystocele of size 'd'. The black 'putative' portion represents the historical understanding in the year 2002 (when this dissertation research was started). The dark grey 'novel' portion represents the contribution of this dissertation. In particular, the idea of focusing on the pressure differential acting on the exposed distal portion of vagina as the driving force to the development of prolapse (Chapter 4 & 5) is held to be a key contribution. The light grey 'potential' portion represents tissue adaptational mechanisms that could act over time and need to be investigated in the future. In this dissertation the effect of a single loading cycle, with different magnitudes of intra-abdominal pressure, IAP, was investigated, but the effect of multiple loading cycles should be investigated in the future. IAP denotes intra-abdominal pressure; PVM: pubovisceral muscle, pubic portion of levator ani muscle; AVW: anterior vaginal wall; α : active contraction of levator ani muscle; P_0: atmosphere pressure; Δp : pressure differential ; T: tension; and ε : strain.

The core concept is that impairment weakening the levator ani muscle's (box 5 in Figure 7-2) resistance to stretch causes an enlarged genital hiatus, which exposes longer the anterior vaginal wall (box 1) to a pressure differential, which causes abnormally larger tensile stress being placed on the paravaginal support (box 4), the apical support (box 7) and the anterior vaginal wall (box 2), causing the abnormal elongation in those structures, eventually causing cystocele formation (model output, "d").

There are some positive feedback mechanisms in this conceptual model which provide insights that help to explain how cystocele can gradually develop over the years. The exposed anterior vaginal wall causes the tension in vaginal tissue because of pressure differential. This tension loads the apical support system and causes apical descent. Then

this apical descent causes a longer length of vagina to be exposed to the pressure differential which in turn causes larger tension in vaginal wall and larger loading on apical support until a new equilibrium is again established in the system. A second positive feedback mechanism is caused by the anterior vaginal wall having a trapezoidal shape - narrower at distal end than at the apex. As increasing vaginal length is exposed to the pressure differential, the area of vagina exposed to the pressure differential will increase non-linearly due to this trapezoidal shape, thereby leading to a non-linear increase in the force dragging down the apex. Thirdly, an impairment during vaginal birth or due to intrabdominal pressure overloading during activities like lifting, tripping or slipping, could injure the apical support system and thereby decrease the stiffness of apical support system material properties; this will cause an even larger apical descent, and eventually a larger cystocele.

This conceptual model provides useful insights that help explain why vaginal parity is the most important risk factor to predict prolapse and how insults to the pelvic floor during vaginal birth in a young woman can cause cystocele formation later in the woman's life (usually starting to become symptomatic in their 50s or 60s).

In this dissertation, we did not directly consider the mechanisms of adaptation in tissues loaded over longer periods of time (Figure 7-2: light grey "future" portion). Our MR imaging studies showed that women with prolapse have slightly larger muscle cross-sectional area in their dorsal portion of levator ani, they also tend to have larger vaginal cross-sectional area and larger vaginal length. These findings suggest tissue can slowly adapt to abnormally increased loading placed onto them as the result of muscle impairment. This might be another reason for the delay we see in cystocele formation over the years between vaginal delivery and when cystocele is first noticed.

There are several limitations to the approach used in this dissertation. First, all the MRI measurements were landmark-based and relied on considerable anatomical expertise. Second, subject's levator ani muscle activity during Valsalva maneuver is difficult to control. Even though we did carefully train subjects to relax their muscle when increasing

their intra-abdominal pressure, variation in Valsalva effort and activity of levator ani muscle during a Valsalva can occur, cystocele formation during the Valsalva can be trial- and subject specific. However the effect of active muscle contraction has yet to be incorporated into our model simulations. Clearly, voluntary or involuntary increases in levator activity would tend to stiffen the muscle by engaging more muscle cross bridges in the strongly bound state, thereby increasing its resistance to stretch deformation, and vice versa. So the higher the levator stiffness the more resistance there is to hiatal expansion. Third, material properties were assumed to be classically hyper-elastic in nature. Time-dependent factors such as a tissue's viscous properties and the effects of loading rate, number of loading cycles were not addressed in the model. It would certainly have been better to have used visco-hyperelastic properties in the models had they been available, which was not the case at the time of writing. Fourth, the tissue failure criteria and the possibility of tissue adaptation (whereby a tissue loaded repetitively over time might change its material properties such as stiffness by changing its structure or density) were not considered in this model. Fifth, impairments in support structures were simulated simply by decreasing their stiffness; the initial geometry changes caused by impairment were also not considered at present time. In the case of the apical support, the 50% decrease in stiffness was simply an arbitrary value. It remains to be seen whether future experimental measurements show impairments of this magnitude. Sixth, the anatomy of some regions, especially the paravaginal attachments, and the attachments of the distal vagina remain to be defined in detail, so these need to be studied in the future and incorporated into the model. For example, it is likely that the distal end of the vagina is not fixed in every patient and its attachment can deform and even translate distally under abdominal pressure loading in some patients. Seventh, even though our models have been shown to be able to reproduce a similar size and shape of cystocele as that of seen in the real patient, a more extensive, specific and quantitative model validation method is still in the future. Also, we did not consider inertial loading effects caused by any deceleration of abdominal content momentum by the apical support and pelvic floor. Presumably these inertial effects are small during the slow movements associated with a Valsalva. But they can be large during vigorous physical activity such as jump landings.

Despite these limitations, we believe the model captured many of the important features of cystocele formation and the results support the working hypothesis posited in Chapter 1.

Chapter 8

Conclusions

This dissertation is a first attempt to understand the biomechanical mechanisms underlying an anterior vaginal wall prolapse using MR imaging and biomechanical modeling approach. We evaluated the effect of pathological changes in three components of anterior vaginal wall support: 1) levator ani muscle, 2) vaginal wall, and 3) paravaginal and apical suspension. The following conclusions were drawn:

1. Women with major defects exhibited a smaller (i.e., 50% less than women without defect) cross-section area in the ventral portion of the levator ani muscle, whereas in the posterior portion of the muscle, women with major defects exhibited a slightly larger (17%) cross-section area compared to those without defects. However cross-sectional area measurements did not show statistically significant differences between women with and without prolapse for each level of defect. There was evidence of compensatory muscle adaptation and hypertrophy in the region of the levator ani adjacent to the defect site.
2. Using a similar technique, vaginal cross-sectional area was larger for women with prolapse compared to women with normal support. Positive correlations were found between anterior vaginal wall descent, cystocele size, and anterior vaginal wall length. Combined with apical descent, these parameters explained 77% of cystocele size.

3. A 2-D, sagittal plane, lumped parameter model showed that a combined impairment in both muscular and connective tissue support of the anterior vaginal wall was needed to produce

4. the largest cystocele. A 90% impairment of apical support led to a 530% increase in anterior wall prolapse in the presence of a 60% pubovisceral muscle impairment.

4. A 3-D, subject-specific, anatomically accurate, finite element model demonstrated that realistically-shaped and -sized cystoceles can develop due to a levator defect. This allows a pressure differential to act across the distal vaginal wall, thereby tensioning the vaginal wall and its apical supports, which in turn causes the prolapse to form in the distal vagina. This sequence of events helps to explain the clinical observations of hiatal size and muscle weakness in women with AVP.

5 By simultaneously measuring intra-abdominal pressure as the displacement of the most dependent bladder point, the compliance of the anterior vaginal wall support system in women with prolapse was estimated as 0.5 mm / cm H2O, or 67% higher than was found in healthy age-matched controls. This suggests that in women with prolapse, apical support compliance is increased relative to controls.

Chapter 9

Suggestions for Future Research

This dissertation provides useful insights into biomechanical mechanisms underlying an anterior vaginal wall prolapse. We focused on the interplay among: 1) levator ani muscle, 2) anterior vaginal wall, and 3) apical and paravaginal connective tissue support. We also investigated the mechanical factors resulting from the alterations in these supports that are involved in the development of prolapse. There are many factors that remain to be investigated, such as the effect of vaginal childbirth, the effect of aging on tissues, the effect of occupations involving heavy lifting and chronic coughing which both heavily load the pelvic floor, and the effects of collagen and elastin disorders, neuromuscular dysfunction, hormonal effects as well as tissue adaptation over time. These effects are all worthwhile investigating in the future.

The initial geometry used in the present model was based on the anatomy of a single woman with normal support. How abnormal initial geometry might affect the stress distributions in different support structures and lead to cystocele formation remains to be investigated. Also the morphological variation in the anterior vaginal wall support system that exists in a population needs to be delineated, as do how those variations affect the formation of the cystocele.

The present 3D model has a simplified structure and geometry. The model can be improved by incorporating the perineal body and its support, and a separated posterior vaginal wall and rectum, so that organ competition during the development of

prolapse can be studied. Also in some regions, the functional anatomy of the paravaginal support needs to be further clarified and implemented in the model.

Studies are needed to provide the model with more accurate material properties. Because most tissues are highly anisotropic, biaxial test data will be needed along with muscle fiber and collagen fiber mapping. The lack of representation of striated levator and smooth muscle tone and activity also needs to be remedied. Finally, data are needed on the visco-hyperelastic behavior and injury criteria of the salient tissues. Once available, the effects of different pressure and inertial loading rates can usefully be examined. Finally a more specific and extensive model validation technique is needed for future models that take into account any inter-individual and ethnic morphological differences.

Appendices

Appendix A

Cardinal and Uterosacral Ligament Load-Sharing Depends on Their Relative Orientations

ABSTRACT

Objective: The aim of this project is to use a 2-D biomechanical model to investigate how variation in cardinal and uterosacral ligament inclinations affect the tension in each ligament as it supports the pelvic viscera ("pelvic load") in static equilibrium. Data for the 2-D model was derived from 3-D models of the cardinal and uterosacral ligaments of women with normal pelvic support.

Methods: Supine MRI scans of volunteers with normal support on POP-Q (all points at least 1 cm above the hymen) examination were obtained from a study of pelvic organ support. 3-D models were constructed from a convenience sample of 15 women in whom axial and coronal proton density MR scans clearly showed ligament anatomy that could be reconstructed using the 3-D Slicer© software. Each model was segmented into equal parts using I-DEASTM software, whereupon the centroid of each model segment was found. The 3-D lines-of-action of the four ligaments were then determined either using these centroids or their approximate origin and insertion points. The angles between the ligaments (U-C) and of each ligament relative to the cranio-caudal body axis (C, U) were measured. We represented the averaged actions of the left and right uterosacral ligaments in the sagittal plane by a single cable (whose tension is Tu) and, similarly, the left and right cardinal ligaments by a second cable [tension: Tc]. A "pelvic load" (arbitrarily set at 1 Newton [N]) was suspended from each ligament and deflected by the levator plate whose angle was set using MRI measurements. Tu and Tc were then calculated for each individual in the upright posture using their measured angles.

Results: Tc was 51% greater than Tu (P=0.0002). However, the variability (range×100%/mean tension) of Tu was greater (98%) than the variability of Tc (36%). The variance in angle C was larger than the other two angles.

Conclusion: Biomechanical model analysis using data from women with normal support suggests that the cardinal ligaments may carry more tension than the uterosacral ligaments. However, the variability in uterosacral tension is greater across individuals. Comment: Individual differences in ligament geometry might predispose a certain woman to ligament injury under conditions of increased ligament load (e.g. loss of pelvic muscle support).

Introduction

The cardinal and uterosacral ligaments have long been credited with contributing to utero-vaginal support. Varying anatomists have studied these structures from cadaveric dissections and cross-sectional anatomy (Blaisdell 1917, Campbell 1950, Range 1964, DeLancey 1992). These studies have provided some understanding of the structures' histologic content and structural arrangement. However, a biomechanical understanding of how the ligaments function to provide pelvic organ support has been lacking. The biomechanical relationship of the ligaments can be simplified as being analogous to a light suspended by two cables. In this example, the light represents the pelvic viscera and provides the "load" or force placed on the cables. The cables are the cardinal and uterosacral ligaments. The angles of inclination of the cables or the ligaments affect the tension placed on each ligament as it supports the pelvic viscera. These angles can be estimated from 3-D models of the cardinal and uterosacral ligaments constructed from magnetic resonance images. These calculations can then be used to develop 2-D biomechanical models to investigate how variation in inclination of the cardinal and uterosacral ligaments affect the tension in each ligament as it supports the pelvic viscera ("pelvic load") in static equilibrium.

Materials and Methods

Supine MRI scans of 15 volunteers with normal support (all points at least 1 cm above the hymen) on POP-Q examination and clearly defined cardinal and uterosacral ligament

anatomy were selected from a larger study of over 300 women with and without normal pelvic organ support. All MR scans were obtained as multiplanar two-dimensional fast spin proton density MR images (echo time 15 ms, repetition time 4000 ms) using a 1.5 T superconducting magnet (General Electric Signa Horizon LX) with version 9.1 software. The field of view in axial and coronal images are both 16x16 cm and the field of view in the sagittal images is 20x20 cm. All three views had slice thicknesses of 4 mm with a 1 mm gap between slices.

Axial and coronal MR-images were imported into a three-dimensional (3-D) imaging program (3-D Slicer, version 2.1b1) and aligned using anatomic landmarks. The uterosacral ligament was traced on axial MR images (Figure A-1) and the cardinal ligament was identified and traced on coronal MR images (Figure A-2).

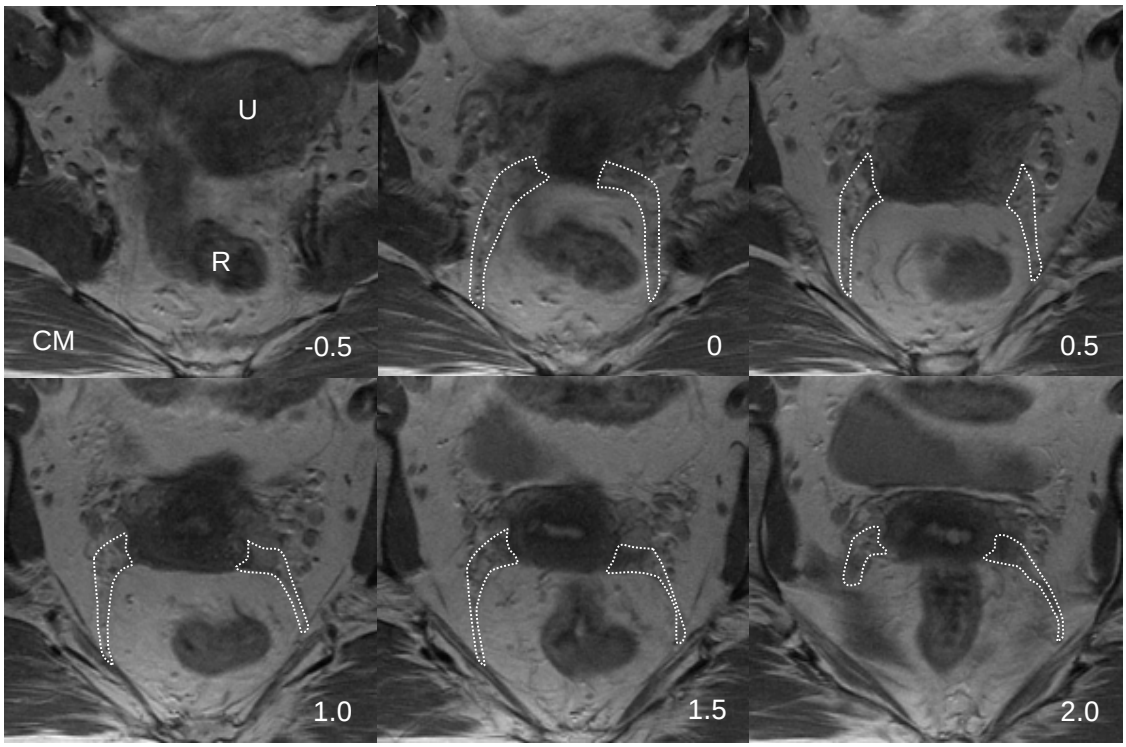

Figure A-1. Tracings of the uterosacral ligament on axial MR images.

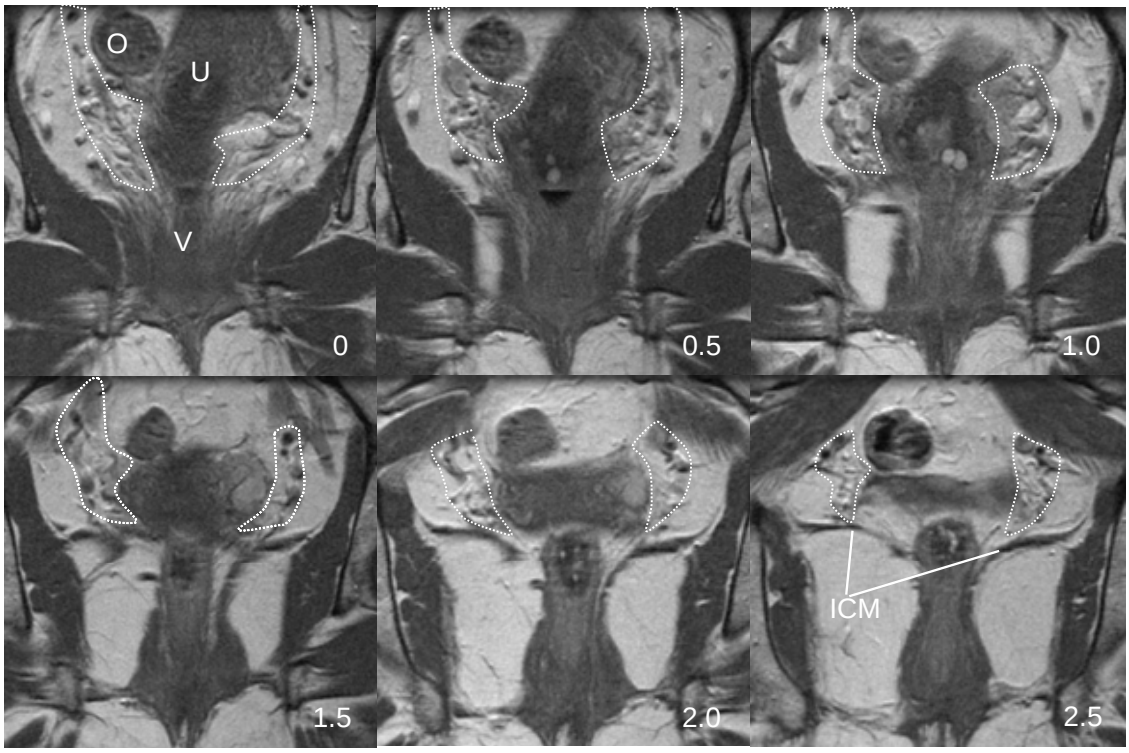

Figure A-2. Tracings of the cardinal ligament on coronal MR images.

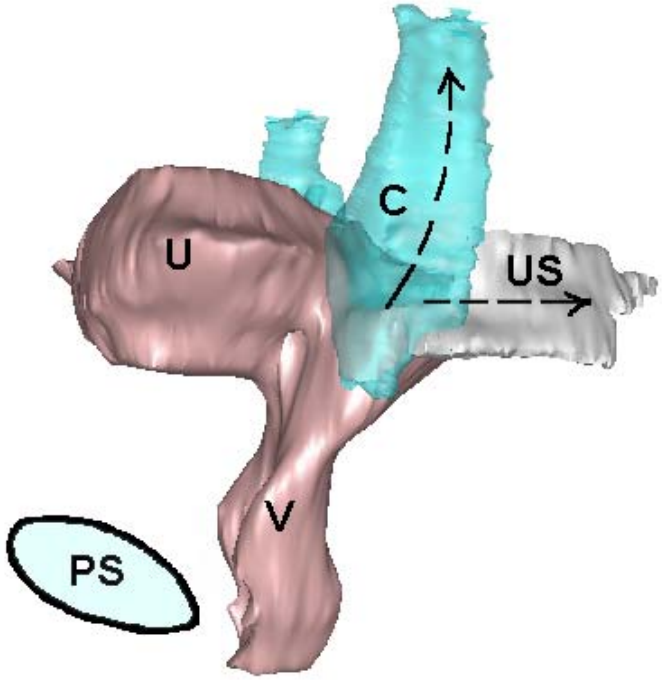

Figure A-3. Left lateral view of 3-D cardinal and uterosacral ligament models. Arrows demonstrate the line of action of the ligaments. C: cardinal ligament; US: uterosacral ligament PS:pubic symphysis; U: uterus; V: vaginal;

3-D volumetric models were constructed from these axial- and coronal traces using the 3-D Slicer© software (Figure A-3). The 3-D models were then imported into I-DEASTM version 9.0 (EDS, Plano, TX), an engineering graphics software. Each model was segmented into equal parts using I-DEAS, and the centroid of each model segment was found. The 3-D lines-of-action for the four ligaments were determined by using the best fitted straight line of the centroid (Figure A-4). For four of our models, subjects had very curved uterosacral ligaments because of the supine acquisition of the MR scans. For those models we determined the line-of-action by connecting the origin and insertion points.

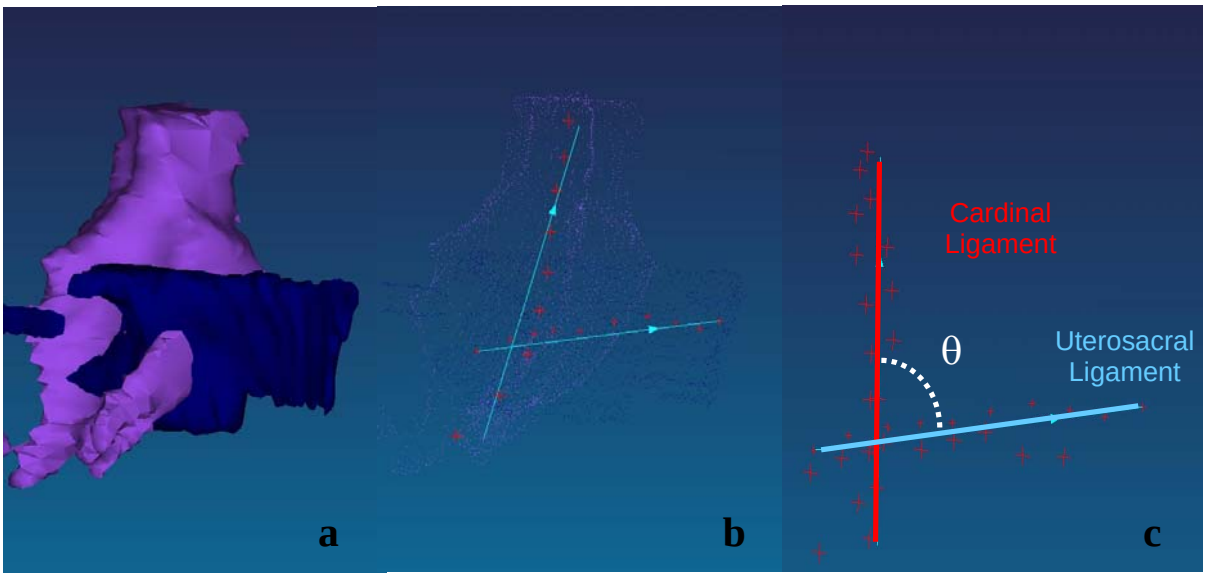

Figure A-4. Determining the lines of action of the ligaments. a) 3D models of the right cardinal and uterosacral ligament. b) Using best fit line through centroids to determine the axis of ligaments. c) Measuring the angle between the cardinal and uterosacral ligament.

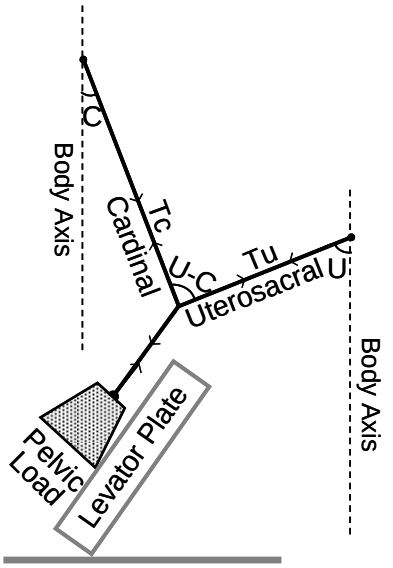

Figure A-5: Suspension model

The angles between the uterosacral and cardinal ligaments (U-C) and of each ligament relative to the cranio-caudal body axis (C, U) were measured in 3-D space. These angles were then projected onto the sagittal plane and used for the angles in the 2-D biomechanical model (Figure A-5). In this model, we represented the averaged actions of the left and right uterosacral ligaments in the sagittal plane by a single cable (whose tension is Tu) and, similarly, the left and right cardinal ligaments are represented by a second cable (Tc). A "pelvic load" (arbitrarily set at 1 Newton [N]) was suspended from the ligaments and deflected by the levator plate (Figure A-1) whose angle was set at 45^{o} from the horizontal (using MRI measurements of women with normal support). We calculated the tension placed on the cardinal and uterosacral ligaments using these parameters. Secondary analysis was performed using levator plate angle (LPA) of 54^{o} based on measurements of prolapse patients. Tu and Tc were then calculated for each individual in upright posture using their measured angles.

Results

The variance in angle C was larger than the other two angles. Using the levator plate angle of women with normal support (45^{o}), the tensions in the cardinal and the uterosacral ligaments were almost the same. Changes in the levator plate angle caused changes in the tension on the ligaments. If the levator plate was changed to 54^{o} as in

prolapse geometry, Tc (0.74 N) was 51% greater than Tu (0.49 N) (P=0.0002). However, the variability (range×100% / mean tension) of Tu was greater (98%) than the variability of Tc (36%).

Table A-1 Result

	Mean ± SD	Min	Max
C (o)	25.0 ± 8.6	13.2	47.0
U (o)	81.0 ± 5.9	69.0	92.5
U-C (o)	73.5 ± 8.1	59.0	80.6
Tc (N) LPA=45o	0.62± 0.09	0.47	0.77
Tu (N) LPA=45o	0.63±0.120.12	0.36	0.77
Tc (N) LPA=54o	0.74 ±0.08	0.63	0.89
Tu (N) LPA=54o	0.49 ±0.13	0.19	0.67

Discussion

The geometry of the cardinal and uterosacral ligaments and their orientation relative to the direction of the force placed upon them affects their tension. Changing the angles of the ligaments relative to the body axis also changes their angles relative to the loading force thereby changing ligament tension. The ligament which is more aligned to the loading direction will have a greater tension than the ligament that is less aligned. Finally, changing the levator plate angle from 45^{o} (normal women) to 54^{o} (prolapse women) increases the difference between the angles of the ligaments relative to the load, thereby increasing the difference between Tc and Tu. The cardinal ligaments then carry more tension than the uterosacral ligaments because they are better aligned with the pelvic load force than the uterosacral ligament. Moreover, inter-individual variation in the calculated tension in the uterosacral and the cardinal ligaments varies widely. Therefore, there may be certain individuals who, because of their geometry, have ligaments subjected to greater tension for any given pelvic load.

The uterosacral and cardinal tissues are critical components of Level I support and provide support for the vaginal apex (DeLancey et al 1992). The cardinal ligaments are oriented in a relatively vertical axis (in the standing posture) while the uterosacral

ligaments are more dorsal in their orientation. Neither are true ligaments in the sense of a skeletal ligament that is composed of dense regular connective tissue similar to knee ligaments. They are "visceral ligaments" that are similar to bowel mesentery. They are made of blood vessels, nerves, smooth muscle, and adipose tissue intermingled with irregular connective tissue. They have a supportive function in limiting the excursion of the pelvic organs much as the mesentery of the small bowel limits the movement of the intestine. When these structures are placed on tension, they form condensations that surgeons refer to as ligaments (Campbelln 1950, Range et al 1964).

Both the cardinal and the uterosacral ligaments are visible from pelvic MR images. The cardinal ligament is a mass of retroperitoneal areolar connective tissue in which blood vessels predominate; it also contains nerves and lymphatic channels (Range et al 1964). It has a configuration similar to that of "chicken wire" or a fishing net in its natural state but when placed under tension assumes the appearance of a strong cable as the fibers align along the lines of tension (Range et al 1964). Because of it relatively vertical orientation, it is best seen on the coronnal MR images. It is demarcated by the vessels and lymphatic elements lateral to the pelvic organs (Figure A-2). The 3-D models of the cardinal ligaments often have an amorphous "cloud-like" appearance which at times made approximations of their lines of action challenging.

The uterosacral ligaments are bands of tissue running under the rectovaginal peritoneum composed of smooth muscle, loose and dense connective tissue, blood vessels, nerves, and lymphatics (Campbell 1950). They originate from the postero-lateral aspect of the cervix at the level of the internal cervical os and from the lateral vaginal fornix (Campbell 1950). Because of their relatively antero-posterior orientation, they are best seen in the axial scan images. While macroscopic investigation observed insertion of the ligament to the levator ani, coccygeus, and the presacral fascia (Blaisdell 1917), MRI examination showed the uterosacral ligaments overlie the sacrospinous ligament and coccygeus in 82% of the cases and over the sacrum in only 7% of the cases (Umeck et al 2003). The difference between the appearance of these structures in MRI and on dissection may have to do with the tension placed on the structures during dissection and will require further research to clarify. The 3-D models from the tracings showed the uterosacral ligaments to have a "band-like" appearance.

This study is unique in its attempt to understand how the orientation of the cardinal and uterosacral ligaments affects load sharing. It also nicely demonstrates the important contribution of the levator plate angle to this arrangement. Small changes to the levator plate angle in the 2-D model changed the tensions on both of the ligaments. The technique developed in this study of using 3-D measurements and applying them to simplified biomechanical models is an important tool in furthering our understanding of pelvic organ support. The limitation is that these are preliminary results which will likely need refinement. We hope to continue this work in the future.

References

Blaisdell FE. The anatomy of the sacro-uterine ligaments. Anat Record 1917; 12:1-42.

Campbell, R. M.: The anatomy and histology of the sacrouterine ligaments. American Journal of Obstetrics & Gynecology, 1950;59: 1

DeLancey, J. O.: Anatomic aspects of vaginal eversion after hysterectomy. American Journal of Obstetrics & Gynecology, 1992;166: t

Range, R. L. and Woodburne, R. T.: The gross and microscopic anatomy of the transverse cervical ligaments. American Journal of Obstetrics & Gynecology, 1964;90: 460

Umek WH, Morgan DM, Ashton-Miller JA, DeLancey JO. Quantitative analysis of uterosacral ligament origin and insertion points by magnetic resonance imaging. Obstet Gynecol. 2004 Mar;103(3):447-51

Appendix B

Vaginal Wall Deformation Estimation Using Non-Rigid Image Registration

ABSTRAT

Anterior compartment support system composed of a variety of structures: levator ani muscle, apical and paravaginal connective tissue and anterior vaginal wall itself. The unique mechanical properties of each of these structures form the composite compliance of anterior compartment support in living women. It would be helpful to be able to associate anterior vaginal wall deformation pattern under intra-abdominal pressure loading with structural impairment. In this chapter, we present an approach toward the quantification of anterior vaginal wall deformation via non-rigid registration of serial dynamic MR images when women perform Valsalva using the framework implemented in the Insight toolkit. Demons registration method was shown to perform well. This lay the groundwork for more sophisticated validation of biomechanical modeling using the finite element method.

Introduction

The interactions of levator ani muscles, apical connective tissue in the form of the cardinal and uterosacral ligaments and the connective tissues forming the anterior vaginal wall combine to form a complicated anterior compartment support system.

By observing from mid-sagittal dynamic MR sequence during Valsalva, we noticed that the deformations of pelvic floor region are distinguished between women with normal support and women with AVP. Even within the women with AVP, the deformation patterns are very different in some from the others.

Previously we assess the anterior compartment compliance in vivo by tracing the location of most independent bladder point. However, during cystocele formation, the vaginal wall stretch is highly un-uniformed. And because of the anatomy of anterior vaginal wall, it is hard to identify enough visible landmarks to accurately estimate the deformation in different portion of anterior vaginal wall. The non-rigid image registration technique has been successfully used to detect the deformation of biological tissue and organ in other parts of the body, such as myocardial contraction, abdominal deformation due to respiration, lung deformation during respiration cycle and tissue changes secondary to tumor growth (Rueckert 1999, Petitjean 2004, Rohlfing 2004, Perperidis, 2003 Sundaram 2005). The goal of this chapter is to investigate the feasibility of use non-rigid image registration technique to estimate the vaginal wall deformation when women are performing Valsalva.

Method

Image Requistion

For dynamic imaging, a multiphase, single level image of the pelvis in the midsagittal plane was obtained approximately every second for 23–27 s using a T2-weighted single-shot fast spin-echo sequence (time at rest=1,300 ms, time of excitation=60 ms, slice thickness=6 mm, field of view=32–36 cm, matrix=256×160, one excitation and half-Fourier acquisition). The time needed to acquire each of the images was determined by the patients' weight and was approximately a second. A set of 20 successive images were acquired in 23–27 s during rest and a graded Valsalva effort as follows: The operator instructed the subject to hold her breath in inspiration and initiated the scan and after 5 s of imaging during rest, the operator instructed the subject to strain minimally for 5 s, moderately for 5 s, and maximally for 5 s, then to breath normally and relax for another 5–7 s before ending the acquisition. Usually, three images were acquired at rest during suspended inspiration, 12 during the graded Valsalva effort, and five during post-Valsalva relaxation and normal breathing.

Demons deformable registration

Intensity-based automatic deformable image registration algorithm, known as the 'Demons', was used to estimate the deformation between images. This method computes a deformable registration based on intensity changes and is derived from the work by Thirion (Thirion 1998). The registration is driven by the concept of optical flow and was initially used in computer vision research. Optical flow calculates an image velocity approximating image motion from sequential time-ordered images. The demons algorithm is based on gradient calculations from the fixed image to determine the demons force required to deform the moving image. The diffusion model assumes that so-called "demons" at

every voxel from the fixed (reference) image are applying forces that push the voxels of the moving image into matching up with the fixed image. The inputs to the registration are a moving image m and a fixed image f. The optical flow velocity can then be written as

$$\vec{v} = \frac{(m-f)\vec{\nabla} f}{\left|\vec{\nabla} f\right|^2 + K^2 (m-f)^2} \quad (7\text{-}1)$$

v is the displacement during the time $\vec{\nabla} f$ interval between the two image frames.

Represents the relationship between the neighboring points in the fixed image (such as an dege), K is the reciprocal of the diagonal of a pixel and the (m-f) term represents the differential force of the interaction between the fixed and the moving images. Equation (7-1) is calculated iteratively; after each iteration, the optical flow computation is followed by regularization of the deformation field using a Gaussian filter. This method was implemented in ITK. Figure 7-1 showed the framework of image registration.

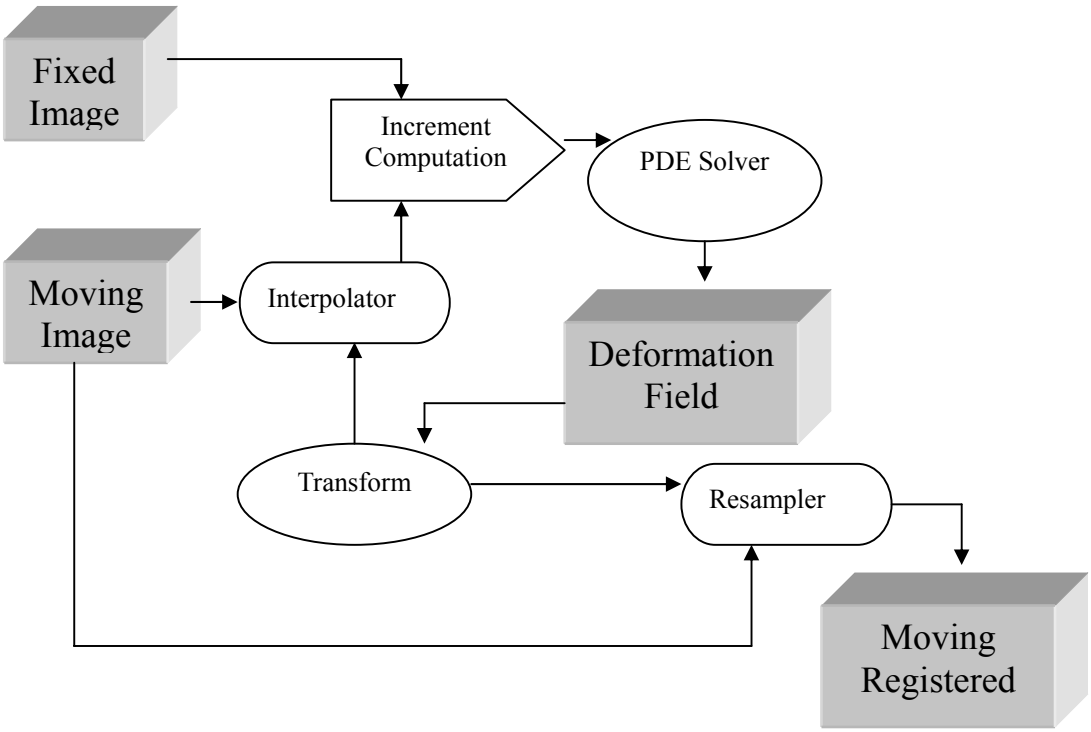

Figure B-1 Image registration framework implemented using ITK

Result

Sequential MR images during one Valsalva loading cycle were registered using Demons algorithm. The previous image was set to be moving image and was registered toward image at later time point. Deformation field was calculated and represented as deformed grid. To validate the registration, anterior vaginal wall at first image was traced. And it was deformed according to calculated deformation field between first and second image, 2' was the deformation result. As you can see that anterior vaginal wall in 2' matches well with that in MR image 2. Then sequentially 3',4', 5' was generated by deform anterior vaginal wall based on calculated deformation field. They all match well with that in original MR images.

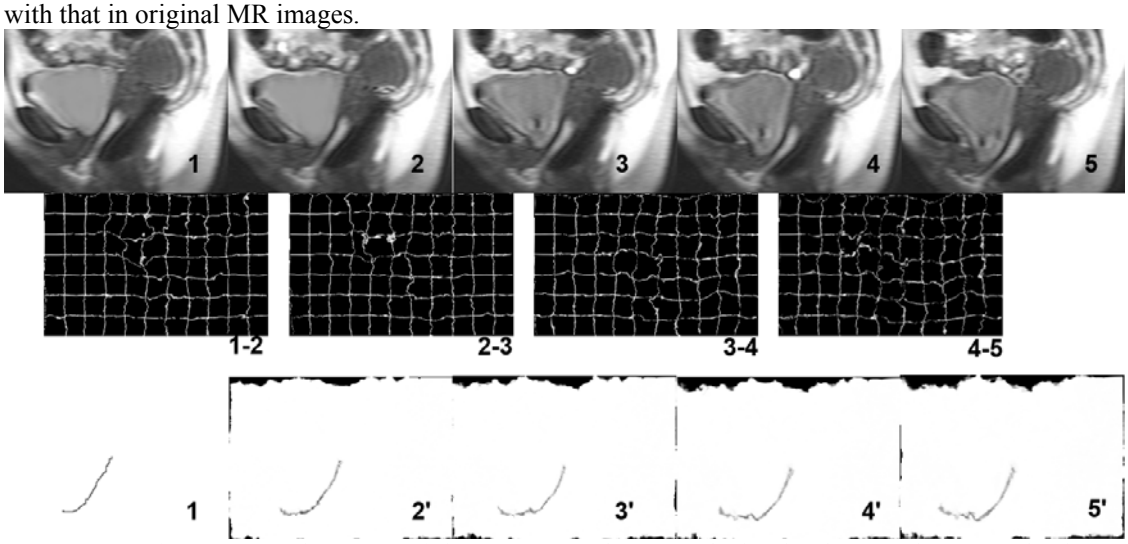

Figure B-2 First row are the sequential MR images during Valsalva loading cycle. Second role are the calculated deformation field between adjacent images. For example 1-2 means deformation field between image 1 and 2. Third role, first image is the tracing of anterior vagina wall at first image. 2', 3', 4' and 5' are the calculated location of anterior vaginal wall.

Discussion for future work

This chapter provided a framework to estimated deformation field of anterior vaginal wall support system using demons deformable image registration technique. We can assess the system compliance in different support structure by analyzing the deformation in different region associated with intra-abdominal pressure. This lay the groundwork for more sophisticated validation of biomechanical modeling using the finite element method.

References

Perperidis, D., Rao, A., Mohiaddin, R., Rueckert, D., 2003. Non-rigid spatio-temporal alignment of 4D cardiac MR images. In: Gee, J.C.,

Maintz, J.B.A., Vannier, M.W. (Eds.), Proceedings of the 2nd International WBIR, LNCS 2717, pp. 191–200.

Petitjean, F.P.C., Rougon, N., 2004. Building and using a statistical 3d motion atlas for analyzing myocardial contraction in MRI. In: Proceedings SPIE Conference on Image Processing – SPIE International Symposium Medical Imaging_04, San Diego, CA, vol. 5370.

Rohlfing, T., O_Dell Jr., C.R.M.W.G., Zhong, J., 2004. Modeling liver motion and deformation during the respiratory cycle using intensity-based nonrigid registration of gated MR images. Med. Phys. 31, 427–432.

Rueckert, D., Sonoda, L.I., Hayes, C., Hill, D.L.G., Leach, M.O.,

Hawkes, D.J., 1999. Nonrigid registration using free-form deformations: application to breast MR images. IEEE TMI 18 (8), 712–721.

Sundaram TA, Gee JC. Towards a model of lung biomechanics: pulmonary kinematics via registration of serial lung images. Medical Image Analysis 2005;9: 524–537

Thirion JP, Image matching as a diffusion process: an analogy with Maxwell's demons, Medical Image Analysis 1998;2(3):243-60.